THE BIOCHEMICAL AND DRUG BINDING CHARACTERISTICS OF TWO ABC TRANSPORTERS

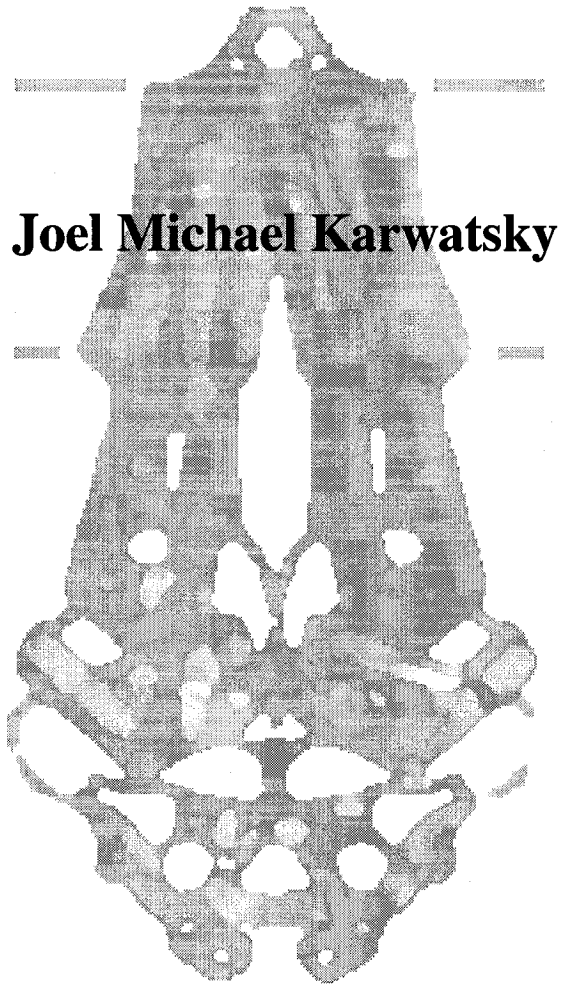

Joel Michael Karwatsky

Institute of Parasitology
McGill University, Montreal

A thesis submitted to McGill University in partial fulfillment of the requirements of the degree of Doctor of Philosophy

© Joel Michael Karwatsky

Library and Archives Canada

Published Heritage Branch

395 Wellington Street
Ottawa ON K1A 0N4
Canada

Bibliothèque et Archives Canada

Direction du Patrimoine de l'édition

395, rue Wellington
Ottawa ON K1A 0N4
Canada

Your file Votre référence
ISBN: 978-0-494-21662-0
Our file Notre référence
ISBN: 978-0-494-21662-0

NOTICE:
The author has granted a non-exclusive license allowing Library and Archives Canada to reproduce, publish, archive, preserve, conserve, communicate to the public by telecommunication or on the Internet, loan, distribute and sell theses worldwide, for commercial or non-commercial purposes, in microform, paper, electronic and/or any other formats.

The author retains copyright ownership and moral rights in this thesis. Neither the thesis nor substantial extracts from it may be printed or otherwise reproduced without the author's permission.

AVIS:
L'auteur a accordé une licence non exclusive permettant à la Bibliothèque et Archives Canada de reproduire, publier, archiver, sauvegarder, conserver, transmettre au public par télécommunication ou par l'Internet, prêter, distribuer et vendre des thèses partout dans le monde, à des fins commerciales ou autres, sur support microforme, papier, électronique et/ou autres formats.

L'auteur conserve la propriété du droit d'auteur et des droits moraux qui protège cette thèse. Ni la thèse ni des extraits substantiels de celle-ci ne doivent être imprimés ou autrement reproduits sans son autorisation.

In compliance with the Canadian Privacy Act some supporting forms may have been removed from this thesis.

While these forms may be included in the document page count, their removal does not represent any loss of content from the thesis.

Conformément à la loi canadienne sur la protection de la vie privée, quelques formulaires secondaires ont été enlevés de cette thèse.

Bien que ces formulaires aient inclus dans la pagination, il n'y aura aucun contenu manquant.

Canada

For my parents, Sue and Mike.

General Abstract

Chemotherapy is used in the treatment of cancer. Unfortunately, drugs often fail due to multidrug resistance (MDR) caused by P-glycoprotein (P-gp1 or ABCB1) and the multidrug resistance-associated protein (MRP1 or ABCC1). These proteins bind and transport drugs out of cancer cells, thereby conferring MDR.

The second chapter of this thesis addresses an unexplained phenomenon that accompanies P-gp1 expression, collaterally sensitive to verapamil. The collective results of this work demonstrated that treatment of cells that over-express P-gp1 with verapamil induces apoptosis. Furthermore, the findings show that the ATPase activity of P-gp1 was activated by verapamil. The degree of ATPase activation was proportional to the level of apoptosis and the increased demand for ATP resulted in the production of reactive oxygen species (ROS). Finally, the production of ROS led to cell death mediated by apoptosis in that experimental model system.

Chapters three and four are devoted to understanding the binding characteristics of MRP1 with two of its physiological substrates, glutathione (GSH) and leucotriene C_4 (LTC_4). Photoreactive derivatives of these substrates were synthesised to address this objective, IAAGSH and $IAALTC_4$. Photolabelling and transport studies showed that these derivatives have similar binding characteristics as the native compounds. In addition, photolabelling of MRP1 occurred with a high specificity with both compounds. IAAGSH and $IAALTC_4$ were also used to determine the locations of GSH and LTC_4 binding sites. This was accomplished using MRP1-variants containing hemagglutinin (HA) epitopes at specific locations in the amino acid sequence. Through photoaffinity labelling, immunoprecipitation, and trypsin digestion, a map of binding sites for IAAGSH or $IAALTC_4$ was obtained. Both LTC_4 and GSH bound to transmembrane (TM) regions 10-11 and 16-17 which have been previously implicated in drug binding. Furthermore, novel binding sites for both substrates were discovered. $IAALTC_4$ photolabelled a novel site within the first five TMs (TMD0) of MRP1, whereas IAAGSH labelled two

cytoplasmic regions (L1 and L0). These may represent specific binding sites for LTC_4 and GSH.

The work within this thesis explores some of the biochemical characteristics of P-gp1 and MRP1 that are not directly related to drug resistance and may lead to new strategies in cancer treatment.

Résumé Général

La chimiothérapie est utilisée comme traitement contre le cancer. Malheureusement, les drogues utilisées manquent souvent à leur tâche du au phénomène de résistance aux drogues (MDR) causée par la P-glycoprotéine (P-gp1 ou ABCA1) et par la « multidrug resistance-associated protein » (MRP1 ou ABCC1). Ces protéines lient et transportent les drogues hors des cellules cancéreuses, conférant ainsi la MDR.

Le deuxième chapitre de cette thèse adresse un phénomène inexpliqué associé à l'expression de P-gp1, la sensibilisation au vérapamil. Les résultats démontrent que le traitement au vérapamil induit l'apoptose chez les cellules qui sur-expriment P-gp1. De plus, les résultats montre que l'activité ATPase de P-gp1 est induite par le verapamil. Le degré d'activation de l'ATPase est proportionnelle au niveau d'apoptose et l'augmentation de la demande en ATP cause une production de « reactive oxygen species » (ROS). Finalement, la production de ROS conduit à la mort cellulaire par le biais de l'apoptose.

Les chapitres trois et quatre sont dévoués à la compréhension des caractéristiques de liaison de MRP1 avec deux de ses substrats physiologiques, la glutathione (GSH) et la leucotriène C_4 (LTC_4). Des dérivés photoréactifs de ces substrats (l'IAAGSH et l'$IAALTC_4$) ont été synthétisés pour étudier cette questiom. Les études de photomarquage et de transport ont montré que ces deux dérivés ont des caractéristiques de liaison similaires à celles de leur homologue naturel. Par surcroît, le photomarquage de MRP1 se fait de façon très spécifique avec les deux produits. L'IAAGSH et l'$IAALTC_4$ ont été utilisés pour déterminer les sites de liaison de la GSH et de la LTC_4. Ceci a été accompli en utilisant des variants de MRP1 contenant un épitope de l'hemmaglutinin (HA) inséré à des positions spécifiques de la séquence d'acides aminés. En utilisant le photomarquage suivit par une immunoprécipitation et une digestion à la trypsine, une carte des sites de liaison pour l'IAAGSH ou l'$IAALTC_4$ a été obtenue. Les deux, LTC_4 et GSH, se lient aux régions transmembranaires (TM) 10-11 et 16-17 auparament impliquées dans la

liaison aux drogues. De plus, de nouveaux sites de liaison pour les deux substrats ont été découverts. L'IAALTC$_4$ photomarque un nouveau site entre les cinq premiers TMs (TMD0) de MRP1, tandis que IAAGSH marque deux régions cytoplasmiques (L1 et L0). Ceux-ci pourraient représenter des sites de liaisons spécifiques pour LTC$_4$ et GSH.

Le travail présenté dans cette thèse explore quelques caractéristiques biochimiques de P-gp1 et de MRP1 qui ne sont pas directement reliées à la résistance aux drogues et qui pourrait conduire à de nouvelles stratégies pour le traitement du cancer.

Table of Contents

Acknowledgements

First and foremost, I must extend many thanks to my thesis supervisor Dr. Elias Georges. His scientific creativity and know-how have been indispensable for the successful completion of this thesis. Furthermore, his guidance was honest, which is something I cherish. Several other people have had a direct impact on the successful completion of my studies. Firstly, Mara Leimanis has been a wonderful co-worker and friend for many years. Her presence has enriched my experiences both scientifically and personally; I wish her happiness and success in her future endeavours. Four other lab-mates also contributed significantly to my experience at the Institute of Parasitology, Roni Daoud, Omar Alqawi, Abrahem Abrahem, and Rémi-Martin. Each of them taught me a great deal about science, culture, and friendship, I owe them many thanks. There have been many other lab-mates, and each one played an important part in my experience, thus I would like to thank Ying, Max, Bayo, and Anne. Although I have not worked closely with Dr. Gros' lab, I must extent a special thanks to him and Dr. Jie Cai for their support and the materials they provided which greatly facilitated my work.

While working at the Institute of Parasitology, I made many friends who helped me through my PhD. Jake, Darcy, Cat, Nick, and Anne have been constant companions and I thank them for their friendship. Peter Lee helped many people at the Institute including myself; I owe him special thanks for always being there when I needed his expertise and his understanding. The time I spent with Sureemas and Iracema was illuminating; they taught me about their culture and I consider them friends for life. Adam and Kim Belley provided wonderful camaraderie during the first few years of my studies, and remain good friends. I would also like to express my gratitude to Dr. Jim Smith and Dr. Robin Beech for their help. Finally, Shirley, Gordie, Kathy and Christien have been essential to the completion my studies; I will always remember their efforts and kindness.

I must express my appreciation to Debbie Zimmerman for the companionship and wisdom she has shared with me in the last years of my PhD. My grandparents (Baba, Gramma Jean, Didi, and Isabelle) and family have provided much of the energy I needed to stay focused. I regret that my grandfather (Grumps) will not be able to see me graduate; his loving support over the years has truly been appreciated. Finally, the gratitude I have for my parents is immeasurable. The love and unconditional support they have given me made my studies and this thesis possible, thank you.

Contributions of Authors

The majority of experimental work in this thesis was designed and performed by the author under the supervision of Dr. Elias Georges. The contribution of the co-authors added significantly to the quality of each study, and in some cases, the studies would not have been possible without their input. In the first manuscript (chapter 2), several of the experiments shown in figures 1 to 5 were performed by Maximilian C. Lincoln, a previous student in Dr. Elias Georges' laboratory. In the second manuscript (chapter 3), Dr. Roni Daoud, a previous student of Dr. Georges', played a significant role in the synthesis of IAAGSH. In the second and third manuscript (chapters 2 and 3), the purified plasma membranes containing MRP1-variants with hemagglutinin epitopes were produced by Dr. Jie Cai from the laboratory of Dr. Philippe Gros in the department of Biochemistry, McGill University. The transport studies in the third manuscript (chapter 3) were performed with help from Mara Leimanis. The western blots in figure 5 of chapter 3 were performed with significant help from Nicolas Patocka. Finally, Christiene Trudeau and Rémi-Martin Laberge translated the general abstract into French.

Statement of Originality

Joel Karwatsky, the PhDcandidate, contributed the following original material and original scholarship in the domain of biochemical cancer research.

Manuscript 1 (chapter 2). Karwatsky J., Lincoln M.C., Georges E. 2003. A Mechanism for P-Glycoprotein-Mediated Apoptosis As Revealed by Verapamil Hypersensitivity. *Biochemistry, Vol.42,* pages 12163-12173.

The aim of this manuscript was to investigate the phenomenon of collateral sensitivity to verapamil in P-glycoprotein 1 (P-gp1) expressing cells. This study showed for the first time that cell mortality in CHO cells that over-express P-gp1 is mediated by apoptosis. Beyond this, the mechanism linking P-gp1 activity and expression to apoptosis was also elucidated. The key biochemical link between P-gp1 activity and apoptosis was the activation of P-gp1 ATPase by low concentrations of verapamil, an effect that correlated with the production of reactive oxygen species and apoptosis.

Manuscript 2 (chapter 3). Karwatsky J., Daoud R, Cai J., Gros P., Georges E. 2003. Binding of a Photoaffinity Analog of Glutathione to MRP1 (ABCC1) within Two Cytoplasmic Regions (L0 and L1) as well as Transmembrane Domains 10-11 and 16-17. *Biochemistry, Vol.42,* pages 3286-3294.

In order to understand the interaction between MRP1 and its natural substrate, glutathione (GSH), a novel photoreactive analogue was synthesised, IAAGSH. Using this compound, it was found that IAAGSH interacts with MRP1 with high specificity. In addition, binding competition studies showed that the degree of photoaffinity labelling correlates with the transport activity of MRP1. This was made evident by the ability of verapamil and vincristine to enhance labelling of MRP1 in much the same way that they

enhance GSH transport by MRP1. IAAGSH interacts with two drug binding sites found in transmembrane (TM) regions 10-11 and 16-17. Furthermore, two novel cytoplasmic photoaffinity labelling regions were identified in linker domains L0 and L1 and may correspond to GSH-specific binding sites.

Manuscript 3 (chapter 4). Karwatsky J., Leimanis M., Cai J., Gros P., Georges E. 2005. The Leucotriene C_4 Binding Sites in Multidrug Resistance Protein 1 (ABCC1) Include the First Membrane Multiple Spanning Domain. *Biochemistry, Vol 44, pages 340-351.*

A novel photoreactive analogue of leucotriene C_4 (LTC_4) was synthesised to investigate the interactions between MRP1 and its primary physiological substrate. The photoreactive analogue, $IAALTC_4$, was used to determine precise binding sites within MRP1. To this effect, it was found that LTC_4 interacts with known drug binding sites in TM 10-11 and 16-17. In addition to these regions, $IAALTC_4$ photoaffinity labelled the first membrane multiple spanning domain in MRP1, a region that was previously not known to play a role in substrate binding and may form part of a LTC_4-specific binding site. Finally, TM 12 was efficiently labelled, indicating that it is in close proximity to TM 16-17 of the properly folded protein.

List of Figures

Appendix 1

Common Abbreviations

agosterol A	AG-A
aryl azido-glutathione	AAGSH
aryl azido-leucotriene C_4	$AALTC_4$
[^{125}I]11-azidophenyl agosterol A	[^{125}I]azidoAG-A
ATP-binding cassette	ABC
Breast Cancer Resistant Protein	BCRP1 (ABCG2)
17β-estradiol 17-(β-D-glucuronide)	$E_2$17βG
[^{3}H]estrone 3-sulfate	[^{3}H]E_1SO_4
glutathione (oxidised)	GSSG
glutathione (reduced)	GSH
hemagglutinin A	HA
[^{125}I]iodoaryl azido-rhodamine 123	IAARh123
[^{125}I]iodoaryl azido-leucotriene C_4	$IAALTC_4$
[^{125}I]iodoaryl azido-glutathione	IAAGSH
leukotriene C_4	LTC_4
linker domain 0 or 1	L0 or L1
membrane spanning domains	MSD
monoclonal antibodies	mAbs
multidrug resistance	MDR
multidrug resistance protein 1	MRP1 (ABCC1)
N-(hydrocinchonidin-8'-yl)-4-azido-2-hydroxybenamide	IACI
N-{4-[1-hydroxy-2-(dibutyl-amino)ethyl] quinolin-8-yl}-4-azidosalicylamide	IAAQ
nucleotide binding domain	NBD
P-glycoprotein-1 (class I)	P-gp1 (ABCB1)
rhodamine 123	Rh123
transmembrane	TM

Statement from Thesis Office

In accordance with the "Guidelines concerning thesis preparation" of the Faculty of Graduate and Postdoctoral Studies, manuscript which have been published have been incorporated in this thesis. The following is quoted directly from the guidelines:

"Candidates have the option of including, as part of the thesis, the text of one or more papers submitted, or to be submitted, for publication, or the clearly-duplicated text (not the reprints) of one or more published papers. These texts must conform to the "Guidelines for Thesis Preparation" with respect to font size, line spacing and margin sizes and must be bound together as an integral part of the thesis."

"The thesis must be more than a collection of manuscripts. All components must be integrated into a cohesive unit with a logical progression from one chapter to the next. In order to ensure that the thesis has continuity, connecting texts that provide logical bridges preceding and following each manuscript are mandatory."

"The thesis must conform to all other requirements of the "Guidelines for Thesis Preparation" in addition to the manuscripts. The thesis must include the following: (1) a table of contents; (2) a brief abstract in both English and French; (3) an introduction which clearly states the rational and objectives of the research; (4) a comprehensive review of the literature (in addition to that covered in the introduction to each paper); (5) a final conclusion and summary; (6) a thorough bibliography; (7) Appendix containing an ethics certificate in the case of research involving human or animal subjects, microorganisms, living cells, other biohazards and/or radioactive material."

"As manuscripts for publication are frequently very concise documents, where appropriate, additional material must be provided (e.g., in appendices) in sufficient detail to allow a clear and precise judgment to be made of the importance and originality of the research reported in the thesis."

"In general, when co-authored papers are included in a thesis the candidate must have made a substantial contribution to all papers included in the thesis. In addition, the candidate is required to make an explicit statement in the thesis as to who contributed to such work and to what extent. This statement should appear in a single section entitled "Contributions of Authors" as a preface to the thesis. The supervisor must attest to the accuracy of this statement at the doctoral oral defence. Since the task of the examiners is made more difficult in these cases, it is in the candidate's interest to clearly specify the responsibilities of all the authors of the co-authored papers."

General Introduction

The family of ABC (ATP-binding cassette) transporters is one of the largest protein families yet identified. ABC transporters play a significant role in cell physiology due to their ability to move molecules across cell membranes against a concentration gradient. The cell membrane separates the external environment from the cytoplasm. Without it, it would not be possible to maintain a different chemical composition in their cytoplasm compared to the external environment in all living organisms. The cell's ability to control the chemical makeup of its cytoplasm is crucial for regulating the basic biochemical processes needed for survival. A multitude of membrane bound proteins are used to selectively move molecules across the membrane. Many of these proteins permit passive (energy independent) transport of molecules, while the movement of molecules against a concentration gradient requires active (energy dependent) transport. The ABC transporters are the largest and most diverse group of active transport proteins. They transport a wide variety of molecules from one side of the membrane to the other using ATP as a source of energy. Although the majority of the proteins transport a single unique substrate, some possess the ability to transport a variety of different substrates. In fact, some ABC transporters can transport structurally and functionally different toxic drugs out of living cells, thereby conferring multidrug resistance. It is this feature that has given prominence to ABC transporters in the field of cancer treatment with small molecule drugs.

Cancer is a disease that is present in all higher organisms and has accompanied human civilization for countless generations [1]. The pictures and writings of many ancient civilisations have described cancers, and bone cancers; the presence of these cancers was confirmed upon examination of Egyptian mummies. Sir Percival Pott initiated one of the earliest scientific examinations of cancer in 1775. He found that men who worked as chimney sweeps as children had a high rate of death due to cancer of the scrotum. This finding was significant because it demonstrated that a causative agent or carcinogen was

responsible for disease development. Furthermore, this early work demonstrated the extended latent period between exposures to the carcinogen and cancer development [1].

One of the most effective means of treating cancer is through the use of toxic drugs, or chemotherapy. Unfortunately, tumour cells can and do develop resistance to some 50 different anti-cancer drugs. Several mechanisms have been identified that confer resistance to anti-cancer drugs. One of the most extensively studied mechanisms of drug resistance involves the transport of drugs out of cancer cells, a process that is caused by certain ABC transporters. The most studied, and best characterized of these are the multidrug transporters P-glycoprotein 1 (P-gp1 or ABCB1) [2] and Multidrug Resistance Protein 1 (MRP1 or ABCC1) [3]. P-gp1 and MRP1 function as broad-specificity drug pumps that bind and transport drugs [4]. Both proteins confer resistance to many of the same anti-cancer drugs including: epipodophyllotoxins, vinca alkaloids, and certain anthracyclines [5-7]. It is surprising that these ABC transporters have such similar substrates since they share only 15% amino acid sequence identity [3]. In addition to the similarity in substrates, a number of differences do exist. For example MRP1 transports drugs that are conjugated to: glutathione, sulphate, or glucuronidate [8-10], while these conjugated organic anions are poor substrates for P-gp1.

Although much emphasis has been placed on the ability of P-gp1 and MRP1 to cause multidrug resistance in tumour cells, both proteins also have important roles in normal cells. For example, several potential physiological substrates of MRP1 have been identified, these include: conjugated bile salts, prostaglandin A_2, glutathione (GSH), and leukotriene C_4 (LTC_4) [8,9,11,12]. These molecules play diverse roles within a healthy body. LTC_4 participates in several normal processes in the lungs, and GSH is a crucial component of detoxifying pathways in mammalian cells. Despite the role of MRP1 in regulating the movement of these important physiological molecules, the majority of work published on MRP1 has focused on its interaction with anti-cancer drugs; knowledge of the way MRP1 interacts with its natural physiological substrates has been lacking. The work presented within the current thesis addresses this issue by examining the interactions between MRP1 and its natural physiological substrates LTC_4 and GSH.

Unlike MRP1, the ABC transporter P-gp1 does not possess any known physiological substrates. In fact, P-gp1 has probably evolved to fulfill the role of protecting

organs from a wide variety of natural toxins found in the environment. This protective role against toxins is supported by the observation that P-gp1 is found within the body at sites that protect sensitive organs such as the brain and testes. Furthermore, P-gp1 has been implicated in the transport of lipids [13,14]. Although this classical protective function of P-gp1 has been well studied, its biochemical effects on cells may extend beyond the transport of antibiotics. In fact, since its discovery as a multidrug transporter, an interesting cellular artefact has been associated with P-gp1 expression. Along with causing multidrug resistance, the presence of P-gp1 often increases the sensitivity of cells to low doses of a relatively non-toxic compound, verapamil. This characteristic is called collateral sensitivity and has been widely reported in cells that contain P-gp1. As of yet, no satisfactory explanation for this effect has been presented.

Briefly, the first chapter is an introductory review of (1) multidrug resistance in cancer, (2) substrate binding in P-gp1 and MRP1, and (3) the mechanism of apoptotic cell death. The second chapter includes the first study, and describes the mechanism of collateral sensitivity to verapamil, detailing how P-gp1 expressing cells die by apoptosis. Chapters three and four detail the interactions of MRP1 with its natural substrates GSH and LTC_4, respectively. In addition, the locations of binding for both compounds are presented.

References

1. Tannock, I., and Hill, R. P. (1998) *The basic science of oncology*, 3rd Ed., McGraw-Hill Health Professions Division, New York
2. Ling, V. (1975) *Can J Genet Cytol* **17**(4), 503-515
3. Cole, S. P., Bhardwaj, G., Gerlach, J. H., Mackie, J. E., Grant, C. E., Almquist, K. C., Stewart, A. J., Kurz, E. U., Duncan, A. M., and Deeley, R. G. (1992) *Science* **258**(5088), 1650-1654
4. Germann, U. A. (1996) *Eur J Cancer* **32A**(6), 927-944
5. Cole, S. P., Sparks, K. E., Fraser, K., Loe, D. W., Grant, C. E., Wilson, G. M., and Deeley, R. G. (1994) *Cancer Res* **54**(22), 5902-5910
6. Gao, M., Yamazaki, M., Loe, D. W., Westlake, C. J., Grant, C. E., Cole, S. P., and Deeley, R. G. (1998) *J Biol Chem* **273**(17), 10733-10740

7. Hooijberg, J. H., Broxterman, H. J., Kool, M., Assaraf, Y. G., Peters, G. J., Noordhuis, P., Scheper, R. J., Borst, P., Pinedo, H. M., and Jansen, G. (1999) *Cancer Res* **59**(11), 2532-2535

8. Evers, R., Cnubben, N. H., Wijnholds, J., van Deemter, L., van Bladeren, P. J., and Borst, P. (1997) *FEBS Lett* **419**(1), 112-116

9. Jedlitschky, G., Leier, I., Buchholz, U., Barnouin, K., Kurz, G., and Keppler, D. (1996) *Cancer Res* **56**(5), 988-994

10. Loe, D. W., Stewart, R. K., Massey, T. E., Deeley, R. G., and Cole, S. P. (1997) *Mol Pharmacol* **51**(6), 1034-1041

11. Leier, I., Jedlitschky, G., Buchholz, U., Center, M., Cole, S. P., Deeley, R. G., and Keppler, D. (1996) *Biochem J* **314 (Pt 2)**, 433-437

12. Leier, I., Jedlitschky, G., Buchholz, U., Cole, S. P., Deeley, R. G., and Keppler, D. (1994) *J Biol Chem* **269**(45), 27807-27810

13. Bosch, I., Dunussi-Joannopoulos, K., Wu, R. L., Furlong, S. T., and Croop, J. (1997) *Biochemistry* **36**(19), 5685-5694

14. van Helvoort, A., Smith, A. J., Sprong, H., Fritzsche, I., Schinkel, A. H., Borst, P., and van Meer, G. (1996) *Cell* **87**(3), 507-517

Chapter 1

Literature review

ABC TRANSPORTERS AND MULTIDRUG RESISTANCE

"The question was, which would the chemo kill first: the cancer or me?"

Lance Armstrong

ABC Transporters

Members of the ABC protein family have been found in all cells from bacteria to plants to man. The number of different ABC proteins, or ABC transporters, is well represented in these organisms; for example, the *Escherichia coli* chromosome encodes approximately 70 ABC transporters, making up 4.8% of the genome [1]. The yeast genome encodes 30 ABC transporters [2], and 48 are found in the human genome [3]. The history of ABC proteins in scientific research began unknowingly in the field of genetics. *Drosophila* eye colour, which is controlled by an ABC transporter, was being used as a model system for genetic research. It wasn't until the 1970s that ABC transporters were formally identified and characterised in bacteria. Some of the initial work began with studies on nutrient uptake in *E. coli* and *Salmonella typhimurium*. It was observed that these species have multiple independent transport systems for nutrients, of which one class was fuelled by ATP hydrolysis [4]. In 1982, the first complete genetic sequence of the ABC histidine transporter (HisQ, M, and P) of *S. typhimurium*, was published [5]. Soon after, the sequence of the *E. coli* maltose transporter (MalK) was also determined. Both MalK and HisP were found to be similar, suggesting that they may have evolved from a common ancestor [6]. Sequence analysis of other homologous proteins showed that each of these proteins contained a consensus nucleotide binding motif [7] termed the "Walker" A and B motifs [8]. These domains use the energy derived from ATP hydrolysis to transport nutrients across biological membranes [9,10]. It became apparent that proteins containing

these ATP-binding subunits make up a large family of proteins with a distinct organisation of four core domains: two transmembrane domains (TMDs) and two nucleotide binding domains (NBDs). The amino acid sequence of the ABC domain contains three major conserved regions which include the Walker A and B motifs (commonly found in ATPases), in addition to an ABC signature motif. The ABC signature motif, also known as the linker peptide, usually begins with the amino acid sequence Leu-Ser-Gly-Gly- [11].

Although much of the initial biochemical characterisation of ABC transporters was derived from bacterial proteins, the eventual discovery of mammalian ABC proteins contributed significantly to the field. The first eukaryotic ABC transporter to be discovered was the human P-glycoprotein (P-gp1 or ABCB1). It was first identified by its ability to confer a multidrug resistance phenotype onto cancer cells [12,13]. P-gp1 was subsequently sequenced and characterised more thoroughly by the groups of Victor Ling, Michael Gottesman, Phillipe Gros, and Igor Roninson [14-16]. This work determined that P-gp1 *exports* its substrates out of cells unlike the *import* of nutrients by many bacterial transporters. Furthermore, P-gp1 was found to interact with its substrates directly, whereas the bacterial transporters depend on periplasmic binding proteins to recognise their substrates.

To understand the mechanism by which ABC transporters move molecules across biological membranes, structural data is needed. Obtaining this information has proven to be very challenging. High resolution three dimensional crystal structures would be invaluable; unfortunately they are difficult to obtain for ABC transporters. The difficulties stem from problems in both the over-expression and purification of these membrane-bound proteins. When over-expressed, ABC transporters are often toxic to cells or are improperly folded. Purification of these proteins can pose even greater problems since the lipid environment within the plasma membrane is important for integral membrane proteins to fold correctly. During the protein purification process used to obtain crystal structures, the natural lipids must be removed and then replaced with detergent, a process that may irreversibly denature the proteins. Given these difficulties, some structural data has been obtained; single-particle analyses and electron crystallography have produced: low- to medium-resolution structures for P-gp1[17-20], the

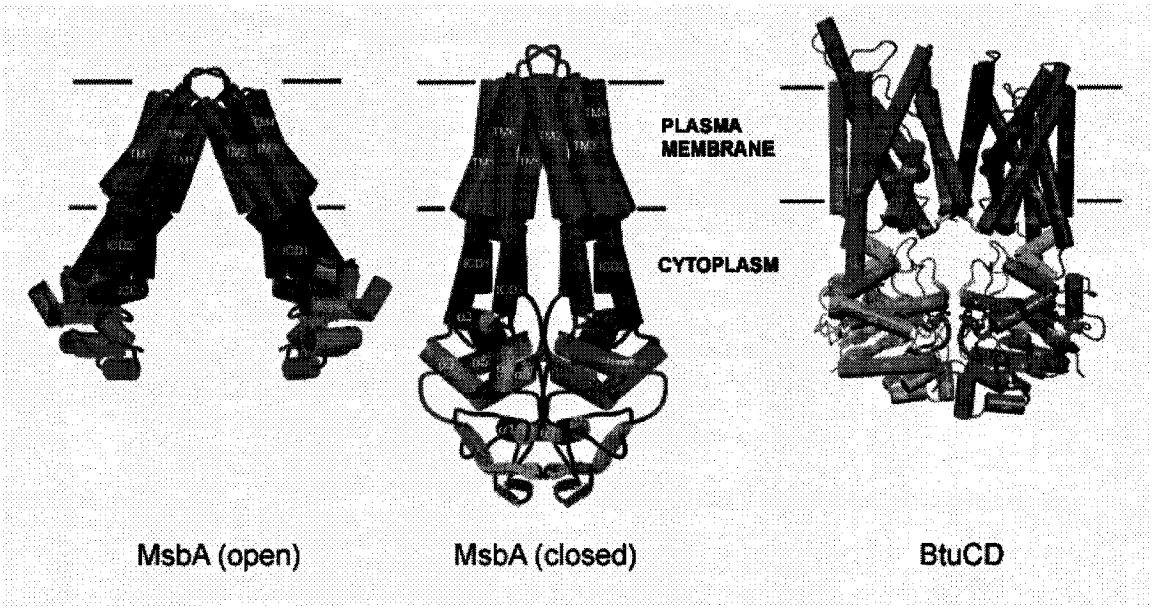

Figure 1

The structure of the lipid flippase MsbA by x-ray crystallography from: *Escherichia coli* in the open configuration (4.5 angstroms resolution), *Vibrio cholera* in the closed configuration (3.8 angstrom resolution), and *E. coli* BtuCD transporter that mediates vitamin B12 (3.2 angstrom resolution). This image was modified from previously published figures [21-23].

peptide transporter TAP (TAP1/TAP2 or ABCB2/ABCB3) [24], a yeast multidrug transporter Pdr5p [25], and the multidrug transport protein 1 (MRP1 or ABCC1) [26]. Interestingly, the structures for P-gp1 showed large scale conformational changes upon nucleotide binding, indicating that ATP hydrolysis is coupled to transport. In comparison to eukaryotic transporters, higher resolution structures have been published for two bacterial ABC transporters, MsbA and BtuCD [21-23]. Figure 1 shows a side view of the structure of these proteins derived from the X-ray crystallography data. There is no significant structural homology between the transmembrane regions of these two proteins because BtuCD has twenty membrane spanning α-helices as opposed to twelve in MsbA. Indeed, there is low homology in the primary sequence of the transmembrane domain segments within the family ABC proteins in general. Furthermore, the functions of ABC transporters vary widely. These factors point to the possibility of varied arrangements and mechanisms of transport among ABC proteins, making it difficult to generalise about the structure of these proteins, however this early crystallography work has given some insight into the 3-dimensional structure within a very diverse family of proteins

Remarkably, there is an ABC transporter for almost any class of molecule: small molecules, large molecules, charged molecules, hydrophobic molecules, inorganic ions, sugars, amino acids, proteins, lipids, and complex polysaccharides [27]. Most ABC transporters are highly substrate specific, but some ABC proteins such as P-gp1 and MRP1 can transport a wide variety of molecules. These proteins have the ability to transport a diverse assortment of chemotherapeutic drugs; a trait that has given P-gp1 and MRP1 an important role in cancer drug resistance. Over-expression of these proteins prevents toxic drugs from entering cancer cells, thereby causing multidrug resistance and rendering treatment ineffective. Therefore, understanding the biology of multidrug transport proteins has become important in clinical oncology.

Cancer, Chemotherapy, and Multidrug Resistance

Tumours grow due to the proliferation of their cells, and these cells may metastasize when malignant cells spread from primary tumours to other sites. Under normal conditions, the body of a healthy animal is composed of a diverse assortment of cells that reproduce by mitosis and are organised into collaborative assemblies of tissues and organs. In many ways the relationship between cells is similar to an ecosystem, with processes such as: cell births, deaths, habitats, territorial limitations, and the maintenance of population sizes. To maintain a healthy body, many somatic (differentiated) cells are committed to die at a specific stage of their life, or after a certain number of cellular divisions. If needed at a later date, these cells are then renewed by specific progenitor stem cells. Thus, the turnover and renewal of healthy cell populations occurs constantly in the development and maintenance of tissues. For example in the blood system, billions of neutrophils die every day and are regenerated by haemopoietic stem cells. Cancer develops when this highly regulated process of cell growth is altered, thereby producing a population of cells without regulated cell division or that are not terminated at the appropriate time. Cancer cells are defined by: (1) their ability to reproduce in defiance of normal restraints, and (2) invade and colonise regions of the body normally reserved for other cell types. Furthermore, these abnormal traits are heritable, passing from one generation to the next. Eventually, these cells can become malignant when they invade

surrounding tissues and form metastases. This may result in the end of the whole cellular society, leading to the death of the entire organism [28].

Chemotherapy is commonly used to treat malignant tumours in cancer patients. The first use of chemotherapy can be traced to the discovery of nitrogen mustard as a treatment for non-Hodgkin's lymphoma in 1942. Its usage was based on autopsy findings from soldiers dying of exposure to sulphur mustard gas during the First World War. These fallen soldiers had lymphoid hypoplasia and myelosuppression. Given these findings, Louis Goodman, Alfred Gilman and colleagues reasoned that controlled doses of a similar agent might cause regression of a lymphatic tumour. Indeed, tumours regressed in the first patients treated with nitrogen mustard, although the disease progressed again after a few weeks, [29]. Since then, great leaps have been made in cancer chemotherapy, and today drugs such as paclitaxel (Taxol) and imatinib mesylate (Gleevec) have reduced morbidity and mortality in many cancer patients.

Ideally, treatment of cancer with chemotherapeutic drugs leads to a cure or long-term remission with few side effects. It is believed that toxic drugs accomplish this by targeting and killing a subpopulation of tumour stem cells which have a very large potential for cell proliferation. Stem cells may constitute only a small proportion of a cancer but are the major contributors to a cancer's uncontrolled proliferation. Thus, many of the anti-cancer drugs exploit the differences in metabolism and the division rate between proliferating neoplastic cells and normal differentiated cells. For example, the anti-cancer drug vincristine inhibits microtubule polymerisation, thereby inhibiting the formation of a mitotic spindle during mitosis and preventing cell division. The drug methotrexate inhibits the metabolic pathway used to produce a crucial nucleoside precursor, dTMP. Without dTMP, a cell's ability to synthesise and replicate its DNA is inhibited, preventing cell division [30]. Unfortunately, the toxicity of these drugs can affect normal tissues, thereby limiting the dose and frequency of drug administration. Normal tissues with a high cellular proliferation are more sensitive to this collateral toxicity. The tissues that are most often affected include: bone marrow, intestinal mucosa, hair follicles, and gonads. Nausea, vomiting, and carcinogenesis are some of the common side effects. Severe toxicity leading to patient death can also be caused by anti-cancer drugs. Fortunately, many of these side effects have been avoided with newer generation

drugs. These compounds target signalling networks that regulate proliferation and survival. Often these networks are radically altered in cancer cells and allow for 'targeted therapy' against cancers. Some examples of targeted drugs include Gleevec, which inhibits of specific kinases that are active in chronic myeloid leukaemia (CML) and certain other cancers.

Chemotherapy is used as the primary treatment for several types of malignancies such as lymphoma, acute leukemia in children, and testicular cancer in men. Chemotherapy is also used for palliative treatment in advanced cancers and as an adjuvant therapy along-side surgery and radiotherapy. Unfortunately, many tumour cells are resistant, or develop resistance to a variety of different anti-cancer drugs. Resistance to anti-cancer drugs may be due to intrinsic or acquired drug resistance. Intrinsic resistance is observed in several cancers that have an inherently low probability of responding to chemotherapy such as colon cancer and non small-cell lung cancer. In these cancers, resistance is present prior to drug exposure or may emerge after brief exposure to low concentrations of drugs. Alternatively, some cancers may respond to treatment, but eventually acquire resistance. This form of drug resistance is seen in tumours such as breast cancer, ovarian cancer, and small-cell lung cancer. Acquired resistance probably arises from the selection of drug resistant subpopulations in tumours. Studies using *in vitro* tumour cell lines have found that under controlled selection conditions, malignant cell lines can acquire resistance by repeated exposure to increasing concentrations of anti-cancer drugs. Although several mechanisms of acquired drug resistance have been observed in laboratory cell lines, it is unclear if they are relevant within *in vivo* models and clinical situations [30]. In an early study of acquired resistance Ling observed that a colchicine-resistant mutant of Chinese hamster ovary cells displayed cross-resistance to a variety of unrelated compounds, a phenotype termed multidrug resistance (MDR) [12]. Later, the genes responsible for the MDR phenotype were cloned from human, hamster, and mouse cells [31-33]. The human gene, *mdr1*, associated with MDR encodes the ABC transporter P-gp1, a membrane glycoprotein with a molecular weight of 170 kDa.

To date, several mechanisms have been identified that may confer MDR to anti-cancer drugs: (1) the drug transport mechanisms due to ABC transporters such as P-gp1

[13], the Multidrug Resistance Protein 1 (MRP1 or ABCC1) [34], and the Breast Cancer Resistant Protein (BCRP1 or ABCG2) [35,36], (2) resistance to apoptosis caused by non-functional p53 [37,38] or over-expressed Bcl-2 [39], (3) decreased activity of topoisomerase II, which allows for conformational changes in DNA [40,41], (4) DNA repair mechanisms mediated by O^6-alkylguanine DNA alkyltransferase [42], and (5) drug detoxification mechanisms such as Glutathione S-transferases [43] and Cytochrome P450 mixed function oxidases [44]. The focus of the following sections will be on P-pg1 and MRP1 as mediators of MDR.

ABC transporters such as P-gp1 and MRP1 are found in cell plasma membranes. These proteins cause MDR by pumping anti-cancer drugs out of a cell preventing the accumulation of drugs to toxic levels. Many of the substrates for these transporters are either natural product drugs or their derivatives, such as: anthracyclines (doxorubicin, daunorubicin, epirubicin), vinca alkaloids (vincristine, vinblastine), epipodophyllotoxins (etoposide, teniposide), and paclitaxel (Taxol). These are compounds that were isolated from plants, fungi, or bacteria, and include chemically modified agents that were derived from the original natural products. The mechanism of action of these drugs varies greatly. Within this category of anti-cancer drugs are compounds that interfere with topoisomerase II activity (e.g. doxorubicin and etoposide); that inhibit microtubule polymerisation (e.g. vincristine, etoposide); or inhibit microtubule depolymerisation (e.g. Taxol) [30].

P-Glycoprotein 1 (P-gp1 or ABCB1)

One of the first steps towards determining how P-gp1 functions is to create a model of P-gp1 based on its known amino acid sequence. The human P-gp1 is composed of 1280 amino acids. Structurally, P-gp1 can be regarded as a molecule with two closely related halves. Each half consists of a membrane spanning domain (MSD) made up of six transmembrane (TM) α-helices and one nucleotide binding domain (NBD) that hydrolyses ATP [45]. In total, P-gp1 has twelve TM α-helices which are divided into MSD1 and MSD2, and two NBDs (NBD1 and NBD2). Each half of P-gp1 contains one MSD and one NBD; each half is connected by a highly charged intracellular linker region (L1). The overall topology of P-gp1 is: MSD1-NBD1-L1-MSD2-NBD2, with both the

N- and C-termini located within the cytoplasm [18]. Studies using antibodies directed against defined extracellular epitopes have been consistent with this model [46]. In humans, P-gp1 has two family members that are not involved in MDR, these include MDR3 or P-gp3 (ABCB4) and the Sister of P-glycoprotein (ABCB11 or the bile salt exporter protein, BSEP), these proteins share 75% and 50% sequence identity to P-gp1, respectively. The physiological substrate of MDR3 is phosphatidylcholine, which is indispensable in normal bile formation. MDR3 is located in the liver and acts as a flipase, transporting phosphatidylcholine from the inner to the outer leaflet of the plasma membrane [47,48]. A definite role for MDR3 in drug resistance has not been established although it transports some anti-cancer drugs at lower rates than P-gp1 [49]. The Sister of P-glycoprotein is involved with the export of bile salts through the liver canicular membrane [50]. Thus, P-gp1 remains the only family member with an exceptional aptitude to cause multidrug resistance.

By measuring drug transport into plasma membrane vesicles derived from multidrug resistant cell lines, it has been shown that drug efflux requires ATP hydrolysis [51]. The ATPase activity of P-gp1-rich plasma membranes can also be measured by measuring the conversion of ATP to ADP in the presence of drug substrates [52]. Unlike other ATPase-driven transporters such as the Na^+K^+- and Ca^{2+}-ATPases, P-gp1 exhibits a high level of constitutive ATPase activity in the absence of any substrates. This is in contrast with other ATPases that only hydrolyse ATP when a substrate is presented to the protein [53-55]. The high basal ATPase activity of P-gp1 has been attributed to transport of endogenous lipids or hydrophobic peptides [56,57]. It is also possible that uncoupled ATPase activity in the absence of drug substrates contributes to its basal activity. Inhibitors of other ion-translocating ATPases such as ouabain and sodium azide do not inhibit P-gp1 ATPase, whereas vanadate does inhibit activity but at higher concentrations than are required for other ATPases [58]. Perhaps this is because P-gp1 ATPase has an unusually high *Km*, indicating that it has a very low affinity for ATP as compared to other translocating ATPases [59-61].

Several systems have been used to determine how ATP hydrolysis, drug binding, and drug transport are related in the P-gp1 catalytic cycle. One approach examined the ability of various drug substrates to bind P-gp1 in the presence of an ATP analog (8-

azido-[α^{32}P]-ATP) and vanadate trapping of ADP [45,62]. This work found that two rounds of ATP hydrolysis must occur to complete the transport cycle. Furthermore, both NBDs must be functional for ATP hydrolysis to occur in P-gp1 [63], although the two ATP binding domains do not hydrolyse ATP simultaneously, each domain alternates ATP hydrolysis [64]. Given this work and many other studies, the current model predicts that substrates interact with P-gp1 at a high affinity binding site followed by the hydrolysis of one ATP molecule. ATP hydrolysis shifts the substrate into a low affinity binding site on the protein whereby it is released into the outer plasma membrane leaflet or the extracellular environment [45]. Hydrolysis of a second ATP molecule at the other NBD then resets the conformation of P-gp1 to accept a new substrate [65,66]. With numerous rounds of ATP hydrolysis and drug transport, P-gp1 proteins can significantly reduce the cellular concentration of anti-cancer drugs.

One of the most interesting features of P-gp1 is its ability to recognise and transport a wide variety of substrates while still displaying a greater affinity to certain compounds. The interactions between P-gp1 and its substrates obviously do not adhere to the classic "lock and key" or "induced fit" models. These classic models describe the interactions of enzymes or transporters with hydrophilic substrates, whereas a large number of P-gp1 substrates are hydrophobic or amphiphilic. Consequently, it has been proposed that the multidrug binding site may be made up of a simple hydrophobic pocket which can bind non-specifically to hydrophobic or amphiphilic molecules [67]. This possibility has largely been dismissed because there tends to be large differences in the binding affinities of individual substrates. In fact there appears to be a high binding affinity for some molecules and low affinity for others. Thus, the multidrug binding site in P-gp1 cannot be viewed as non-specific hydrophobic pocket, nor do classic binding models apply. The TM regions are believed to contain the necessary sequences to bind neutral or positively charged hydrophobic drugs because these substrates interact with P-gp1 within the lipid bilayer [58]. The list of P-pg1 substrates is very large and includes many categories of molecules: anti-cancer drugs (e.g. anthracyclines, vinca alkaloids, epipodophyllotoxins, paclitaxel, actinomycin D, and topotecan), cyclic and linear peptides (e.g. gramicidin D and valinomycin), HIV protease inhibitors (e.g. Ritonavir, Indinavir, and Saquinavir), and many others (colchicines, ethidium bromide, Hoechst

33342, and Rhodamine 123) [68]. Some of these compounds were identified as substrates by *in vitro* studies, while their role as P-gp1 substrates *in vivo* remains unclear.

Based on this broad substrate list and several studies, it has been suggested that the principal physiological role of P-gp1 is to protect organisms from toxic substances. P-gp1 expression is found in regions of the body that are involved in drug excretion and at toxin sensitive "sanctuary sites" including: the epithelium of the gastrointestinal tract, the renal proximal tubule, the canicular surface of hepatocytes, and the blood brain barrier [69,70]. P-gp1 knockout mice are exceptionally sensitive to P-gp1 substrates, however these mice are otherwise healthy and reproduce normally [71-73]. Therefore, although P-gp1 is necessary for the excretion of toxic substrates, cells do not require P-gp1 for basic survival processes.

Clinical Importance of P-gp1

Having established that P-gp1 causes multidrug resistance *in vitro*, it became important to examine its effect on clinical treatment in cancer patients. To assess the role P-gp1 plays in cancer treatment, the presence of P-gp1 in tumours must be established, a task that has not been without difficulty. The methods to detect P-gp1 been problematic, making it difficult to confirm its' presence in cancers. Protein expression in clinical samples has primarily been documented by reverse transcription-polymerase chain reaction (RT-PCR) to identify mRNA transcripts, and by immunohistochemistry (IHC) to directly visualise protein levels. Difficulties with these techniques such as contamination of tumour tissue for RT-PCR, and poor sensitivity and specificity with IHC have led to large variability between studies and as a result complicated data analysis. Yet despite these problems, some valid data has appeared, especially with acute myelogenous leukemia (AML). Several clinical studies show that P-gp1 is expressed in about 30 % of AML patients at the time of diagnosis, and increases to over 50 % at the time of relapse [74-76]. A variety of clinical trials have also attempted to determine if P-gp1 expression in AML patients results in a poor clinical outcome. Indeed, several trials report that a higher level of P-gp1 expression is correlated to a reduced complete response rate and overall survival [77-80]. Studies in solid tumours have been more variable. For example, detection rates in breast cancer vary from 0 % to 71 % as measured by IHC using the same antibody [81,82]! Yet P-

gp1 does appear to be more highly expressed in relapsed breast, ovarian, and lung cancer [27]. In addition to varying methods of detection, the inconsistencies in solid tumours appear to be due to patient therapeutic history, the type of tumour, and the tumour grade. Despite the difficulties in determining the incidence and significance of P-gp1 in solid tumours, it does appear to play an important role in clinical oncology.

Inhibition of P-gp1

The pharmacological reversal or inhibition of MDR was first reported in 1981 by Tsuruo and coworkers [83]. They showed that two clinical drugs, verapamil and trifluoperazine, were capable of improving the anti-neoplastic activity of vincristine in a murine leukaemia cell line. Since then, a diverse group of compounds have been identified that are capable of sensitising resistant cells to anti-cancer drugs. These have been termed chemosensitisers or reversing agents. The method by which chemosensitisers enhance the efficacy of anti-cancer drugs is by directly inhibiting the drug efflux activity of P-gp1. The molecular basis of chemosensitisation is not well understood but two general mechanisms are probably responsible, these are based on either competitive or non-competitive inhibition P-gp1 transport activity. Competitive inhibition of P-gp1 occurs when the chemosensitiser reduces the toxicity of a drug by directly competing for the drug binding site. If the inhibitor occupies all of the drug binding sites, then the anti-cancer drugs will not interact with P-gp1 or be transported. Photoreactive verapamil analogs have been demonstrated to bind specifically to the protein; this interaction could be inhibited in a dose dependent manner by verapamil and vinblastine [84,85]. This suggests that the mechanism of inhibition is through competition for drug binding sites. Alternatively, some reversing agents of P-gp1 exert their effect through non-competitive inhibition. A non-competitive inhibitor binds outside the multidrug site and causes an allosteric change in the conformation of P-gp1. The structural change reduces the affinity of substrates for the multidrug binding site, thereby preventing interactions of anti-cancer drugs with P-gp1 and inhibiting transport. For instance, P-gp1 transport of vinblastine is allostrerically inhibited by azidopine, a photoactive dihydropyridine calcium channel blocker [86].

Effective chemosensitisers would be very useful in preventing P-gp1 mediated drug resistance in cancer patients. For this reason much effort has been directed towards finding effective P-gp1 reversing agents. Early work lead to the characterisation of the "first generation" reversing agents such as: the calcium channel blocker verapamil, other calcium channel blockers, calmodulin inhibitors, cardiovascular drugs, hormonal steroidal derivatives, antibiotics, and cyclosporins [58,87-89]. These compounds were not designed as MDR inhibitors and had previously been used for other pharmacological applications. Although they showed promise *in vitro*, they fell short of preventing clinical drug resistance. These compounds were not very potent and needed to be used at high concentrations (micromolar) that were prohibitively toxic to patients [90]; this created a need for more specific and potent agents. The newly developed second generation agents were typically analogues of the first generation molecules. Among these were R-verapamil, VX-710 (biricodar), and PSC 833 (valspodar). A significant number of studies tested PSC 833 in clinical settings. The most notable finding was the need to reduce the dose of the anti-cancer drugs used in combination with PSC 833 because of unforeseen toxicity [91,92]. Initially, it was thought that reductions in the concentration of anti-cancer drugs would still be effective because of the longer drug half-life in the body and longer exposure time. This assumption proved to be wrong. In actuality, the dose reductions with PSC 833 led to under-treatment, indicating that the original high concentration of anti-cancer drugs were probably the most effective against tumours [90,93]. Moreover, undue toxicity in combination therapy with PSC 833 was also observed and may have been caused by several pharmacokinetic interactions: (1) liver and renal P-gp1 inhibition; (2) inhibition of drug metabolising cytochrome P450s; and (3) impaired bile flow, perhaps from inhibition of ABCB11 [27]. Another second generation agent VX-710 has the added capability to restore sensitivity to both P-gp1 and MRP1-expressing cells *in vitro*. Several initial clinical studies have showed some promising results with this inhibitor in combination with paclitaxel and doxorubicin to treat breast cancer and soft tissue sarcomas, respectively [94,95]. Third generation modulators are now being investigated. As a result of more advanced approaches to drug development, many of these agents do not affect the activity of cytochrome P450s and appear not to interact with many of the other ABC transporters [96,97], and unlike their predecessors, they non-

competitively inhibit P-gp1 [98]. Some of these compounds that are in clinical development include: XR9576 (tariquidar) [99], LY335979 (zosuquidar) [96,100], and ONT-093 [101]. The very recent and limited clinical work with these agents has been promising. As a result of their enhanced specificity, both XR9576 and LY335979 have caused fewer alterations in the pharmacokinetics of the co-administered anti-cancer drugs [94,102]. These preliminary results offer new hope for clinical inhibition of P-gp1.

Collateral Sensivity to Verapamil

A very interesting feature of some cell lines that develop acquired resistance is the development of collateral sensitivity to relatively non-toxic drugs. In other words, these MDR cell lines become more susceptible to specific non-toxic drugs than the parental cell lines. This property was first observed in colchicine-resistant CHO cells. These cells displayed an increase in sensitivity to a variety of local anaesthetics, steroid hormones and detergents such as Triton-X compounds [103]. Since then, the group of compounds that cause collateral sensitivity in MDR cell has been expanded to include polyamine analogs and calcium channel blockers [104,105].

The phenomenon of collateral sensitivity to verapamil in multidrug resistant cells has been widely reported [106-112]. One study found that verapamil was much more toxic to multidrug resistant cells than to the sensitive cells even though the resistant cells still had reduced amounts of intracellular verapamil [104]. Another study using a CHO cell line was able to demonstrate that loss of MDR phenotype by reducting P-gp1 levels was subsequently accompanied by a similar loss of collateral sensitivity to verapamil. These studies suggest that both the resistant phenotype and collateral sensitivity to verapamil are mediated by a common mechanism [111].

The mechanism and the role of P-gp1 in the development of collateral sensitivity are still not clear. Study of this topic has been confounded by the observation that not all P-gp1 expressing cells are hypersensitive to verapamil [112]. To date, several explanations have been put forwards to explain this phenomenon. It has been proposed that collateral sensitivity to verapamil occurs due to a genetic mutation in P-gp1 during the selection process with toxic drugs [108]. The mutant protein may have similar properties as compared to normal MDR P-gp1, while causing additional toxic processes. Alternatively,

verapamil sensitivity could be caused by changes in the expression level of an unrelated protein. Finally, high P-gp1 levels may destabilise the membrane or cause a metabolic change which is deleterious to cell survival [112]. None of these mechanisms have adequately explained this perplexing phenomenon.

Multidrug Resistance Protein 1 (MRP1 or ABCC1)

In the late 1980s, after the biochemical characterisation of P-gp1, several drug-selected cell lines were identified that had a classical MDR phenotype without an increase in P-gp1 expression. This was seen in the small cell lung cancer cell line H69 which was used to derive the MDR cell line H69AR by intermittent exposure to doxorubicin [113,114]. MRP1 was identified in H69AR by examining the mRNAs that are over-expressed in H69AR relative to H69 [34]. It was eventually found that MRP1 is part of the ABCC sub-group of ABC transporters [115]. Four other MRP-related proteins in the ABCC group have been associated with some form of drug resistance, MRP2-5 (ABCC2-5). Another clinically important member of this sub group that is not associated with drug resistance is the cystic fibrosis transmembrane conductance regulator (CFTR or ABCC7) [27].

The topology of MRP1 is similar to P-gp1 although MRP1 has an additional five α-helices making up a third membrane spanning domain at the N-terminal (MSD0), this makes for a total of 17 TM helices. MSD0 is connected through an intracellular linker domain (L0) to a P-gp1-like core. The predicted topological organization of MRP1 is: MSD0-L0-MSD1-NBD1-L1-MSD2-NBD2 [116,117]. Unlike P-gp1, MRP1 has an extracytosolic N-terminal; this was made evident by N-Glycosylation of Asn^{19} and Asn^{23} [117].

Like P-gp1, MRP1 functions as a broad-specificity drug efflux pump that binds drugs and transports them against a concentration gradient using ATP hydrolysis as an energy source [118,119]. MRP1 confers resistance to many of the same natural product drugs as P-gp1, including: epipodophyllotoxins, vinca alkaloids, and certain anthracyclines [120-122] [120-122], although they share only 15 % amino acid sequence identity [34]. Several methods have been used to determine the roster of MRP1 substrates. The most commonly used technique has been to measure the ATP-dependent uptake of radiolabelled substrates into inside-out membrane vesicles prepared from MRP1-

transfected cell lines. In fact, most substrates have been identified by their ability to inhibit the uptake a well characterised radiolabelled substrate such as LTC_4. MRP1 substrates can be divided into several categories based on substrate characteristics and mechanisms of transport. Firstly, MRP1 transports structurally diverse organic anions that are conjugated to either: glutathione (GSH), sulfate, or glucuronate [123-126]. These conjugates include several compounds that are found endogenously in the body: the proinflammatory leucotriene C_4 (LTC_4), 17β-estradiol 17-(β-D-glucuronide) ($E_2$17βG), estrone-3-sulfate, oxidized glutathione (GSSG), and prostaglandin A_2 [123,125,127,128]. A second category of substrates is made up of substrates that are co-transported with GSH, such as vincristine, daunorubicin, and aflatoxin B_1 [126,129-131]. The possibility that co-transport with GSH depends on a redox reaction at its cysteine residue has been discounted because non-reducing GSH derivatives such as S-methyl-GSH also stimulate co-transport [130,132]. A third category is made up of molecules that are neither conjugated, nor co-transported; these include methotrexate and folate [122,133]. A sub-category of MRP1 substrates include compounds that stimulate GSH transport by MRP1, but that do not themselves get transported. For instance, verapamil stimulates GSH transport into inside-out membrane vesicles containing MRP1 [134,135]. In addition, several dietary flavanoids have also been found to increase GSH transport while showing no evidence of their own transport [136,137]. The mechanism by which GSH and other molecules enhance MRP1-mediated transport of conjugated and unconjugated compounds is still not well understood.

Like P-gp1, it is fascinating that MRP1 transports a plethora of chemically unrelated substrates. For example, LTC_4 and aflatoxin B_1, two structurally different compounds, both have high affinities for MRP1 transport (K_m $LTC_4 \approx 0.1$ μM, K_m aflatoxin $B_1 \approx 0.2$ μM) [126,129]. Considering these two molecules are so dissimilar, it is interesting that MRP1 can also discriminate between some compounds with very similar structures. This is evidenced by the low affinity MRP1 has for LTD_4 and LTE_4. Both of these molecules are metabolites of LTC_4 that have lost γ-glutamate, or γ-glutamate and glycine, respectively, from the glutathione moiety in LTC_4 [127]. Another example of MRP1 substrate specificity is found in the positioning of the glucuronide moiety in $E_2$17βG. Other estrogens that are glucuronidated at the 17β position of the D-ring are

believed to be transported because they are effective competitors for $E_2$17βG transport. A shift in glucuronidation to the 16α position results in a reduced ability to inhibit $E_2$17βG transport, while conjugation to the A-ring of an estrogen abolishes MRP1 interactions [126,138]. These examples demonstrate that MRP1 can transport a broad group of structurally diverse molecules while maintaining a high level of specificity, a common characteristic of multi-specific binding sites.

Physiological and Clinical Importance of MRP1

MRP1 has been detected in all normal tissues except for healthy adult liver. The highest detectable levels are found in the: lung, testis, kidney, skeletal muscle, and heart [34,139]. Studies with *mrp1*$^{-/-}$ mice have shown LTC_4 to be an important natural substrate of MRP1 due to their impaired LTC_4–mediated inflammatory response [140]. LTC_4 is a mediator of immediate hypersensitivity reactions, acting as a potent agonist of bronchoconstriction and vascular permeability [141,142]. MRP1 may also play an important role in protecting cells from injury due to drugs or toxins. This possibility is supported by the localization of the protein at the blood-organ interfaces of several toxin sensitive regions such as the central nervous system, the testis, and the placenta [143-145]. Furthermore, *mrp1*$^{-/-}$ mice are more sensitive to etoposide and have abnormal spermatogenesis [140]. Thus, MRP1 may play a dual role by mediating inflammatory responses and protecting tissues against toxins.

Although MRP1 has been detected in many solid and haematological tumours, the evaluation of its clinical significance is impeded by the expression of the protein in many of the tissues from which the tumours originate. Notably high levels of MRP1 have been detected in lung cancer, particularly of the non-small cell variety (NSCLC) which accounts for approximately 80 % of all lung cancers [146]. Furthermore, MRP1 expression was reported as a negative indicator of patient survival in the squamous cell carcinoma form of NSCLC [147]. Only a few studies have shown that MRP1 expression has an impact on the clinical outcome of cancers. One group reported a correlation between MRP1 expression in breast cancer (as detected by IHC) and relapse-free survival [148]. In bladder cancer, the MRP1 expression level, as determined by RT-PCR, was found to be 2.4-fold greater post-chemotherapy compared to untreated patients [149]. Despite the difficulties

associated with determining the clinical significance of MRP1, current data suggests that it may play a role in tumour drug resistance.

PHOTOAFFINITY LABELLING OF MRP1

"There is a single light of science, and to brighten it anywhere is to brighten it everywhere."

Isaac Asimov

Photoaffinity Labelling Techniques

The interactions between a protein and its substrate generally involve a specific domain or "active site" within the folded protein. Generally, the affinity of a specific ligand or substrate towards an active site is high. The surface of an active site is lined with amino acids, and the R-groups of these amino acids interact with, and bind the substrate. These interactions between an active site and a substrate are made-up of several weak, non-covalent interactions including hydrogen bonds, hydrophobic interactions, and ionic interactions. A common approach in the identification of a protein active site involves the use of chemically modified ligands that can form covalent bonds within the active site of a protein. Once a substrate is covalently bound to its active site, the entire protein-substrate complex can be extensively manipulated and the substrate will remain bound to the protein. The use of these chemically modified ligands is known as affinity labelling. A commonly used form of this technique is called photoaffinity labelling, or photolabelling. It has become an invaluable tool for determining ligand/protein interactions. In photolabelling, the ligand or photoaffinity probe is "activated" by electromagnetic radiation (commonly UV light) to form a covalent bond. The probe must be easily detectable, for example by containing a radioactive isotope within its molecular structure. In the past decade, photoreactive probes have been used to determine the substrate specificity and location of binding sites in ABC transporters.

Several features are crucial for the development of a photoreactive probe. A probe must include a detectable tag (i.e., radioactive, fluorescent, or immuno-reactive) so that it can be located after photolabelling to a protein. Many of the probes that are used for photolabelling of ABC transporters have one of the following radioactive tags: [^{125}I], [^{35}S], or [^{3}H]. An effective photoaffinity probe should also have similar binding affinity and chemical characteristics as its parent compound. The more similar a probe is to its parent compound, the more likely it is to have high affinity interactions with its target protein. To ensure specific interactions with the binding site, the UV-generated excited state of a photoaffinity probe must also have a lifetime shorter than the dissociation from the binding site, but long enough to stay within proximity of the target site for covalent linkage. Several other features are also favourable such as stability in aqueous solutions and ambient light, as well as high specific radioactivity [150].

Three principal photoactive groups exist for the generation of photoactive probes, these include: arylazide, diazirine, and benzophenone photophores. The most widely used photoactive groups in the study of ABC transporters are arylazides. The azide component of these probes can be converted into highly reactive nitrene intermediates, which then form a covalent bond within a binding site. Nitrenes are derivatives of nitrogen that are extremely unstable due to a valence deficiency and are produced from azides through the loss of molecular nitrogen. The generation of a stable N_2 molecule from the photolabelling reaction results in a favourable free-energy change which drives the production of a nitrene intermediate (Scheme 1). The energy from a low dose of UV-irradiation is sufficient to drive the reaction forward [150].

Scheme 1 $\qquad R - N = N = N \rightarrow R - N: + N_2$

When using an arylazide photoaffinity probe in a photolabelling experiment, tissue homogenates are first incubated with the photoaffinity probe to establish reversible equilibrium binding with target proteins. UV-irradiation then converts the probe into a highly reactive and short lived nitrene intermediate which forms a covalent linkage at or near to the protein binding site(s). This reaction allows for the identification of proteins that specifically bind to the photoaffinity probe.

Some limitations exist in photolabelling experiments. Modifying a parent compound with a photoreactive moiety may alter some of its chemical characteristics. It is therefore important to demonstrate competition between the photoaffinity analog and the parent compound. In addition, the photoreactive group may label the target protein close to, but not directly at the actual binding site. Despite these limitations, photolabelling has provided some of the most precise information on substrate binding in multidrug transport proteins and other receptor proteins.

Photolabelling P-gp1

One of the most important observations derived from photolabelling experiments was that P-gp1 mediates drug transport via direct binding to drugs. Many of the photolabelling techniques and strategies used to understand MRP1 binding were first developed with P-gp1. The initial photolabelling studies of P-pg1 were conducted using a photoaffinity analog of vinblastine named [^{125}I]N-(p-azido-[3-^{125}I salicyl)-N'-β-aminoethylvindesine ([^{125}I]NASV) [85]. This compound specifically binds to P-gp1 in many cells lines that express P-gp1 [85,151,152]. These studies led to the development of a prolific number of photoreactive analogs of cytotoxic agents and MDR modulators that specifically interact with P-gp1, including derivatives of daunorubicin and doxorubicin [152-155]. Photolabelling with these compounds was inhibited with known P-gp1 substrates, including natural product alkaloids and antibiotics. Other photoreactive analogs of MDR1-related drugs were also examined. These include [^{125}I]iodoaryl azido-rhodamine 123 (IAARh123) and [^{125}I]ASA-benzimidazole [156]. Interestingly, the former also binds to other family members of ABC proteins, including MRP1 [157,158], MRP6 [159], and LmrA [160].

Photoreactive derivatives of P-gp1 reversing agents have also proven useful in the investigation of its binding sites. The first such compound shown to bind to P-gp1 was a photoaffinity analog of dihydropyridine, [^{3}H]azidopine [161]. Analogs of the potent inhibitor verapamil were also used, such as N-(p-azido-3-^{125}I]salicyl) aminomethylverapamil ([^{125}I]NAS-VP). The binding of these compounds to P-gp1 is competitively inhibited by vinblastine, verapamil, and several other calcium channel blockers [84,155].

Photoaffinity probes also played a critical role in identifying P-gp1 drug binding domains. In these studies, site-directed antibodies were used in conjunction with [^{125}I]arylazidoprazosin ([^{125}I]AAP) and [^{3}H]azidopine, [162-164]. These compounds bind within, or immediately to the C-terminal side of TM 6 and TM 12. Interestingly, these results were later confirmed by using several other techniques. For example, mutational analysis has shown that the regions encompassed by TM 5-6 and TM 11-12 are involved in drug transport and substrate specificity [165-167]. Further information on P-gp1 drug binding was gained by using thiol-reactive analogs of dibromobimane, MTS-verapamil, and rhodamine in conjunction with mutant P-gp1 containing single cysteine residues [165-171]. These findings indicate that amino acid residues within TM 4-6, TM 10-12, and perhaps TM 9, contribute to P-gp1 drug binding. In contrast, several photoaffinity studies have found that binding occurs only in the N-terminal half of P-gp1. These results showed that analogs of verapamil, azidopine, and spiperone bound to at least one common binding domain within or on the C-terminal side of TM 6 [86,172]. Similarly, photolabelling with [^{125}I]iodomysin was restricted to a region which includes TM 4 and part of TM 5 exclusively in the N-terminal half of P-gp1 [173]. Interestingly, two photoaffinity analogs of paclitaxel bearing similar modifications at different loci, showed different binding regions. The compound 3'BzDC interacts with TM 12, whereas 7-DzDC reacts within TM 7 and half of TM 8 [174]. The exact nature of P-gp1 binding sites is still unclear but enough evidence has been gathered to form rational theories. One model proposes the existence of two drug binding sites, one for substrates such as vinblastine, melfloquine and tamoxifen, and another for molecules such as verapamil [175,176]. It has also been proposed that P-gp1 contains three drug binding sites [177]. The latter model predicts the existence of two drug sites with different drug specificities and a third allosteric site. The initial photoaffinity studies with P-gp1 have proven to be germane for work with MRP1.

Photolabelling of MRP1 with [^{3}H]LTC$_4$

Although, MRP1 is known for its role in causing multidrug resistance to a wide array of anti-cancer drugs, LTC_4 remains one of the highest affinity substrates ($K_m \approx 100$ nM). Work with *mrp1*$^{-/-}$ mice has shown that LTC_4 is an important natural substrate of MRP1

[140]. It has also been demonstrated that dendritic cell mobilization and trafficking into lymphatic vessels is reduced in *mrp1*$^{-/-}$ mice, an effect that was restored by exogenously adding LTC_4 [178]. Thus, knock-out mice have proved a valuable *in situ* tool to confirm that LTC_4 is a natural substrate of MRP1.

To investigate the interactions between LTC_4 and MRP1, several studies have taken advantage of the intrinsically photoreactive nature of LTC_4 to photolabel MRP1 [125,129,138,179,180]. The first evidence that [^{3}H]LTC_4 directly binds to MRP1 was demonstrated by the photolabelling of a 190 kDa protein in plasma membranes from the autonomous malignant mastocytoma subline L138C3-10a from Balb/c mouse derived bone marrow mast cells [179]. The inhibition of MPR1 photolabelling with MK571 (an LTD_4 receptor antagonist and an inhibitor of MRP1 mediated drug transport [181]) provided further evidence for the direct binding of LTC_4 and MRP1. Continued examination of these cells [129] confirmed the identity of the 190 kDa protein by immunoprecipitation with a mixture of MRP1-specific monoclonal antibodies: QCRL1, QCRL2, and QCRL3 [129,182]. Interestingly, MRP1 photolabelling was inhibited by QCRL3 at a concentration that is known to abolish [^{3}H]LTC_4 transport. These initial studies which took advantage of the photoreactive properties of LTC_4 demonstrated that the endogenous substrate does indeed interact directly with MRP1.

Several limitations exist when photolabelling MRP1 with [^{3}H]LTC_4, such as low cross-linking efficiency and low specific radioactivity. Despite these obstacles, [^{3}H]LTC_4 has been instrumental in yielding information on the binding characteristics of MRP1. For example, [^{3}H]LTC_4 was used to examine the interactions between MRP1 and several compounds conjugated to glucuronide. Glucuronidation results from the conjugation of glucuronic acid with chemical and bacterial toxins such as alcohols, phenols, enols, carboxylic acid, amines, hydroxyamines, carbamides, sulphonamides and thiols, as well as some normal metabolites. For most individuals, glucuronidation is a supplementary detoxification pathway. Export of glucorinated molecules by MRP1 may aid in the detoxification of some tissues. Some of the glucuronidated compounds that have been investigated include the naturally occurring estrogen 17β-estradiol 17-(β-D-glucuronide) ($E_2$17βG) as well as several cholestatic and non-cholestatic steroid glucuronides [138]. $E_2$17βG inhibits photolabelling of MRP1 with [^{3}H]LTC_4 in a concentration dependent

manner, with an IC_{50} of approximately 50 μM. Single concentrations (100 μM) of the cholestatic steroids: glycolithocholate-3-sulfate, $E_2$17βG, $E_2$3$SO_4$17βG and $E_3$17βG also effectively inhibited photolabelling of MRP1. Conversely, the non-cholestatic compounds $E_2$3βG and $E_3$3βG had negligible effects. These observations are consistent with transport studies in which the cholestatic, but not the non-cholestatic, compounds reduced transport of [^{3}H]LTC_4. These studies show that natural substrates of MRP1 such as LTC_4 and $E_2$17βG may interact at similar regions within the protein. These examples illustrate how [^{3}H]LTC_4 can be applied to determine the binding characteristics of MRP1, though its usefulness has been extended further.

Photolabelling with [^{3}H]LTC_4 has been used to identify the specific regions of MRP1 that interact with LTC_4 [180]. A bacculovirus expression system was used to produce truncated forms of MRP1 in Sf21 insect cells. Photolabelling occurred efficiently only when two truncated half molecules of MRP1 (amino acids 1-932 and 932-1531) were co-expressed, while expression of either half alone did not produce efficient labelling. This indicates the need for a cooperative interaction between the N- and C-terminal halves of the protein. Furthermore, both halves of MRP1 were photolabelled, indicating the presence of at least two sites that interact with LTC_4. Efficient photolabelling of MRP1 was also dependent on the presence of all or part of the L0 region, but not MSD0. Specifically, it was shown that part of L0, from Asp^{204} to Leu^{281}, is required for high affinity binding of LTC_4; interestingly, L0 itself was not photolabelled by [^{3}H]LTC_4. These observations demonstrate how and where MRP1 interacts with an endogenous substrate.

Photolabelling of MRP1 with Unconjugated Drugs

The first evidence that MRP1 binds to an unaltered (non-conjugated) cytotoxic drug was demonstrated using a quinoline based compound with an [^{125}I] label, N-{4-[1-hydroxy-2-(dibutyl-amino)ethyl] quinolin-8-yl}-4-azidosalicylamide (IAAQ) [183,184]. IAAQ photoaffinity labels MRP1 derived H69/AR cells, but not parental H69 cells. Despite the frequent observed role of GSH in MRP1 function, photolabelling with IAAQ was not dependent on the presence of free GSH. Molar excess of LTC_4, MK571, vinblastine, or chloroquine inhibited the photolabelling of MRP1 in cells and purified plasma

membranes. Inhibition of photolabelling with these drugs correlates with previously observed transport functions of MRP1. For example, vinblastine was the least effective inhibitor of IAAQ labelling of MRP1 as well as a poor substrate of MRP1 mediated transport [120]. Moreover, IAAQ is believed to interact with physiologically relevant sites because its photolabelling was effectively inhibited with LTC_4. Interestingly, it was proposed that inhibition of IAAQ photolabelling with MK571 and chloroquine may be due to the quinoline moiety which is found in each of these molecules. This line of reasoning was investigated using photolabelling experiments with several other quinoline containing drugs: chloroquine, quinine, quinidine, and primaquine [185]. Each of these drugs, except for primaquine, inhibited the MRP1 photolabelling with IAAQ in a concentration-dependent manner. These studies indicate that the quinoline moiety may be important for MRP1-substrate recognition. The molecular structure of IAAQ as well as other compounds that photolabel MRP1 independent of GSH are shown in figure 2.

A second unaltered cytotoxic quinoline-based drug containing [^{125}I] has been, N-(hydrocinchonidin-8'-yl)-4-azido-2-hydroxybenamide (IACI) [186]. The identity of a 190 kDa membrane protein that was photolabelled by IACI was confirmed by its binding to three MRP1-specific mAbs, QCRL1, MRPr1 and MRPm6 [187]. Similar to IAAQ, photolabelling of MRP1 in H69/AR cells with IACI occurred independent of free GSH. LTC_4 inhibited photolabelling of MRP1, indicating that IACI also binds to physiologically relevant sites. Furthermore, the specific photolabelling of MRP1 was inhibited with increasing concentrations of known MRP1 substrates: colchicine, chloroquine, doxorubicin, and MK571. The most effective inhibitors of labelling were MK571 and LTC_4. These further establish quinoline-based drugs as a class of compounds that interact directly with MRP1.

Rhodamine 123 (Rh123) is a cationic fluorescent dye that accumulates selectively in mitochondria [188] and is transported by P-gp1 [156,189]. A photoreactive analogue of Rh123, IAARh123, was used to label MRP1 in purified plasma membranes isolated from MRP1-transfected HeLa cells [158]. The ability of various compounds to inhibit the IAARh123 photolabelling was consistent with results obtained with IAAQ and IACI. These observations confirm that IAARh123 binds specifically to MRP1 and shares the same or overlapping binding site(s) as MK571 and LTC_4. Interestingly, each of these

iodinated photoreactive probes (IAAQ, IACI, and IAARh123) can bind and photolabel MRP1 independent of GSH. Since photolabelling occurs independent of GSH, it appears as if GSH is only required for the binding and transport of certain classes of drugs.

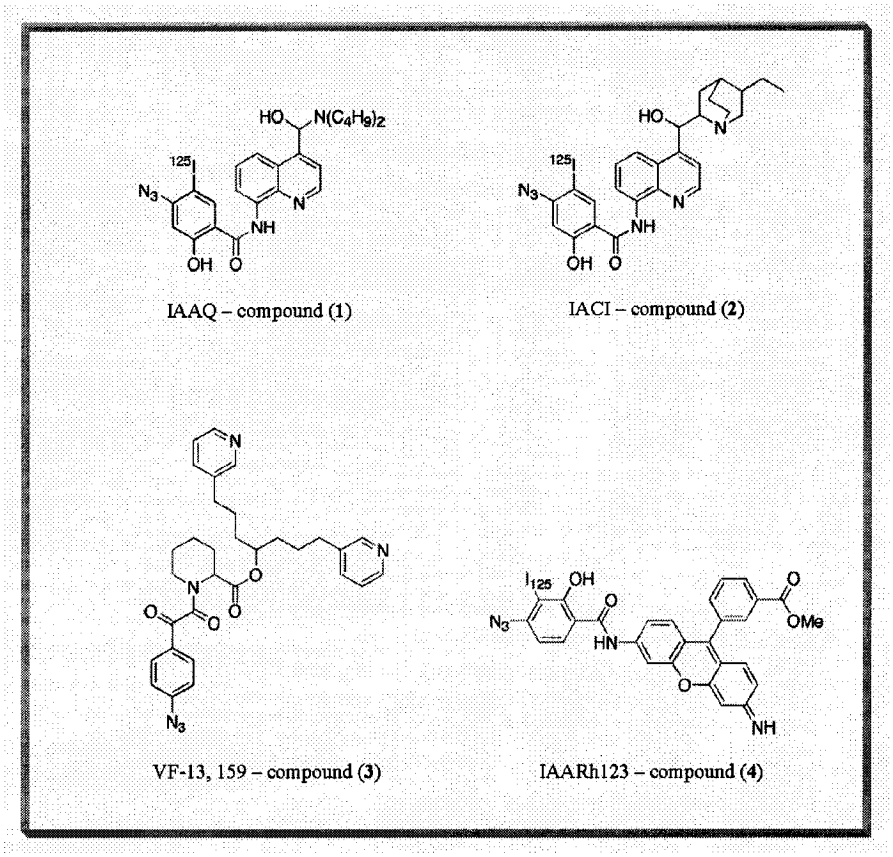

Figure 2

The organic structures of diverse compounds: (N-{4-[1-hydroxy-2-(dibutyl-amino)ethyl] quinolin-8-yl}-4-azidosalicylamide (IAAQ) (**1**), N-(hydrocinchonidin-8'-yl)-4-azido-2-hydroxybenamide (IACI) (**2**), VF-13, 159 (**3**), and Iodo-aryl azido-rhodamine 123 (**4**) that bind specifically to MRP1. These compounds are capable of photolabelling MRP1 independent of GSH.

Several features of IACI and IAARh123 made them suitable to identify substrate binding sites within MRP1 [158,186]. This was accomplished by localising trypsin-derived peptides of MRP1 that are bound to IACI or IAARh123. Mild trypsin digestion of purified MRP1 produced two polypeptides that were photolabelled with IACI or IAARh123: 111 and 85 kDa; these peptides make up the N- and C-terminal halves of the

protein (respectively). They are produced from digestion at a trypsin sensitive site located in the L1 linker domain connecting MSD0-MSD1 with MSD2 [117]. Exhaustive proteolysis of these two halves produced several small peptides that were photolabelled with IACI or IAARh123: a 6 kDa polypeptide in the N-terminal half (111 kDa), and two 4 and 6 kDa polypeptides in the C-terminal half (85 kDa) of MRP1. The labelling of these individual peptides implies that up to three binding sites exist in MRP1 for IACI and IAARh123.

To determine a more precise location of these binding sites, a series of MRP1 mutants containing hemagglutinin A (HA) epitopes were used [157]. Each mutant contains HA epitopes inserted at a single location in the MRP1 sequence. Eight separate MRP1 HA-variants were generated with epitopes inserted after amino acids: 4, 163, 271, 574, 653, 938, 1001, or 1222 [190,191]. To identify drug binding sites, each HA-variant was first photolabelled with IAARh123 or IACI. The labelled proteins were then digested with varying concentrations of trypsin (1/800 to 1/25, trypsin/protein). Based on the locations of the HA-epitopes and the sizes of the photolabelled peptides, interactions with MRP1 were found to occur in two regions. One region is located between Ser^{542} and Arg^{593} containing TM 10-11, and the other from Cys^{1205} to Glu^{1253}, comprising TM 16-17 (figure 3). Interestingly, alignment of the predicted secondary structures for MRP1 and P-gp1 indicates the labelled regions in MRP1 correspond to photoaffinity labelled regions of P-gp1 in TM 5-6 and TM 11-12 [163,167,177,192]. This suggests that similar drug binding domains may be found in different ABC transporters. This latter finding was unexpected considering the low degree of amino acid sequence identity between the two proteins [34]. Each of these compounds, IAAQ, IACI, and IAARh123 are good substrates of MRP1.

The pipecolinate derivative VX-710 has been shown to be a good reversing agent for P-gp1 as well as MRP1 [193,194]. VX-710 restored the sensitivity of MRP1-expressing HL-60/ADR cells to doxorubicin and etoposide (VP-16). Using a tritiated photoaffinity analog of VX-710, called [^{3}H]VF-13,159, it was shown that VX-710 may exert its affect on resistance at least in part by direct binding to MRP1. [^{3}H]VF-13,159 had the same or overlapping binding sites as VX-710 since photolabelling was specifically inhibited by an excess of VX-710 in a concentration-dependent manner.

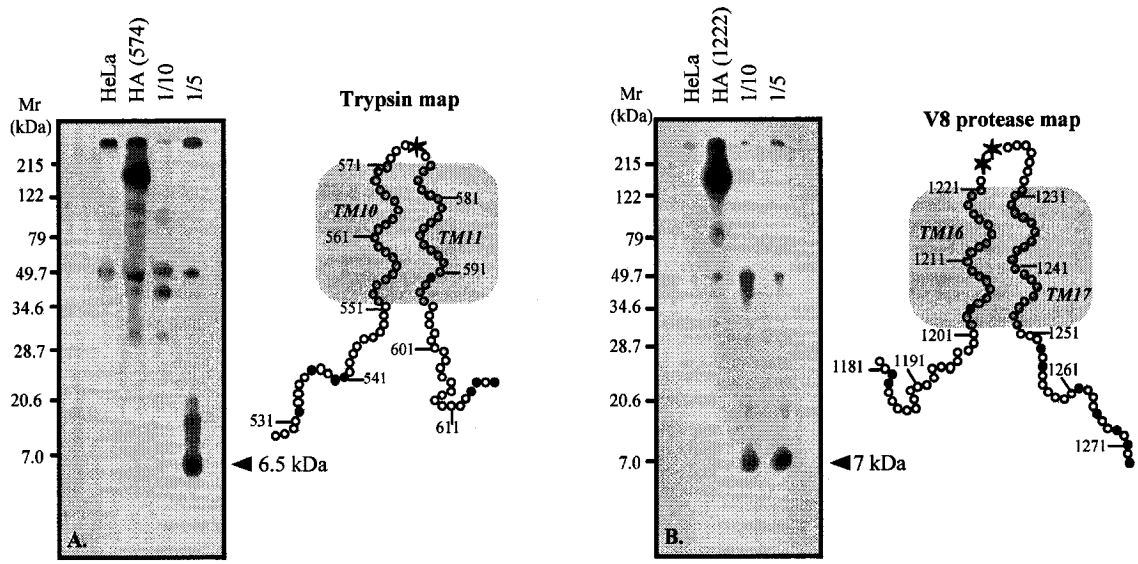

Figure 3

Exhaustive digestion of IAARh123-photoabeled MRP1-HA(574) and MRP1-HA(1222) variants. Panels A and B show exhaustive trypsin and V8 protease digestions of IAARh123-photolabeled membranes from MRP1-HA(574) and MRP1-HA(1222), respectively. The smallest immunoprecipitable IAARh123-photolabeled peptides attainable after trypsin digestion of MRP1-HA(574) or V8 protease digestion of MRP1-HA(1222) were 6.5 and 7 kDa, respectively. The schematic to the right of panels A and B represents the corresponding domains in MRP1. The grey region shows amino acids within the TM domains. Black circles are the trypsin-sensitive arginines and lysines (*A*) or V8-sensitive aspartic and glutamic acids (*B*). This figure was reproduced from Daoud *et al.*, 2001 [157].

It is interesting that a variety of photoreactive compounds are able to interact with MRP1 without free GSH. This attribute may indicate that the dependence on GSH may be limited to the transport process of certain compounds and therefore not important for the initial step of substrate binding. The next section discusses how several other photoreactive molecules interact with MRP1 in a GSH-dependent manner.

GSH-Dependent Photolabelling of MRP1

P-gp1 and MRP1 both confer resistance to several commonly used natural product anti-cancer drugs such as anthracyclines, vinca alkaloids, and epipodophyllotoxins, although some differences exist. Unlike P-gp1, considerable evidence indicates that GSH is required for MRP1 to transport certain unmodified drugs such as vincristine and daunorubicin [130,131,138]. An early study demonstrated that resistance to doxorubicin, daunorubicin, vincristine, and VP-16 in MRP1-transfected lung carcinoma cells could be inhibited by depleting cellular GSH with DL-buthionine (S,R)-sulfoximine [195]. Efflux of daunorubicin from these cells was inhibited by the depletion of GSH. In addition, MRP1 was shown to increase GSH export from transfected cells. This effect was enhanced with arsenite, possibly due to co-transport [195]. These studies suggest that GSH is required for the transport of several compounds by MRP1. However, the details of how GSH exerts its effects on MRP1 and its substrates are still unclear. GSH may act as a transport activator by facilitating substrate binding and/or transport [196]. Consistent with these observations, several photoreactive probes have been identified which only photolabel MRP1 in the presence of GSH. The molecular structure of compounds that photolabel MRP1 in a GSH-dependent manner are shown in figure 4.

The first such compound was derived from a polyhydroxylated sterol acetate isolated in a marine sponge (*Spongia* sp.), named agosterol A (AG-A). AG-A inhibits MRP1-mediated LTC_4 transport in human KB carcinoma cells [196]. To characterise how it interacts with MRP1, a photoaffinity analog of AG-A was synthesized, [^{125}I]11-azidophenyl agosterol A ([^{125}I]azidoAG-A) [196]. Specific photolabelling of MRP1 with [^{125}I]azidoAG-A occurred only in the presence of GSH, and increased proportional to the amount of GSH, up to 2 mM. Interestingly, S-methyl-GSH also stimulated photolabelling, which is consistent the observation that S-methyl-GSH stimulates transport as well [130]. Two other GSH derivatives with extended alkyl chains, S-ethyl-GSH and S-octyl-GSH, did not affect labelling.

The binding sites of [^{125}I]azidoAG-A may be similar to, or overlap the binding sites of several known substrates of MRP1. Among anti-cancer agents, vincristine and adriamycin inhibited labelling most effectively, with half-maximal inhibition at 33.9 and 30.4 μM. The MRP1 reversing agent, 4-oxo-8-[p-(4-phenylbutyl-oxy)benzoylaminol]-2-

(trtrazol-5-yl)-4H-1-benzo-pyran hemihydrate (ONO-1078) completely inhibited labelling at 200 μM. LTC_4 caused the highest inhibition with half-maximal inhibition at 1.3 μM. Several other compounds had an inhibitory effect on MRP1 labelling with [^{125}I]azidoAG-A: $E_2$17βG, VP-16, PAK-104P, and MK571. Interestingly, a drug accumulation study with parental KB/CV and resistant KB/MRP cells revealed no differences in azidoAG-A transport with these inhibitors. The authors took this to imply that the affinity of the drug for the binding site is so high that dissociation occurs at an extremely low rate. This illustrates the distinction between binding and transport, suggesting that the two processes are linked but not necessarily sequential.

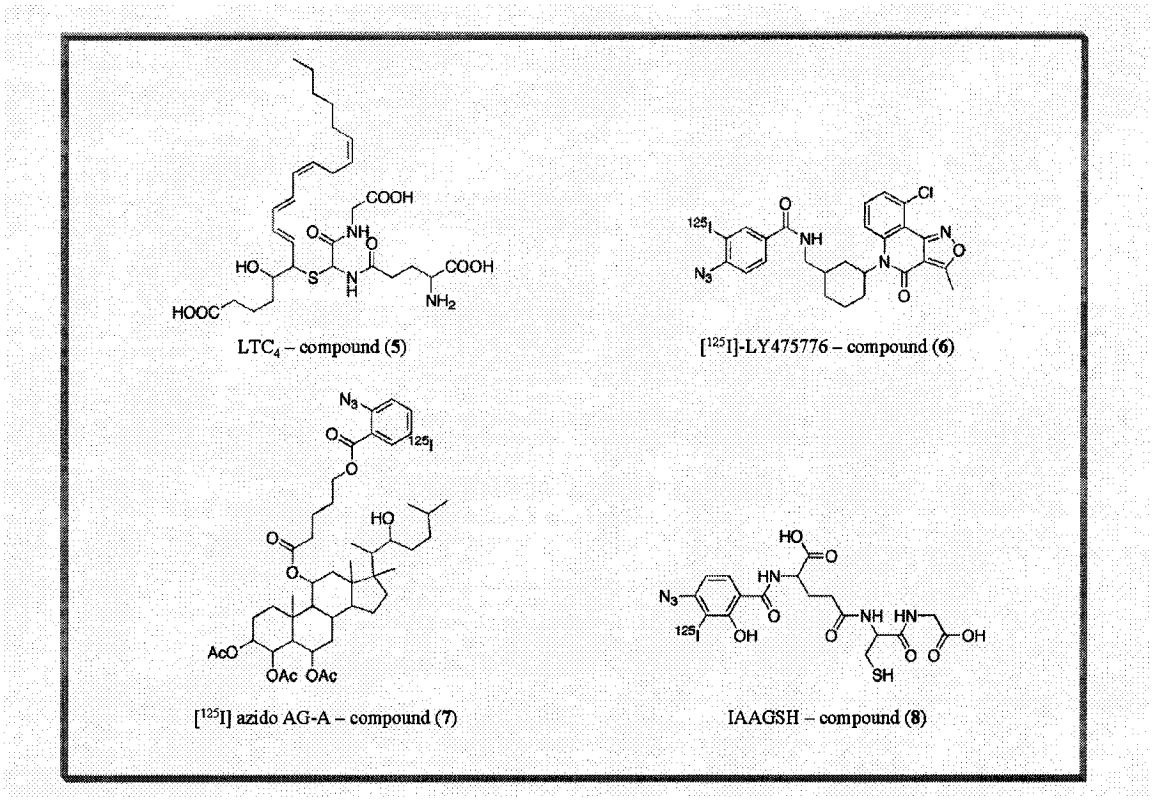

Figure 4

The organic structures of various compounds that photoaffinity label MRP1. These compounds are asocciated with GSH. LTC_4 (**5**) is conjugated to GSH and is intrinsically photoreactive. [^{125}I]-LY475776 (**6**), [^{125}I] AG-A (**7**), and Iodoaryl-azido-GSH (IAAGSH) (**8**) are modified through addition of an arylazide moiety. The photolabelling of [^{125}I] AG-A and [^{125}I]-LY475776 is GSH-dependent.

The binding regions of [^{125}I]azidoAG-A within MRP1 were determined using several techniques [196,197]. An initial study examined the photolabelling of each half of MRP1 [117]. Photolabelling of the C-terminal half of MRP1 is competitively inhibited with AG-A, whereas labelling of the N-terminal half can not be inhibited. The study concluded that the photolabelled N-terminal fragment was in fact a non-specific polypeptide. Further characterization of [^{125}I]azidoAG-A binding sites were determined using a bacculovirus co-expression system to express truncated fragments of normal and mutated MRP1. Co-expression of the N-terminal ($MRP1_{1-932}$) and C-terminal ($MRP1_{932-1531}$) halves of MRP1 resulted in the labelling of the C-terminal half alone although co-expression of the N-terminal half is required for efficient labelling. The binding region was further narrowed to a region between amino acids Ala^{932} and Arg^{1222} within TM 14-17. Furthermore, a region that is not labelled, but necessary for binding, exists between amino acids His^{1223} and Phe^{1295} [197]. This region was further investigated by replacing the Arg residue at position 1202 within TM 16 with Gly; the corresponding Arg residue in MRP2 plays an important role in MRP1 activity [198]. Photolabelling of MRP1 R1202G was greatly reduced although it retained transport activity and conferred vincristine resistance. These findings indicate that TM 14-17 and specifically TM 16 are critical for GSH-dependent labelling of MRP1 with azidoAG-A.

The importance of MSD0 and L0 was examined because of the uniqueness of these regions in the MRP family [196]. A mutant MRP1 lacking the first transmembrane domain ($MRP1_{203-1531}$) was generated and successfully photoaffinity labelled with [^{125}I]azidoAG-A. Together with the observation that $MRP1_{1-932}$ is needed for GSH–dependent binding, it appears as if a segment of MRP1 between amino acids His^{203} and Ala^{932} is important for MRP1/substrate interactions.

A second photoreactive drug, [^{125}I]LY475776, was shown to bind MRP1 specifically and in a GSH-dependent manner [199,200]. [^{125}I]LY475776 is an iodinated azido tricyclic isoxazole and has a higher binding affinity than LTC_4 [199,200]. The requirement for GSH in photolabelling MRP1 with this compound can also be substituted with several non-reducing GSH derivatives and peptide analogs. Alkyl-derivatives of GSH stimulate the photolabelling of MRP1 with [^{125}I]LY475776, although their ability to do so diminishes as the length of the alkyl chains increase above three carbon atoms. In

addition, the GSH analog ophthalmic acid, in which the thiol group from the Cys residue has been replaced with a methyl group, stimulates [^{125}I]LY475776 labelling. Moderate labelling is also observed when the Gly residue of GSH is replaced with Ala. Interestingly, a recent report which examined the structural requirements of GSH for MRP1 activity and showed that estrone 3-sulfate (E_1SO_4) transport is stimulated with the same Gly to Ala substitution in GSH [136]. Conversely, changes to the γ-Glu or Cys residues in GSH to Gly greatly diminishes the stimulation of [^{125}I]LY475776 labelling. Another study [136] also shows that substitutions of the γ-Glu results in the loss of [^{3}H]estrone 3-sulfate ([^{3}H]E_1SO_4) transport stimulation. Although modifying GSH structure appears to affect MRP1-mediated transport, it has been consistently observed that the reducing potential of the Cys residue is not significant.

The role of GSH in mediating the interaction between [^{125}I]LY475776 and MRP1 was further solidified by using verapamil and apigenin. These compounds stimulate MRP1-dependent export of GSH and are effective inhibitors of [^{125}I]LY475776 labelling. Since verapamil and apigenin stimulate GSH transport but are not transported themselves, it is postulated that a lower concentration of cytosolic GSH is responsible for the inhibition of [^{125}I]LY475776 binding. It is also possible that verapamil and apigenin compete for the same binding site as [^{125}I]LY475776. Vincristine, which may be co-transported with GSH [130], also inhibits [^{125}I]LY475776 labelling, but to a lesser degree than verapamil or apigenin. In addition to its binding affinity, the binding sites of [^{125}I]LY475776 have also been examined.

Limited trypsin proteolysis of MRP1 has revealed that the major [^{125}I]LY475776-labelling site is located within MSD2 between amino acids Pro^{1150} and Met^{1250}. This region corresponds to the last two predicted transmembrane domains in MSD2, TM 16-17. Furthermore, labelling was reduced by >80 % in mutant MRP1 proteins with substitutions of Trp^{1246} in TM 17. Studies using a bacculovirus expression system demonstrated that co-expression of both halves of the protein, $MRP1_{1-932}$ and $MRP1_{932-1531}$, are required for efficient labelling of the MSD2 binding site [201]. Photolabelling also occurs in mutant MRP1 lacking MSD0, although the presence of L0 is essential. However, unlike [^{125}I]azidoAG-A, S-methy-GSH can induce weak labelling of the N-terminal half of MRP1 with [^{125}I]LY475776.

Interestingly, [^{125}I]LY475776 binds with a much higher affinity to human MRP1 compared to the murine ortholog, mrp1 [201]. This difference in binding affinity was explored more carefully using mrp1 hybrid proteins containing all or part of the MSD2 from the human protein. The findings of that study [201] show that labelling is enhanced in hybrid proteins containing the human segments. This supports the presence of a binding within TM 16-17. Futhermore, a series of amino acids were identified to be important for binding of LY475776 [201]. A mutation of Thr^{1242} to Ala in MRP1 decreases photoaffinity labelling with [^{125}I]LY475776 and supports the possibility of a drug binding sites in TM 17 of MRP1. This residue is required for efficient transport of $E_2$17βG [202].

Taken together, these findings indicate that [^{125}I]LY475776 and [^{125}I]azidoAG-A share many similarities in their interactions with MRP1. Both photoreactive molecules preferentially label the C-terminal half of MRP1. More precisely, binding appears to be localised within the last TM domains of MSD2, TM 16-17. Furthermore, the L0 region appears to be essential for proper photolabelling although it is not labelled itself. Interestingly, the compounds that photolabel MRP1 independent of GSH (IACI and IAARh123) interact efficiently with both halves of MRP1, while the GSH-dependent compounds ([^{125}I]LY475776 and [^{125}I]azidoAG-A) preferentially label the C-terminal half. This could be a product of allosteric changes caused by GSH or may reflect the different techniques used between studies. Either way, these studies have provided accurate and relatively consistent information on the regions of MRP1 that interact with its exogenous substrates.

Photolabelling MRP1 with a Photoreactive GSH Analog

A large body of evidence points to the importance of GSH in MRP1 activity. Many of the preferred substrates of MRP1 are conjugated to GSH including LTC_4 [123,125-127]. GSH is required for MRP1 to transport unmodified drugs such as vincristine and daunorubicin [130,131,138] possibly though co-transport [203]. The common physiological role of GSH is as an antioxidant that detoxifies reactive oxygen species by acting as a substrate for GSH-S-transferases [204]. Thus, MRP1 may play a role in the removal of GSH-associated cell metabolites.

The Photoaffinity labelling of MRP1 was examined with a photoreactive derivative of GSH, azidophenacyl-[^{35}S]GSH [205]. This study found that azidophenacyl-[^{35}S]GSH labels both halves of MRP1. Although L0 is not directly photolabelled, it is still required for efficient photolabelling of other regions of MRP1 with azidophenacyl-[^{35}S]GSH. This finding is similar to observations that the L0 is required for photoaffinity labelling by [^{3}H]LTC$_4$, [^{125}I]azidoAG-A, and [^{125}I]LY475776 [180,196,201]. The precise location within the two halves of MRP1 that interacts with azidophenacyl-GSH is not known. This GSH analog may interact with the same sites as the exogenous drugs or it may bind to an unknown allosteric site.

Significance of Photoaffinity Labelling

Since the initial observation that IAAQ directly and specifically labels MRP1, photoreactive probes have become invaluable in the characterization of drug binding in this protein. One of the reasons why it has been embraced is due to the consistent similarities between photolabelling and transport. Photolabelling of MRP1 can be inhibited with compounds that are known substrates or inhibitors of transport. The most effective inhibitors are the highest affinity substrates such as LTC$_4$. This correlation is further demonstrated with GSH and its alkyl-derivatives. Short alkyl-chain derivatives are effective substitutes for native GSH in transport and binding of photoreactive probes. In contrast, GSH derivatives with longer alkyl-chains have no effect on MRP1-mediated transport or photolabelling. More importantly, photoreactive drug analogs provide a straightforward approach to localize drug binding domains within large ABC proteins. [^{3}H]LTC$_4$ and other photoreactive analogs suggest that the drug binding sites are located within the lipid bilayer, possibly within the last two TM α-helices of MSD1 and MSD2. These sites fit well within the greater context of ABC transporters since equivalent drug binding regions exist in P-gp1. However, photoreactive probes have still not uncovered the precise molecular structure of drug binding sites. The possibility of drug binding sites within the transmembrane regions is consistent with structures derived for the lipid flippase MsbA by x-ray crystallography [21,22]. The structure of an MsbA dimmer shows that a chamber formed by α-helices exists within the lipid bilayer. The inner membrane leaflet side of the chamber contains a cluster of positively charges residues, in contrast to

the more hydrophobic outer membrane leaflet side. This presents an attractive site for substrate binding. Ultimately, higher resolution analysis of MRP1 structure is needed to determine the architecture of binding sites. However, the studies to date have provided insight into the complex interaction between MRP1 and its substrates.

APOPTOSIS AND MITOCHONDRIA

"Why should we be startled by death? Life is a constant putting off of the mortal coil - coat, cuticle, flesh and bones, all old clothes."

Henry D. Thoreau

Apoptosis

The words of Thoreau ring true for all living things, including the fate of eukaryotic cells. At present, the state of knowledge in the field of apoptosis tells us that most eukaryotic cells are at all times primed for death. Many proteins stand ready to initiate a series of regulated biochemical processes that ultimately lead to cell death. It would appear as if cellular life is maintained largely by keeping these death-inducing proteins at bay. Indeed, for these cells "life is a constant putting off of the mortal coil".

Two modes of cell death exist, apoptosis and necrosis, each with distinct morphological and biochemical features. Necrosis places the cell in a more passive circumstance in which death is not within its own control. Necrosis is associated with swelling, rupture of the plasma membrane, and spilling of cellular contents into the extracellular milieu. Alternatively, apoptotic death is a process that is actively regulated from within the cell and is characterised by cell shrinkage, nuclear and cytoplasmic condensation, and chromatin fragmentation [206,207].

In the 1990s, the field of apoptosis has emerged from biomedical obscurity, and has since become one of the most active areas of research. It is now recognised that apoptosis is an essential component of development and tissue homeostasis in all multicellular organisms. For example, proper homeostasis of tissues requires the production of new cells from stem cells, while unwanted, dangerous, or surplus cells are removed by apoptosis. Recently, an appreciation for the role of apoptosis in cancer and

HIV, as well as autoimmune diseases and neurological disorders has emerged. In cancer, the inhibition of apoptosis leads to a disruption in the natural homeostatic balance because cell growth is no longer restricted. This leads to clonal growth of cell populations which may eventually result in the development of a tumour.

The molecular components that control apoptosis are grouped into two quasi-interconnected pathways. One pathway is mediated by death receptors and is triggered by extracellular signals [208]. The other pathway is initiated when mitochondria release pro-apoptotic factors.

Caspases

Caspases are proteolytic enzymes that act as executioners of apoptosis. They are cysteine proteases that typically cleave solely next to aspartate amino acids. The name "caspase" is derived from the mechanism of proteolysis, "c" for cysteine protease, and "asp" for aspartate. Homologous caspase genes are also found in lower organisms within the animal kingdom, including the nematode *Caenorhabditis elegans* and the fruit fly *Drosophila melanogaster* [209]. Caspases are constitutively present in the cytoplasm as an inactive precursor, or pro-caspase, form and vary in size from 30 to 50 kDa. Each pro-caspase consists of one N-terminal pro-domain, one large subunit (~20 kDa), and one small subunit (~10 kDa). Proteolytic cleavage of pro-caspases results in the hetero-dimerisation of the large and small subunits causing caspase activation. After cleavage and hetero-dimerization, caspases can activate other pro-caspases, including those of the same variety. Thus, once activation of a caspase occurs, a cascade of proteolytic activation and amplification of an apoptotic signal begins [210].

Caspases are commonly divided into two groups, the initiators (caspase-2, -8, -9, and -10) and effectors (caspase-3, -6, and -7). Activation of initiator pro-caspases is accomplished with the help of adaptor molecules such as Apaf-1 (mitochondrial pathway) and FADD/MORT1 (receptor-mediated pathway). These adaptors permit auto-processing of pro-caspases, thereby initiating their activity. Activated initiator caspases then start the apoptosis signal cascade by cleaving and activating the effector pro-caspases. Within the mitochondrial pathway, the initiator caspase-9 activates the effector caspases-3 and -7.

Interestingly, there is a hierarchy of substrate specificity within the family of caspases. Upstream caspases possess large N-terminal pro-domains which favour protein-protein interactions with adaptor molecules such as Apaf-1, whereas the pro-domains of downstream caspases are relatively small. Furthermore, upstream caspases prefer specific tetrapeptide substrate cleavage sites that are found within downstream caspases. The form of tetrapeptide cleavage site preferred by downstream caspases are often found in proteins that execute the final cellular stages of apoptosis, including the actin-regulatory gelsolvin and the chromatin-regulatory protein poly-ADP ribosyl polymerase (PARP). These structural differences and substrate preferences are crucial for maintaining the proper sequence of events during apoptosis.

Mitochondria, a Mediator of Life and Death

It wasn't until the 1990s that Horvitz and colleagues derived a molecular pathway for apoptosis in *C. elegans*. This work revealed a group of proteins that regulate apoptosis: Egl-1, Ced-9, Ced-4, and Ced-3 [206,211-213]. Since this groundbreaking work, many mammalian components of apoptosis have been identified including: inhibitors of caspases, regulators of caspase inhibitors, Bcl-2 family members, and cytochrome *c*. Interestingly, each of these proteins is closely associated with mitochondria.

In the mid 1990s, it was revealed that cytochrome *c* plays a significant role in activating apoptosis. This contrasts its classical function as an electron carrying protein that is a crucial component of the energy generating processes within mitochondria. In this regard, it is a component of the electron transport chain (ETC) and resides in the intermembrane space between the inner and outer mitochondrial membranes. Cytochrome *c* shuttles electrons derived from malate and succinate through multiprotein complexes in the ETC. Specifically, cytochrome *c* carries electrons from complex III to complex IV. The electron movement drive the formation of a proton gradient and electric potential ($\Delta\Psi_m$) across the inner mitochondria membrane that is used to produce ATP.

More recently, its role as a component of apoptosis machinery has been elucidated; it is the downstream binding partner of the Apaf-1 protein, a homolog of *C. elegans* Ced-4 [214]. After the initiation of apoptosis, cytochrome *c* is released from the mitochondria and interacts with Apaf-1 to form a huge cytoplasmic protein complex [215].

This complex is termed the apoptosome and its formation leads to downstream activation of caspase-9, the homolog of *C. elegans* Ced-3. The apoptosome possess a unique approach to activating caspase-9. While conventional caspase activation requires proper proteolytic cleavage, the apoptosome activates caspase-9 through constant association in a protein complex [216,217]. Activation of caspase-9 by auto-cleavage also occurs during mitochondria-mediated apoptosis. The activity of processed caspase-9 may be more potent than the apoptosome-caspase structure, suggesting that auto-cleavage acts as a positive feedback loop [218]. Therefore, once mitochondria receive a signal to initiate apoptosis, the release of cytochrome *c* initiates a cascade of events that lead to cell death.

Since the outcome of apoptosis is quite serious, several safe guards have been incorporated such as the inhibitor of apoptosis proteins (IAP). These proteins inhibit caspase activity by directly binding to the active enzymes [219,220]. In the case of caspase-9, it was found that xIAP associates with the active caspase-9-Apaf-1 holoenzyme complex [221]. It has been proposed that xIAP inhibits leaky or unwanted apoptosome-caspase-9 activity [222]. After revealing the role of IAPs, two independent groups identified a protein that inhibits IAPs, SMAC/DIABLO. This protein enhances caspase activity and is also of mitochondrial origin. The first group isolated the protein from HeLa cell membrane extracts that enhanced caspase activity; this protein was called the second mitochondrial-derived activator of caspase (SMAC) [223]. The other group named the protein DIABLO (direct IAP binding protein with low pI) after finding it using a coimmunoprecipitation approach [224]. SMAC/DIABLO interacts tightly with a bacculovirus IAP repeat (BIR) domain in IAP proteins, thereby abrogating their caspase inhibitory activity [225,226]. Another mitochondrial protein named Omi/HtrA2 can also inhibit IAPs, although inactivation occurs through proteolytic cleavage [227,228]. Mitochondria release several other pro-apoptotic proteins in addition to those that regulate the caspase cascade. These include the apoptosis inducing factor (AIF) [229] and endonuclease G (endo G) [230] which are involved in DNA fragmentation and chromosomal condensation during apoptosis.

Why do so many mitochondrial proteins play a central role in apoptosis? Several reasons for this have been proposed. Strategically, it is safer for a cell to separate the pro-apoptotic mitochondrial proteins from their cytosolic targets. For example, cytochrome *c* and SMAC/DIABLO must first be released into the cytoplasm before they can interact

with Apaf-1 and IAP, respectively. Compartmentalisation of cytochrome *c* and SMAC/DIABLO ensures that cell death is initiated only when deliberate and regulated apoptosis signals are present [222]. This is further evidenced from the observation that pro-apoptosis proteins must be processed in the mitochondria before they gain functionality. As a result, they do not illicit apoptosis when they are newly synthesised and transiently exposed to the cytosol. Spatial separation also allows these proteins to be involved in additional processes. For example, cytochrome *c* plays an integral role in energy production and Omi/HtrA2 acts as a molecular chaperone and degrades denatured proteins [231-233]. Taken together, the activity of these proteins firmly establishes a central role for mitochondria in apoptosis.

Mitochondrial Outer Membrane Permeability

A pivotal event in the process of mitochondrial-mediated apoptosis is mitochondrial outer membrane permeability (MOMP). The permeabilisation of the outer membrane of mitochondria during apoptosis occurs suddenly and results in the release of proteins normally found in the intermembrane space such as cytochrome *c* and AIF [234]. Furthermore, a dissipation of $\Delta\Psi m$ frequently accompanies MOMP, although this can occur before, during or after MOMP depending on different mechanisms of apoptosis. Although the mechanisms responsible for MOMP remain controversial, two have been well described; the first mechanism involves both the inner and outer mitochondrial membranes, while only the outer membrane participates in the second.

The first mechanism begins with the opening of the permeability transition (PT) pore in the inner mitochondrial membrane. The PT pore is a complex composed of several polypeptides from both the inner and outer membranes. These proteins operate together at membrane contact sites to form a channel through which molecules that are smaller than or equal to 1.5 kDa can pass through. Several additional proteins have been identified that are believed to regulate the pore, these include the adenine nucleotide (ADP/ATP) transporters (ANTs) in the inner membrane, the voltage-dependent anion channel (VDAC) in the outer membrane, and cyclophilin D, a matrix *cis/trans*-prolyl-isomerase [235]. Opening of the non-selective PT pore allows ions to flow freely into the matrix causing a loss of $\Delta\Psi m$. The new hyperosmotic state within the matrix causes

swelling as water enters. This leads to rupturing of the outer membrane, resulting in MOMP. Thus, opening of the PT pore can be considered an important step leading to the release of apoptogenic proteins such as cytochrome *c*, although it does not exit through the PT pore itself. Several compounds inhibit PT pore opening such as cyclosporine A which binds to cyclophilin D [236]. Studies in which cyclosporin A blocks the loss of $\Delta\Psi m$ and apoptosis suggest that PT marks the point of no return in these cells [237].

The second mechanism that causes MOMP does not appear to involve the PT pore or the inner mitochondrial membrane. It is regulated by the Bcl-2 family of proteins acting directly on the outer mitochondrial membrane.

The Bcl-2 Family

As indicated above, mitochondrial proteins play a central role in apoptosis when they are released from the organelle. A group of "gate keeper" proteins control when the mitochondrial proteins are released, these are members of the B-cell lymphoma/leukemia-2 (Bcl-2) family of proteins. These proteins are divided into two sub-groups, anti-apoptosis death members and pro-apoptosis members. The relative ratios of anti- and pro-apoptotic Bcl-2 family proteins determine the sensitivity or resistance of cells to apoptotic stimuli such as: growth factor deprivation, hypoxia, radiation, anti-cancer drugs, Ca^{2+}, and oxidants [68]. The namesake member of the family, Bcl-2, is a homolog of *C. elegans* Ced-9, and prevents the release of cytochrome *c* from mitochondria, and is thus prevents apoptosis [238]. Four conserved domains have been identified in this protein family based on amino acid sequence alignments; these are called Bcl-2 homology (BH) domains. All the members of this family of proteins share at least one conserved BH domain [239].

The pro-apoptotic Bcl-2 protein subfamily falls into two groups based on the presence of BH domains. The first group of pro-apoptotic proteins share BHl, BH2, and BH3 and include the Bax and Bak proteins. These appear to be effectors of MOMP, causing the release of pro-apoptotic proteins (such as cytochrome *c* and AIF). Prior to apoptosis, Bax exists as a monomeric cytosolic protein in healthy primary tissue cells, while Bak is maintained in an inactive form complexed with the mitochondrial outer-membrane protein VDAC2 [240]. Upon activation by an apoptotic stimulus, Bax and Bak

change their conformation, translocate to mitochondria and form oligomers [241]. This activation induces the release of cytochrome *c*, setting the stage for the amplification of apoptosis through caspases-9 and caspase-3 activities. It remains unknown whether these oligmers directly form channels in mitochondrial membranes or interact with channel-forming proteins to increase MOMP [242-244]. The channel forming hypothesis is based on the finding that Bcl-2 family members are structurally similar to diphtheria toxin, a membrane pore-forming molecule [245]. Mice lacking Bax and Bak fail to undergo MOMP in response to a wide range of signals [246]. Moreover, observations in cell culture and animal models show that down regulation or inactivation of Bax is observed in several human cancers, causing a reduction in cell death within tumours [247-249].

Members of the other pro-death subfamily contain only the BH3 domain; the Egl-1 protein from *C. elegans* was the first BH3-only cell death activator to be discovered. The mammalian counterparts include: Bid, Bad, Bcl-xS, Bmf, Puma, Noxa, and Bim. These BH3-only death factors exert their activity in a variety of ways. They act either by activating Bax and Bak, or by interfering with the anti-apoptotic Bcl-2 family members [250-252]. The mechanisms of activation for these proteins are diverse and include transcriptional activation and proteolitic truncation [239]. Interestingly, several studies demonstrate that BH3-only proteins play a role in the pro-apoptotic activity of anti-cancer agents such as doxorubicin [253] and cisplatin [254].

The first anti-apoptotic family member to be discovered was Bcl-2 itself. The *bcl-2* gene was found through analysis of chromosomal rearrangements that occur in human tumours. In the majority of follicular B-cell lymphomas, the *bcl-2* gene is moved from its normal chromosomal position, into the immunoglobulin heavy chain locus. This increases the transcription of *bcl-2* by the immunoglobulin's intron enhancer [255-257]. Initially, it was suspected that *bcl-2* was another growth promoting oncogene, however it was eventually determined that the Bcl-2 protein enhances cell survival and interferes with apoptosis [258,259]. Since then, other members of the anti-apoptotic Bcl-2 subfamily have been found, these include: Bcl-2, Bcl-xL, Bcl-w, A1/Bfl-1, Boo/Diva/Bcl-B, and Mcl-1. These proteins contain three to four BH domains which are required for them to function. It is commonly believed that Bcl-2 and its anti-apoptotic homologues inhibit apoptosis by preserving the integrity of the mitochondrial membrane. They inhibit the

activity of Bax and Bak by preventing Bax/Bak oligomerisation, possibly by forming heterodimers with them and preventing MOMP [241].

Given the potent ability of Bcl-2 to inhibit apoptosis, it may be possible for overexpression of the protein to immortalise cells and initiate cancer. Despite its potent anti-apoptotic ability, Bcl-2 over-expression alone is not sufficient for tumourigenesis [259]. Rather, Bcl-2 may play a part in maintaining a clonal population until other tumourigenic mutations arise. Along this line of reasoning, recent studies have identified a potential new role for Bcl-2. siRNA studies show that silencing Bcl-2 induces massive p53-dependent apoptosis [260]. Furthermore, this occurs under conditions without p53 induction. Normally, the tumour suppressor protein p53 stimulates the transcription of pro-apoptotic genes in certain cell types. The authors speculate that Bcl-2 constitutively suppresses a previously unidentified pro-apoptotic function of p53. Although our understanding is still incomplete, rapidly emerging data on this protein family may lead to novel approaches to cancer treatment.

Mitochondria and Reactive Oxygen Species (ROS)

Although mitochondria are a fundamental component of the apoptosis pathway, their primary function is to produce energy through a process called oxidative phosphorylation. This process is more efficient at producing ATP than glycolysis or fermentation. The inner mitochondrial membrane contains the components necessary for oxidative phosphorylation. Oxidative phosphorylation involves the reduction of O_2 to H_2O with electrons derived from NADH and $FADH_2$. The electronegative O_2 "pulls" the electrons from the donor molecules through a series of protein complexes (complexes I-IV) in the inner mitochondrial membrane that make up the ETC. The flow of electrons through the ETC causes the transport of protons from the inner mitochondrial matrix into to intermembrane space. The movement of protons is mediated by H^+ pumps of the ETC (complex I = NADH dehydrogenase, III = cytochrome *c* reductase, and IV = cytochrome *c* oxidase). The movement of protons into the intermembrane space produces a chemical and electrical gradient across the inner membrane forming the membrane potential, $\Delta\Psi m$. Finally, protons flow back into the matrix through the ATP synthase protein complex (complex V). The movement of protons into the matrix provides the free energy needed

to synthesise ATP. Therefore, the process of oxidative phosphorylation couples O_2-mediated proton movement ("oxidative") to ATP synthesis ("phosphorylation"). The rate and efficiency of electron transport in mitochondria is controlled by the cellular needs for ATP and heat production [28].

The evolutionary origin of mitochondria is still under debate although it is widely believed that they are derived from primitive aerobic bacteria that began an endosymbiotic relationship with anaerobic eubacteria-like host cells. This symbiotic relationship may have evolved in response to an increase in atmospheric O_2 produced as a by-product of photosynthesis. Oxygen is highly toxic to many life forms because it readily accepts electrons from other molecules, forming toxic free radicals (molecules with unpaired electrons). Since, proto-mitochondria were capable of oxidative phosphorylation and consequently were exposed to O_2, they developed mechanisms to protect themselves against free radicals. Therefore, by entering into a symbiotic relationship with primitive aerobic bacteria, the progenitor to today's eukaryotic cells evaded oxygen toxicity and gained a highly efficient means of producing chemical energy.

Why is oxygen such a hazardous molecule to use as a terminal electron acceptor in mitochondrial oxidative phosphorylation? Its toxicity is primarily a result of reactive oxygen species (ROS) produced during oxidative phosphorylation. Normally, electron transport in mitochondria is extremely efficient, with a majority of the electrons being used to reduce O_2 in complex IV. A fraction of the electrons escape from the ETC and lead to the formation of ROS. The loss of electrons occurs more frequently or at a higher rate when the ETC turns over more quickly to produce more ATP. In fact, mitochondrial ROS generation correlates well with a cells metabolic rate [261,262]. The loss of electrons from the ETC is widely accepted, although the amount that is lost and the precise site where ROS are formed are still not clear. ROS are possibly formed from incomplete reduction of O_2 in complex IV, though it is more likely that ROS are generated at an upstream site in the ETC. The primary ROS species produced in mitochondria is the superoxide radical ($O^-_2\cdot$). This radical is derived from the ubisemiquinone radical intermediate (QH·) during the Q cycle at complex III [263-265]. $O^-_2\cdot$ can then be transformed into hydrogen peroxide (H_2O_2) by spontaneous dismutation or by

superoxide dismutase (SOD). An iron-catalyzed reaction (Fenton Reaction) can add another electron to H_2O_2 and form the hydroxyl radical (OH·) [266]. Of these ROS, the most reactive species is OH·, which is believed to cause the majority of damage to biological molecules. It is such a reactive molecule that damage occurs only in a small region limited by diffusion of the radical. ROS can also cause the uncoupling of the ETC resulting in a feedback loop which induces the mitochondria to produce more ROS [267,268].

ROS can readily react with cellular macromolecules and damage them through chemical interactions [269]. The reason behind their toxicity stems from the fact that they are free radicals, or lead to the formation of free radicals. A free radical is any species capable of independent existence that contains one or more unpaired electrons; an unpaired electron is one that occupies an atomic or molecular orbital by itself. Free radicals are highly reactive because they absorb electrons from other molecules to fill their unpaired orbital. The loss of an electron oxidises a molecule setting off a chain of oxidising reactions as subsequent molecules attempt to regain lost electrons. Interestingly, the oxygen molecule as it occurs naturally is itself a radical: it has two unpaired electrons. Each of the unpaired electrons in O_2 has the same spin quantum number. Fortunately for the life on Earth, the oxygen molecule is not highly reactive because its two orbitals must be filled by electrons that both have the same antiparallel spin. A pair of electrons in a molecular orbital would not meet this criterion since they must have opposite spins in accordance with Pauli's exclusion principle. This restriction on the reactivity of molecular oxygen is fortunate; otherwise organic molecules would immediately combust in the presence of O_2 from normal air. When a single electron is added to oxygen it becomes the superoxide ion which is more reactive and can begin propagating damage throughout a biological system [270].

ROS and Apoptosis

Exposure to low doses of ROS is not severe enough to induce necrosis in cells but may leave cells with a permanently mutated genome. One mechanism of counteracting this effect would be to rid the body of these mutated cells. Perhaps for this reason, low doses of ROS will often induce apoptosis. In fact, early studies in apoptosis showed that low doses of H_2O_2 could induce apoptosis, while the addition of antioxidants inhibited this

effect [271,272]. More recently, ROS have been implicated in apoptotic cell death associated with several diseases. The heart disease condition of ischemia-reperfusion injury is believed to be related to oxidative stress during re-oxygenation which leads to apoptosis [273]. In cultured human lymphocytes from patients with Graves disease (hyperthyroidism), thyroid hormones induced the formation of ROS and subsequent apoptosis [274]. Apoptosis caused by the production of ROS has been implicated in the pathology of diabetes-specific microvascular diseases [274], and under conditions of high glucose, ROS production may lead to apoptosis in primary root ganglion neurons and affect the pathogenesis of neurodegenerative diseases such as Alzheimer's disease, Huntington's disease, and muscular dystrophies [275]. The large number of diseases associated with ROS production and apoptosis demonstrates why these processes have been extensively studied.

The precise mechanisms that govern the induction of apoptosis by ROS are varied and still being elucidated. Given this, it is commonly believed that the addition of exogenous ROS initiates apoptosis by inducing PT pore opening [276-278]. ROS activate the PT pore by altering glutathione-mediated cross-linking of Cys^{159} and Cys^{256} on one of the adenine nucleotide transporters (ANTs); under these condition ADP binding is inhibited and cyclophilin D binding is enhanced [279]. PT pore opening also appears to be accompanied by a burst of ROS which may act in a positive feedback loop to enhance the opening of the pore [280,281].

ROS have been shown to initiate apoptosis by a variety of mechanisms. For example, ROS activate p53 [282]. In addition, ROS may create oxidized lipids in the membrane which are known inducer of apoptosis [283]. It has also been proposed that ROS can activate the genes responsible for apoptosis such as ced-3 and ced-4 in the nematode model system. In this regard, it may mediate apoptosis through oxidative stress-responsive nuclear transcription factors such as NF-κB [284]. Moreover, ROS are associated with the activity of many transcription factors that may be involved in apoptosis. ROS have been seen to activate the redox-sensitive c-Jun N-terminal kinase/stress activated protein kinase (JNK/SAPK), which is necessary for the transcriptional activation of pro-apoptotic genes [285]. Indirect evidence has shown that many cytotoxic drugs may induce apoptosis by increasing ROS production [285]. This

effect has been observed recently with the induction of apoptosis in cancer cells by the nonsteroidal anti-inflammatory drug (NSAID) sodium salicylate [286]. Despite the many roles played by ROS in mediating apoptosis, it is generally believed that ROS are not required to activate the apoptosis program [287].

Recent evidence has suggested that a low concentration of ROS participate in cell signalling and may act as "second messengers" in receptor mediated cell signalling [288-290]. Therefore, the act of aerobic metabolism is a delicate balancing act in which the mitochondrion acts to maximise the amount of ATP synthesis while maintaining ROS production to a low level.

Antioxidants

The life of aerobic cells can be viewed as being under constant oxidative stress from ROS since O_2 and its by-products are ubiquitous. Fortunately, or by necessity, aerobic life forms have developed defence systems against ROS. The cell's ability to ward off oxygen toxicity takes the form of a diverse group of antioxidants defences. These defences comprise: (1) enzymes that catalytically remove free radicals and ROS, including superoxide dismutase, catalase, peroxidase, and thioredoxin; (2) proteins that block the availability of pro-oxidants by sequestering transition metals (such as iron ions, copper ions, and haem) which can serve as a source of electrons; (3) proteins that protect biomolecules from damage by other mechanisms such as heat shock proteins; and finally (4) low molecular mass agents such as glutathione that scavenge ROS [291]. The deleterious effects of ROS in mitochondria are prevented by a variety of these antioxidant systems. Within the intermembrane space of mitochondria, the production of $O^-_2\cdot$ is controlled by several mechanisms. This compartment has a SOD composed of two protein subunits, each of which have an active site containing one copper and one zinc ion (CuZnSOD). All CuZnSODs catalyse the dismutation of $O^-_2\cdot$ by the following reaction:

$$O^-_2\cdot + O^-_2\cdot + 2H^+ \rightarrow H_2O_2 + O_2$$

Some $O^-_2\cdot$ is also removed by spontaneous dismutation which is facilitated by the low pH of this compartment. Furthermore, within the intermembrane space, cytochrome *c* can be

reduced by $O^{-}_{2}\cdot$ and re-inject an electron in into complex IV of the electron transport chain. The hydrogen peroxide that is produced is primarily decomposed by the enzyme family of glutathione peroxidases [291]. These enzymes catalyze the reaction that removes H_2O_2 by coupling its reduction to H_2O with oxidation of reduced glutathione (GSH) to oxidised glutathione (GSSG):

$$H_2O_2 + 2GSH \rightarrow GSSG + 2\ H_2O$$

GSH is regenerated from GSSG by the NADPH-dependent glutathione reductase. GSH is the predominant low molecular weight thiol in animal cells with cytosolic concentrations as high as 10 mM. The [GSH]:[GSSG] ratio is often used as an indicator of the cellular redox state, and is greater than 10 under normal physiological conditions [292]. Apart from its role as a cofactor for the glutathione peroxidase family, GSH participates in many cellular redox reactions. GSH is involved in the metabolism of many xenobiotics by direct conjugation. The reaction that mediates the conjugation to GSH is catalysed by glutathione S-transferase (GST) enzymes. All eukaryotes have several cytosolic and membrane bound GST enzymes; each has distinct substrate specificities and a variety of enzymatic properties. Toxic compounds that are metabolised by GSTs in animals include: chloroform, organic nitrates, bromobenzene, aflatoxin, DDT, naphthalene, and paracetamol. LTC_4 synthase is also a GST although it does not play a role in xenobiotic metabolism. The liver contains a relatively high concentration of GSTs. This results in the excretion of GSH-conjugates into bile using ATP-dependent glutathione S-conjugate efflux pumps [291]. Under conditions of oxidative stress, these pumps are also involved in the export of excessive GSSG. Interestingly, several of the ABC transporters from the MRP family are S-conjugate efflux pumps and may play a significant role in this process.

Taken together, it is difficult to outline a common mechanism or role for ROS and antioxidants in apoptosis. In general, a large body of evidence points to the destructive nature of these free radicals; oxidation of molecules such as DNA and lipids induces caspase cascades that lead to apoptotic cell death. In contrast, it appears as if the cellular machinery has taken advantage of the ubiquitous nature of ROS, and has incorporated

them into various signalling cascades. Most likely, healthy cells regulate the levels of ROS by balancing their production and removal with metabolic processes such as oxidative phosphorylation and enzymes such as glutathione peroxidases.

References

1. Linton, K. J., and Higgins, C. F. (1998) *Mol Microbiol* **28**(1), 5-13
2. Bauer, B. E., Wolfger, H., and Kuchler, K. (1999) *Biochim Biophys Acta* **1461**(2), 217-236
3. Dean, M., Rzhetsky, A., and Allikmets, R. (2001) *Genome Res* **11**(7), 1156-1166
4. Berger, E. A., and Heppel, L. A. (1974) *J Biol Chem* **249**(24), 7747-7755
5. Higgins, C. F., Haag, P. D., Nikaido, K., Ardeshir, F., Garcia, G., and Ames, G. F. (1982) *Nature* **298**(5876), 723-727
6. Gilson, E., Higgins, C. F., Hofnung, M., Ferro-Luzzi Ames, G., and Nikaido, H. (1982) *J Biol Chem* **257**(17), 9915-9918
7. Higgins, C. F., Hiles, I. D., Whalley, K., and Jamieson, D. J. (1985) *Embo J* **4**(4), 1033-1039
8. Walker, J. E., Saraste, M., Runswick, M. J., and Gay, N. J. (1982) *Embo J* **1**(8), 945-951
9. Bishop, L., Agbayani, R., Jr., Ambudkar, S. V., Maloney, P. C., and Ames, G. F. (1989) *Proc Natl Acad Sci U S A* **86**(18), 6953-6957
10. Mimmack, M. L., Gallagher, M. P., Pearce, S. R., Hyde, S. C., Booth, I. R., and Higgins, C. F. (1989) *Proc Natl Acad Sci U S A* **86**(21), 8257-8261
11. Schneider, E., and Hunke, S. (1998) *FEMS Microbiol Rev* **22**(1), 1-20
12. Ling, V. (1975) *Can J Genet Cytol* **17**(4), 503-515
13. Juliano, R. L., and Ling, V. (1976) *Biochim Biophys Acta* **455**(1), 152-162
14. Chen, C. J., Chin, J. E., Ueda, K., Clark, D. P., Pastan, I., Gottesman, M. M., and Roninson, I. B. (1986) *Cell* **47**(3), 381-389
15. Gerlach, J. H., Endicott, J. A., Juranka, P. F., Henderson, G., Sarangi, F., Deuchars, K. L., and Ling, V. (1986) *Nature* **324**(6096), 485-489
16. Gros, P., Croop, J., and Housman, D. (1986) *Cell* **47**(3), 371-380
17. Lee, J. Y., Urbatsch, I. L., Senior, A. E., and Wilkens, S. (2002) *J Biol Chem* **277**(42), 40125-40131

18. Rosenberg, M. F., Callaghan, R., Ford, R. C., and Higgins, C. F. (1997) *J Biol Chem* **272**(16), 10685-10694

19. Rosenberg, M. F., Kamis, A. B., Callaghan, R., Higgins, C. F., and Ford, R. C. (2003) *J Biol Chem* **278**(10), 8294-8299

20. Rosenberg, M. F., Velarde, G., Ford, R. C., Martin, C., Berridge, G., Kerr, I. D., Callaghan, R., Schmidlin, A., Wooding, C., Linton, K. J., and Higgins, C. F. (2001) *Embo J* **20**(20), 5615-5625

21. Chang, G. (2003) *J Mol Biol* **330**(2), 419-430

22. Chang, G., and Roth, C. B. (2001) *Science* **293**(5536), 1793-1800

23. Locher, K. P., Lee, A. T., and Rees, D. C. (2002) *Science* **296**(5570), 1091-1098

24. Velarde, G., Ford, R. C., Rosenberg, M. F., and Powis, S. J. (2001) *J Biol Chem* **276**(49), 46054-46063

25. Ferreira-Pereira, A., Marco, S., Decottignies, A., Nader, J., Goffeau, A., and Rigaud, J. L. (2003) *J Biol Chem* **278**(14), 11995-11999

26. Rosenberg, M. F., Mao, Q., Holzenburg, A., Ford, R. C., Deeley, R. G., and Cole, S. P. (2001) *J Biol Chem* **276**(19), 16076-16082

27. Holland, I. B. (2003) *ABC proteins: from bacteria to man*, Academic Press, London; San Diego, Calif.

28. Alberts, B. (1994) *Molecular biology of the cell*, 3rd Ed., Garland Pub., New York

29. Chabner, B. A., and Roberts, T. G., Jr. (2005) *Nat Rev Cancer* **5**(1), 65-72

30. Tannock, I., and Hill, R. P. (1998) *The basic science of oncology*, 3rd Ed., McGraw-Hill Health Professions Division, New York

31. Endicott, J. A., and Ling, V. (1989) *Annu Rev Biochem* **58**, 137-171

32. Gottesman, M. M., and Pastan, I. (1988) *J Biol Chem* **263**(25), 12163-12166

33. Raymond, M., and Gros, P. (1989) *Proc Natl Acad Sci U S A* **86**(17), 6488-6492

34. Cole, S. P., Bhardwaj, G., Gerlach, J. H., Mackie, J. E., Grant, C. E., Almquist, K. C., Stewart, A. J., Kurz, E. U., Duncan, A. M., and Deeley, R. G. (1992) *Science* **258**(5088), 1650-1654

35. Doyle, L. A., Yang, W., Abruzzo, L. V., Krogmann, T., Gao, Y., Rishi, A. K., and Ross, D. D. (1998) *Proc Natl Acad Sci U S A* **95**(26), 15665-15670

36. Miyake, K., Mickley, L., Litman, T., Zhan, Z., Robey, R., Cristensen, B., Brangi, M., Greenberger, L., Dean, M., Fojo, T., and Bates, S. E. (1999) *Cancer Res* **59**(1), 8-13

37. Harris, C. C. (1996) *J Natl Cancer Inst* **88**(20), 1442-1455

38. Lowe, S. W., Ruley, H. E., Jacks, T., and Housman, D. E. (1993) *Cell* **74**(6), 957-967

39. Hu, Z. B., Minden, M. D., and McCulloch, E. A. (1995) *Leukemia* **9**(10), 1667-1673

40. Eder, J. P., Jr., Chan, V. T., Niemierko, E., Teicher, B. A., and Schnipper, L. E. (1993) *J Biol Chem* **268**(19), 13844-13849

41. Harker, W. G., Slade, D. L., Parr, R. L., Feldhoff, P. W., Sullivan, D. M., and Holguin, M. H. (1995) *Cancer Res* **55**(8), 1707-1716

42. Gerson, S. L., and Willson, J. K. (1995) *Hematol Oncol Clin North Am* **9**(2), 431-450

43. Waxman, D. J., Sundseth, S. S., Srivastava, P. K., and Lapenson, D. P. (1992) *Cancer Res* **52**(20), 5797-5802

44. Schuetz, E. G., Beck, W. T., and Schuetz, J. D. (1996) *Mol Pharmacol* **49**(2), 311-318

45. Ramachandra, M., Ambudkar, S. V., Chen, D., Hrycyna, C. A., Dey, S., Gottesman, M. M., and Pastan, I. (1998) *Biochemistry* **37**(14), 5010-5019

46. Georges, E., Tsuruo, T., and Ling, V. (1993) *J Biol Chem* **268**(3), 1792-1798

47. Ruetz, S., and Gros, P. (1994) *Cell* **77**(7), 1071-1081

48. van Helvoort, A., Smith, A. J., Sprong, H., Fritzsche, I., Schinkel, A. H., Borst, P., and van Meer, G. (1996) *Cell* **87**(3), 507-517

49. Smith, A. J., van Helvoort, A., van Meer, G., Szabo, K., Welker, E., Szakacs, G., Varadi, A., Sarkadi, B., and Borst, P. (2000) *J Biol Chem* **275**(31), 23530-23539

50. Wang, R., Salem, M., Yousef, I. M., Tuchweber, B., Lam, P., Childs, S. J., Helgason, C. D., Ackerley, C., Phillips, M. J., and Ling, V. (2001) *Proc Natl Acad Sci U S A* **98**(4), 2011-2016

51. Horio, M., Gottesman, M. M., and Pastan, I. (1988) *Proc Natl Acad Sci U S A* **85**(10), 3580-3584

52. Litman, T., Zeuthen, T., Skovsgaard, T., and Stein, W. D. (1997) *Biochim Biophys Acta* **1361**(2), 159-168

53. Shapiro, A. B., and Ling, V. (1994) *J Biol Chem* **269**(5), 3745-3754

54. Sharom, F. J., DiDiodato, G., Yu, X., and Ashbourne, K. J. (1995) *J Biol Chem* **270**(17), 10334-10341

55. Urbatsch, I. L., al-Shawi, M. K., and Senior, A. E. (1994) *Biochemistry* **33**(23), 7069-7076

56. Ernest, S., and Bello-Reuss, E. (1999) *J Am Soc Nephrol* **10**(11), 2306-2313

57. Raggers, R. J., Vogels, I., and van Meer, G. (2001) *Biochem J* **357**(Pt 3), 859-865

58. Ambudkar, S. V., Dey, S., Hrycyna, C. A., Ramachandra, M., Pastan, I., and Gottesman, M. M. (1999) *Annu Rev Pharmacol Toxicol* **39**, 361-398

59. al-Shawi, M. K., and Senior, A. E. (1993) *J Biol Chem* **268**(6), 4197-4206

60. Doige, C. A., and Sharom, F. J. (1992) *Biochim Biophys Acta* **1109**(2), 161-171

61. Sharom, F. J., Yu, X., Chu, J. W., and Doige, C. A. (1995) *Biochem J* **308 (Pt 2)**, 381-390

62. Sauna, Z. E., and Ambudkar, S. V. (2000) *Proc Natl Acad Sci U S A* **97**(6), 2515-2520

63. Azzaria, M., Schurr, E., and Gros, P. (1989) *Mol Cell Biol* **9**(12), 5289-5297

64. Hrycyna, C. A., Ramachandra, M., Ambudkar, S. V., Ko, Y. H., Pedersen, P. L., Pastan, I., and Gottesman, M. M. (1998) *J Biol Chem* **273**(27), 16631-16634

65. Sauna, Z. E., and Ambudkar, S. V. (2001) *J Biol Chem* **276**(15), 11653-11661

66. Senior, A. E., and Bhagat, S. (1998) *Biochemistry* **37**(3), 831-836

67. Gottesman, M. M., and Pastan, I. (1993) *Annu Rev Biochem* **62**, 385-427

68. Bertino, J. R. (2002) *Encyclopedia of cancer*, 2nd Ed., Academic Press, San Diego, Calif.

69. Cordon-Cardo, C., O'Brien, J. P., Boccia, J., Casals, D., Bertino, J. R., and Melamed, M. R. (1990) *J Histochem Cytochem* **38**(9), 1277-1287

70. Thiebaut, F., Tsuruo, T., Hamada, H., Gottesman, M. M., Pastan, I., and Willingham, M. C. (1987) *Proc Natl Acad Sci U S A* **84**(21), 7735-7738

71. Borst, P., and Schinkel, A. H. (1996) *Eur J Cancer* **32A**(6), 985-990

72. Schinkel, A. H., Mayer, U., Wagenaar, E., Mol, C. A., van Deemter, L., Smit, J. J., van der Valk, M. A., Voordouw, A. C., Spits, H., van Tellingen, O., Zijlmans, J. M., Fibbe, W. E., and Borst, P. (1997) *Proc Natl Acad Sci U S A* **94**(8), 4028-4033

73. Schinkel, A. H., Smit, J. J., van Tellingen, O., Beijnen, J. H., Wagenaar, E., van Deemter, L., Mol, C. A., van der Valk, M. A., Robanus-Maandag, E. C., te Riele, H. P., and et al. (1994) *Cell* **77**(4), 491-502

74. Chauncey, T. R., Rankin, C., Anderson, J. E., Chen, I., Kopecky, K. J., Godwin, J. E., Kalaycio, M. E., Moore, D. F., Shurafa, M. S., Petersdorf, S. H., Kraut, E. H., Leith, C. P., Head, D. R., Luthardt, F. W., Willman, C. L., and Appelbaum, F. R. (2000) *Leuk Res* **24**(7), 567-574

75. Han, K., Kahng, J., Kim, M., Lim, J., Kim, Y., Cho, B., Kim, H. K., Min, W. S., Kim, C. C., Lee, K. Y., Kim, B. K., and Kang, C. S. (2000) *Acta Haematol* **104**(4), 174-180

76. Zhou, D. C., Zittoun, R., and Marie, J. P. (1995) *Leukemia* **9**(10), 1661-1666

77. Filipits, M., Pohl, G., Stranzl, T., Suchomel, R. W., Scheper, R. J., Jager, U., Geissler, K., Lechner, K., and Pirker, R. (1998) *Blood* **91**(5), 1508-1513

78. Legrand, O., Simonin, G., Beauchamp-Nicoud, A., Zittoun, R., and Marie, J. P. (1999) *Blood* **94**(3), 1046-1056

79. Leith, C. P., Kopecky, K. J., Chen, I. M., Eijdems, L., Slovak, M. L., McConnell, T. S., Head, D. R., Weick, J., Grever, M. R., Appelbaum, F. R., and Willman, C. L. (1999) *Blood* **94**(3), 1086-1099

80. Michieli, M., Damiani, D., Ermacora, A., Masolini, P., Raspadori, D., Visani, G., Scheper, R. J., and Baccarani, M. (1999) *Br J Haematol* **104**(2), 328-335

81. Faneyte, I. F., Kristel, P. M., and van de Vijver, M. J. (2001) *Int J Cancer* **93**(1), 114-122

82. Yang, X., Uziely, B., Groshen, S., Lukas, J., Israel, V., Russell, C., Dunnington, G., Formenti, S., Muggia, F., and Press, M. F. (1999) *Lab Invest* **79**(3), 271-280

83. Tsuruo, T., Iida, H., Tsukagoshi, S., and Sakurai, Y. (1981) *Cancer Res* **41**(5), 1967-1972

84. Safa, A. R. (1988) *Proc Natl Acad Sci U S A* **85**(19), 7187-7191

85. Safa, A. R., Glover, C. J., Meyers, M. B., Biedler, J. L., and Felsted, R. L. (1986) *J Biol Chem* **261**(14), 6137-6140

86. Tamai, I., and Safa, A. R. (1991) *J Biol Chem* **266**(25), 16796-16800

87. Akiyama, S., Yoshimura, A., Kikuchi, H., Sumizawa, T., Kuwano, M., and Tahara, Y. (1989) *Mol Pharmacol* **36**(5), 730-735

88. Foxwell, B. M., Mackie, A., Ling, V., and Ryffel, B. (1989) *Mol Pharmacol* **36**(4), 543-546

89. Safa, A. R., Agresti, M., Bryk, D., and Tamai, I. (1994) *Biochemistry* **33**(1), 256-265

90. Leonard, G. D., Fojo, T., and Bates, S. E. (2003) *Oncologist* **8**(5), 411-424

91. Advani, R., Visani, G., Milligan, D., Saba, H., Tallman, M., Rowe, J. M., Wiernik, P. H., Ramek, J., Dugan, K., Lum, B., Villena, J., Davis, E., Paietta, E., Litchman, M., Covelli, A., Sikic, B., and Greenberg, P. (1999) *Adv Exp Med Biol* **457**, 47-56

92. Visani, G., Milligan, D., Leoni, F., Chang, J., Kelsey, S., Marcus, R., Powles, R., Schey, S., Covelli, A., Isidori, A., Litchman, M., Piccaluga, P. P., Mayer, H., Malagola, M., and Pfister, C. (2001) *Leukemia* **15**(5), 764-771

93. Dorr, R., Karanes, C., Spier, C., Grogan, T., Greer, J., Moore, J., Weinberger, B., Schiller, G., Pearce, T., Litchman, M., Dalton, W., Roe, D., and List, A. F. (2001) *J Clin Oncol* **19**(6), 1589-1599

94. Bramwell, V. H., Morris, D., Ernst, D. S., Hings, I., Blackstein, M., Venner, P. M., Ette, E. I., Harding, M. W., Waxman, A., and Demetri, G. D. (2002) *Clin Cancer Res* **8**(2), 383-393

95. Toppmeyer, D., Seidman, A. D., Pollak, M., Russell, C., Tkaczuk, K., Verma, S., Overmoyer, B., Garg, V., Ette, E., Harding, M. W., and Demetri, G. D. (2002) *Clin Cancer Res* **8**(3), 670-678

96. Dantzig, A. H., Shepard, R. L., Law, K. L., Tabas, L., Pratt, S., Gillespie, J. S., Binkley, S. N., Kuhfeld, M. T., Starling, J. J., and Wrighton, S. A. (1999) *J Pharmacol Exp Ther* **290**(2), 854-862

97. Wandel, C., Kim, R. B., Kajiji, S., Guengerich, P., Wilkinson, G. R., and Wood, A. J. (1999) *Cancer Res* **59**(16), 3944-3948

98. van Zuylen, L., Nooter, K., Sparreboom, A., and Verweij, J. (2000) *Invest New Drugs* **18**(3), 205-220

99. Roe, M., Folkes, A., Ashworth, P., Brumwell, J., Chima, L., Hunjan, S., Pretswell, I., Dangerfield, W., Ryder, H., and Charlton, P. (1999) *Bioorg Med Chem Lett* **9**(4), 595-600

100. Starling, J. J., Shepard, R. L., Cao, J., Law, K. L., Norman, B. H., Kroin, J. S., Ehlhardt, W. J., Baughman, T. M., Winter, M. A., Bell, M. G., Shih, C., Gruber, J., Elmquist, W. F., and Dantzig, A. H. (1997) *Adv Enzyme Regul* **37**, 335-347

101. Newman, M. J., Rodarte, J. C., Benbatoul, K. D., Romano, S. J., Zhang, C., Krane, S., Moran, E. J., Uyeda, R. T., Dixon, R., Guns, E. S., and Mayer, L. D. (2000) *Cancer Res* **60**(11), 2964-2972

102. Thomas, H., and Coley, H. M. (2003) *Cancer Control* **10**(2), 159-165

103. Bech-Hansen, N. T., Till, J. E., and Ling, V. (1976) *J Cell Physiol* **88**(1), 23-31

104. Cano-Gauci, D. F., and Riordan, J. R. (1987) *Biochem Pharmacol* **36**(13), 2115-2123

105. Porter, C. W., Ganis, B., Rustum, Y., Wrzosek, C., Kramer, D. L., and Bergeron, R. J. (1994) *Cancer Res* **54**(22), 5917-5924

106. Cano-Gauci, D. F., Seibert, F. S., Safa, A. R., and Riordan, J. R. (1995) *Biochem Biophys Res Commun* **209**(2), 497-505

107. Croop, J. M., Guild, B. C., Gros, P., and Housman, D. E. (1987) *Cancer Res* **47**(22), 5982-5988

108. Stow, M. W., and Warr, J. R. (1991) *Biochim Biophys Acta* **1092**(1), 7-14

109. Stow, M. W., and Warr, J. R. (1993) *FEBS Lett* **320**(2), 87-91

110. Vickers, S. E., Stow, M. W., and Warr, J. R. (1993) *Cell Biol Int* **17**(5), 477-485

111. Warr, J. R., Anderson, M., and Fergusson, J. (1988) *Cancer Res* **48**(16), 4477-4483

112. Warr, J. R., Quinn, D., Elend, M., and Fenton, J. A. (1995) *Cancer Lett* **98**(1), 115-120

113. Mirski, S. E., Gerlach, J. H., and Cole, S. P. (1987) *Cancer Res* **47**(10), 2594-2598

114. Cole, S. P. (1990) *Cancer Chemother Pharmacol* **26**(4), 250-256

115. Borst, P., Evers, R., Kool, M., and Wijnholds, J. (1999) *Biochim Biophys Acta* **1461**(2), 347-357

116. Bakos, E., Hegedus, T., Hollo, Z., Welker, E., Tusnady, G. E., Zaman, G. J., Flens, M. J., Varadi, A., and Sarkadi, B. (1996) *J Biol Chem* **271**(21), 12322-12326

117. Hipfner, D. R., Almquist, K. C., Leslie, E. M., Gerlach, J. H., Grant, C. E., Deeley, R. G., and Cole, S. P. (1997) *J Biol Chem* **272**(38), 23623-23630

118. Borst, P., and Schinkel, A. H. (1997) *Trends Genet* **13**(6), 217-222

119. Germann, U. A. (1996) *Eur J Cancer* **32A**(6), 927-944

120. Cole, S. P., Sparks, K. E., Fraser, K., Loe, D. W., Grant, C. E., Wilson, G. M., and Deeley, R. G. (1994) *Cancer Res* **54**(22), 5902-5910

121. Gao, M., Yamazaki, M., Loe, D. W., Westlake, C. J., Grant, C. E., Cole, S. P., and Deeley, R. G. (1998) *J Biol Chem* **273**(17), 10733-10740

122. Hooijberg, J. H., Broxterman, H. J., Kool, M., Assaraf, Y. G., Peters, G. J., Noordhuis, P., Scheper, R. J., Borst, P., Pinedo, H. M., and Jansen, G. (1999) *Cancer Res* **59**(11), 2532-2535

123. Evers, R., Cnubben, N. H., Wijnholds, J., van Deemter, L., van Bladeren, P. J., and Borst, P. (1997) *FEBS Lett* **419**(1), 112-116

124. Jedlitschky, G., Leier, I., Buchholz, U., Center, M., and Keppler, D. (1994) *Cancer Res* **54**(18), 4833-4836

125. Leier, I., Jedlitschky, G., Buchholz, U., Cole, S. P., Deeley, R. G., and Keppler, D. (1994) *J Biol Chem* **269**(45), 27807-27810

126. Loe, D. W., Stewart, R. K., Massey, T. E., Deeley, R. G., and Cole, S. P. (1997) *Mol Pharmacol* **51**(6), 1034-1041

127. Jedlitschky, G., Leier, I., Buchholz, U., Barnouin, K., Kurz, G., and Keppler, D. (1996) *Cancer Res* **56**(5), 988-994

128. Leier, I., Jedlitschky, G., Buchholz, U., Center, M., Cole, S. P., Deeley, R. G., and Keppler, D. (1996) *Biochem J* **314 (Pt 2)**, 433-437

129. Loe, D. W., Almquist, K. C., Deeley, R. G., and Cole, S. P. (1996) *J Biol Chem* **271**(16), 9675-9682

130. Loe, D. W., Deeley, R. G., and Cole, S. P. (1998) *Cancer Res* **58**(22), 5130-5136

131. Renes, J., de Vries, E. G., Nienhuis, E. F., Jansen, P. L., and Muller, M. (1999) *Br J Pharmacol* **126**(3), 681-688

132. Leslie, E. M., Ito, K., Upadhyaya, P., Hecht, S. S., Deeley, R. G., and Cole, S. P. (2001) *J Biol Chem* **276**(30), 27846-27854

133. Bakos, E., Evers, R., Sinko, E., Varadi, A., Borst, P., and Sarkadi, B. (2000) *Mol Pharmacol* **57**(4), 760-768

134. Loe, D. W., Deeley, R. G., and Cole, S. P. (2000) *J Pharmacol Exp Ther* **293**(2), 530-538

135. Loe, D. W., Oleschuk, C. J., Deeley, R. G., and Cole, S. P. (2000) *Biochem Biophys Res Commun* **275**(3), 795-803

136. Leslie, E. M., Bowers, R. J., Deeley, R. G., and Cole, S. P. (2003) *J Pharmacol Exp Ther* **304**(2), 643-653

137. Leslie, E. M., Mao, Q., Oleschuk, C. J., Deeley, R. G., and Cole, S. P. (2001) *Mol Pharmacol* **59**(5), 1171-1180

138. Loe, D. W., Almquist, K. C., Cole, S. P., and Deeley, R. G. (1996) *J Biol Chem* **271**(16), 9683-9689

139. Flens, M. J., Zaman, G. J., van der Valk, P., Izquierdo, M. A., Schroeijers, A. B., Scheffer, G. L., van der Groep, P., de Haas, M., Meijer, C. J., and Scheper, R. J. (1996) *Am J Pathol* **148**(4), 1237-1247

140. Wijnholds, J., Evers, R., van Leusden, M. R., Mol, C. A., Zaman, G. J., Mayer, U., Beijnen, J. H., van der Valk, M., Krimpenfort, P., and Borst, P. (1997) *Nat Med* **3**(11), 1275-1279

141. Drazen, J. M., Israel, E., and O'Byrne, P. M. (1999) *N Engl J Med* **340**(3), 197-206

142. Samuelsson, B., Dahlen, S. E., Lindgren, J. A., Rouzer, C. A., and Serhan, C. N. (1987) *Science* **237**(4819), 1171-1176

143. St-Pierre, M. V., Serrano, M. A., Macias, R. I., Dubs, U., Hoechli, M., Lauper, U., Meier, P. J., and Marin, J. J. (2000) *Am J Physiol Regul Integr Comp Physiol* **279**(4), R1495-1503

144. Wijnholds, J., deLange, E. C., Scheffer, G. L., van den Berg, D. J., Mol, C. A., van der Valk, M., Schinkel, A. H., Scheper, R. J., Breimer, D. D., and Borst, P. (2000) *J Clin Invest* **105**(3), 279-285

145. Wijnholds, J., Scheffer, G. L., van der Valk, M., van der Valk, P., Beijnen, J. H., Scheper, R. J., and Borst, P. (1998) *J Exp Med* **188**(5), 797-808

146. Wright, S. R., Boag, A. H., Valdimarsson, G., Hipfner, D. R., Campling, B. G., Cole, S. P., and Deeley, R. G. (1998) *Clin Cancer Res* **4**(9), 2279-2289

147. Ota, E., Abe, Y., Oshika, Y., Ozeki, Y., Iwasaki, M., Inoue, H., Yamazaki, H., Ueyama, Y., Takagi, K., Ogata, T., and et al. (1995) *Br J Cancer* **72**(3), 550-554

148. Nooter, K., Brutel de la Riviere, G., Look, M. P., van Wingerden, K. E., Henzen-Logmans, S. C., Scheper, R. J., Flens, M. J., Klijn, J. G., Stoter, G., and Foekens, J. A. (1997) *Br J Cancer* **76**(4), 486-493

149. Tada, Y., Wada, M., Migita, T., Nagayama, J., Hinoshita, E., Mochida, Y., Maehara, Y., Tsuneyoshi, M., Kuwano, M., and Naito, S. (2002) *Int J Cancer* **98**(4), 630-635

150. Cavalla, D., and Neff, N. H. (1985) *Biochem Pharmacol* **34**(16), 2821-2826

151. Beck, W. T., Cirtain, M. C., Glover, C. J., Felsted, R. L., and Safa, A. R. (1988) *Biochem Biophys Res Commun* **153**(3), 959-966

152. Cornwell, M. M., Safa, A. R., Felsted, R. L., Gottesman, M. M., and Pastan, I. (1986) *Proc Natl Acad Sci U S A* **83**(11), 3847-3850

153. Beck, W. T., and Qian, X. D. (1992) *Biochem Pharmacol* **43**(1), 89-93

154. Busche, R., Tummler, B., Riordan, J. R., and Cano-Gauci, D. F. (1989) *Mol Pharmacol* **35**(4), 414-421

155. Safa, A. R. (1998) *Methods Enzymol* **292**, 289-307

156. Nare, B., Prichard, R. K., and Georges, E. (1994) *Mol Pharmacol* **45**(6), 1145-1152

157. Daoud, R., Julien, M., Gros, P., and Georges, E. (2001) *J Biol Chem* **276**(15), 12324-12330

158. Daoud, R., Kast, C., Gros, P., and Georges, E. (2000) *Biochemistry* **39**(50), 15344-15352

159. Cai, J., Daoud, R., Alqawi, O., Georges, E., Pelletier, J., and Gros, P. (2002) *Biochemistry* **41**(25), 8058-8067

160. Alqawi, O., Poelarends, G., Konings, W. N., and Georges, E. (2003) *Biochem Biophys Res Commun* **311**(3), 696-701

161. Safa, A. R., Glover, C. J., Sewell, J. L., Meyers, M. B., Biedler, J. L., and Felsted, R. L. (1987) *J Biol Chem* **262**(16), 7884-7888

162. Bruggemann, E. P., Currier, S. J., Gottesman, M. M., and Pastan, I. (1992) *J Biol Chem* **267**(29), 21020-21026

163. Greenberger, L. M. (1993) *J Biol Chem* **268**(15), 11417-11425

164. Morris, D. I., Speicher, L. A., Ruoho, A. E., Tew, K. D., and Seamon, K. B. (1991) *Biochemistry* **30**(34), 8371-8379

165. Devine, S. E., Ling, V., and Melera, P. W. (1992) *Proc Natl Acad Sci U S A* **89**(10), 4564-4568

166. Hafkemeyer, P., Dey, S., Ambudkar, S. V., Hrycyna, C. A., Pastan, I., and Gottesman, M. M. (1998) *Biochemistry* **37**(46), 16400-16409

167. Loo, T. W., and Clarke, D. M. (1997) *J Biol Chem* **272**(51), 31945-31948

168. Loo, T. W., and Clarke, D. M. (1999) *J Biol Chem* **274**(50), 35388-35392

169. Loo, T. W., and Clarke, D. M. (2000) *J Biol Chem* **275**(50), 39272-39278

170. Loo, T. W., and Clarke, D. M. (2001) *J Biol Chem* **276**(18), 14972-14979

171. Loo, T. W., and Clarke, D. M. (2002) *J Biol Chem* **277**(46), 44332-44338

172. Tamai, I., and Safa, A. R. (1990) *J Biol Chem* **265**(27), 16509-16513

173. Demmer, A., Thole, H., Kubesch, P., Brandt, T., Raida, M., Fislage, R., and Tummler, B. (1997) *J Biol Chem* **272**(33), 20913-20919

174. Wu, Q., Bounaud, P. Y., Kuduk, S. D., Yang, C. P., Ojima, I., Horwitz, S. B., and Orr, G. A. (1998) *Biochemistry* **37**(32), 11272-11279

175. Ayesh, S., Shao, Y. M., and Stein, W. D. (1996) *Biochim Biophys Acta* **1316**(1), 8-18

176. Shao, Y. M., Ayesh, S., and Stein, W. D. (1997) *Biochim Biophys Acta* **1360**(1), 30-38

177. Shapiro, A. B., Fox, K., Lam, P., and Ling, V. (1999) *Eur J Biochem* **259**(3), 841-850

178. Robbiani, D. F., Finch, R. A., Jager, D., Muller, W. A., Sartorelli, A. C., and Randolph, G. J. (2000) *Cell* **103**(5), 757-768

179. Leier, I., Jedlitschky, G., Buchholz, U., and Keppler, D. (1994) *Eur J Biochem* **220**(2), 599-606

180. Qian, Y. M., Qiu, W., Gao, M., Westlake, C. J., Cole, S. P., and Deeley, R. G. (2001) *J Biol Chem* **276**(42), 38636-38644

181. Gekeler, V., Ise, W., Sanders, K. H., Ulrich, W. R., and Beck, J. (1995) *Biochem Biophys Res Commun* **208**(1), 345-352

182. Hipfner, D. R., Gauldie, S. D., Deeley, R. G., and Cole, S. P. (1994) *Cancer Res* **54**(22), 5788-5792

183. Vezmar, M., Deady, L. W., Tilley, L., and Georges, E. (1997) *Biochem Biophys Res Commun* **241**(1), 104-111

184. Vezmar, M., and Georges, E. (1998) *Biochem Pharmacol* **56**(6), 733-742

185. Vezmar, M., and Georges, E. (2000) *Biochem Pharmacol* **59**(10), 1245-1252

186. Daoud, R., Desneves, J., Deady, L. W., Tilley, L., Scheper, R. J., Gros, P., and Georges, E. (2000) *Biochemistry* **39**(20), 6094-6102

187. Hipfner, D. R., Almquist, K. C., Stride, B. D., Deeley, R. G., and Cole, S. P. (1996) *Cancer Res* **56**(14), 3307-3314

188. Johnson, L. V., Walsh, M. L., and Chen, L. B. (1980) *Proc Natl Acad Sci U S A* **77**(2), 990-994

189. Neyfakh, A. A. (1988) *Exp Cell Res* **174**(1), 168-176

190. Kast, C., and Gros, P. (1997) *J Biol Chem* **272**(42), 26479-26487

191. Kast, C., and Gros, P. (1998) *Biochemistry* **37**(8), 2305-2313

192. Dey, S., Ramachandra, M., Pastan, I., Gottesman, M. M., and Ambudkar, S. V. (1997) *Proc Natl Acad Sci U S A* **94**(20), 10594-10599

193. Germann, U. A., Shlyakhter, D., Mason, V. S., Zelle, R. E., Duffy, J. P., Galullo, V., Armistead, D. M., Saunders, J. O., Boger, J., and Harding, M. W. (1997) *Anticancer Drugs* **8**(2), 125-140

194. Germann, U. A., Ford, P. J., Shlyakhter, D., Mason, V. S., and Harding, M. W. (1997) *Anticancer Drugs* **8**(2), 141-155

195. Zaman, G. J., Lankelma, J., van Tellingen, O., Beijnen, J., Dekker, H., Paulusma, C., Oude Elferink, R. P., Baas, F., and Borst, P. (1995) *Proc Natl Acad Sci U S A* **92**(17), 7690-7694

196. Ren, X. Q., Furukawa, T., Aoki, S., Nakajima, T., Sumizawa, T., Haraguchi, M., Chen, Z. S., Kobayashi, M., and Akiyama, S. (2001) *J Biol Chem* **276**(25), 23197-23206

197. Ren, X. Q., Furukawa, T., Aoki, S., Sumizawa, T., Haraguchi, M., Che, X. F., Kobayashi, M., and Akiyama, S. (2003) *Br J Pharmacol* **138**(8), 1553-1561

198. Ryu, S., Kawabe, T., Nada, S., and Yamaguchi, A. (2000) *J Biol Chem* **275**(50), 39617-39624

199. Norman, B. H., Gruber, J. M., Hollinshead, S. P., Wilson, J. W., Starling, J. J., Law, K. L., Self, T. D., Tabas, L. B., Williams, D. C., Paul, D. C., Wagner, M. M., and Dantzig, A. H. (2002) *Bioorg Med Chem Lett* **12**(6), 883-886

200. Mao, Q., Qiu, W., Weigl, K. E., Lander, P. A., Tabas, L. B., Shepard, R. L., Dantzig, A. H., Deeley, R. G., and Cole, S. P. (2002) *J Biol Chem* **277**(32), 28690-28699

201. Qian, Y. M., Grant, C. E., Westlake, C. J., Zhang, D. W., Lander, P. A., Shepard, R. L., Dantzig, A. H., Cole, S. P., and Deeley, R. G. (2002) *J Biol Chem* **277**(38), 35225-35231

202. Zhang, D. W., Cole, S. P., and Deeley, R. G. (2001) *J Biol Chem* **276**(37), 34966-34974

203. Rappa, G., Lorico, A., Flavell, R. A., and Sartorelli, A. C. (1997) *Cancer Res* **57**(23), 5232-5237

204. Meister, A. (1988) *J Biol Chem* **263**(33), 17205-17208

205. Ciaccio, P. J., Shen, H., Kruh, G. D., and Tew, K. D. (1996) *Biochem Biophys Res Commun* **222**(1), 111-115

206. Horvitz, H. R., Shaham, S., and Hengartner, M. O. (1994) *Cold Spring Harb Symp Quant Biol* **59**, 377-385

207. Kerr, J. F., Wyllie, A. H., and Currie, A. R. (1972) *Br J Cancer* **26**(4), 239-257

208. Ashkenazi, A., and Dixit, V. M. (1998) *Science* **281**(5381), 1305-1308

209. Thornberry, N. A., and Lazebnik, Y. (1998) *Science* **281**(5381), 1312-1316

210. Orrenius, S. (2004) *Toxicol Lett* **149**(1-3), 19-23

211. Hengartner, M. O. (1999) *Recent Prog Horm Res* **54**, 213-222; discussion 222-214

212. Horvitz, H. R. (1999) *Cancer Res* **59**(7 Suppl), 1701s-1706s

213. Liu, Q. A., and Hengartner, M. O. (1999) *Ann N Y Acad Sci* **887**, 92-104

214. Zou, H., Henzel, W. J., Liu, X., Lutschg, A., and Wang, X. (1997) *Cell* **90**(3), 405-413

215. Zou, H., Li, Y., Liu, X., and Wang, X. (1999) *J Biol Chem* **274**(17), 11549-11556

216. Jiang, X., and Wang, X. (2000) *J Biol Chem* **275**(40), 31199-31203

217. Rodriguez, J., and Lazebnik, Y. (1999) *Genes Dev* **13**(24), 3179-3184

218. Zou, H., Yang, R., Hao, J., Wang, J., Sun, C., Fesik, S. W., Wu, J. C., Tomaselli, K. J., and Armstrong, R. C. (2003) *J Biol Chem* **278**(10), 8091-8098

219. Bratton, S. B., Walker, G., Srinivasula, S. M., Sun, X. M., Butterworth, M., Alnemri, E. S., and Cohen, G. M. (2001) *Embo J* **20**(5), 998-1009

220. Ekert, P. G., Silke, J., Hawkins, C. J., Verhagen, A. M., and Vaux, D. L. (2001) *J Cell Biol* **152**(3), 483-490

221. Srinivasula, S. M., Hegde, R., Saleh, A., Datta, P., Shiozaki, E., Chai, J., Lee, R. A., Robbins, P. D., Fernandes-Alnemri, T., Shi, Y., and Alnemri, E. S. (2001) *Nature* **410**(6824), 112-116

222. Jiang, X., and Wang, X. (2004) *Annu Rev Biochem* **73**, 87-106

223. Du, C., Fang, M., Li, Y., Li, L., and Wang, X. (2000) *Cell* **102**(1), 33-42

224. Verhagen, A. M., Ekert, P. G., Pakusch, M., Silke, J., Connolly, L. M., Reid, G. E., Moritz, R. L., Simpson, R. J., and Vaux, D. L. (2000) *Cell* **102**(1), 43-53

225. Chai, J., Du, C., Wu, J. W., Kyin, S., Wang, X., and Shi, Y. (2000) *Nature* **406**(6798), 855-862

226. Liu, Z., Sun, C., Olejniczak, E. T., Meadows, R. P., Betz, S. F., Oost, T., Herrmann, J., Wu, J. C., and Fesik, S. W. (2000) *Nature* **408**(6815), 1004-1008

227. Jin, S., Kalkum, M., Overholtzer, M., Stoffel, A., Chait, B. T., and Levine, A. J. (2003) *Genes Dev* **17**(3), 359-367

228. Yang, Q. H., Church-Hajduk, R., Ren, J., Newton, M. L., and Du, C. (2003) *Genes Dev* **17**(12), 1487-1496

229. Susin, S. A., Lorenzo, H. K., Zamzami, N., Marzo, I., Snow, B. E., Brothers, G. M., Mangion, J., Jacotot, E., Costantini, P., Loeffler, M., Larochette, N., Goodlett, D. R., Aebersold, R., Siderovski, D. P., Penninger, J. M., and Kroemer, G. (1999) *Nature* **397**(6718), 441-446

230. Li, L. Y., Luo, X., and Wang, X. (2001) *Nature* **412**(6842), 95-99

231. Faccio, L., Fusco, C., Chen, A., Martinotti, S., Bonventre, J. V., and Zervos, A. S. (2000) *J Biol Chem* **275**(4), 2581-2588

232. Gray, C. W., Ward, R. V., Karran, E., Turconi, S., Rowles, A., Viglienghi, D., Southan, C., Barton, A., Fantom, K. G., West, A., Savopoulos, J., Hassan, N. J., Clinkenbeard, H., Hanning, C., Amegadzie, B., Davis, J. B., Dingwall, C., Livi, G. P., and Creasy, C. L. (2000) *Eur J Biochem* **267**(18), 5699-5710

233. Spiess, C., Beil, A., and Ehrmann, M. (1999) *Cell* **97**(3), 339-347

234. Goldstein, J. C., Waterhouse, N. J., Juin, P., Evan, G. I., and Green, D. R. (2000) *Nat Cell Biol* **2**(3), 156-162

235. Mattson, M. P., and Kroemer, G. (2003) *Trends Mol Med* **9**(5), 196-205

236. Shi, Y. F., Sahai, B. M., and Green, D. R. (1989) *Nature* **339**(6226), 625-626

237. Chang, L. K., Schmidt, R. E., and Johnson, E. M., Jr. (2003) *J Cell Biol* **162**(2), 245-256

238. Yang, J., Liu, X., Bhalla, K., Kim, C. N., Ibrado, A. M., Cai, J., Peng, T. I., Jones, D. P., and Wang, X. (1997) *Science* **275**(5303), 1129-1132

239. Kirkin, V., Joos, S., and Zornig, M. (2004) *Biochim Biophys Acta* **1644**(2-3), 229-249

240. Cheng, E. H., Sheiko, T. V., Fisher, J. K., Craigen, W. J., and Korsmeyer, S. J. (2003) *Science* **301**(5632), 513-517

241. Borner, C. (2003) *Mol Immunol* **39**(11), 615-647

242. Schlesinger, P. H., Gross, A., Yin, X. M., Yamamoto, K., Saito, M., Waksman, G., and Korsmeyer, S. J. (1997) *Proc Natl Acad Sci U S A* **94**(21), 11357-11362

243. Tsujimoto, Y., and Shimizu, S. (2000) *Cell Death Differ* **7**(12), 1174-1181

244. Zamzami, N., and Kroemer, G. (2001) *Nat Rev Mol Cell Biol* **2**(1), 67-71

245. Muchmore, S. W., Sattler, M., Liang, H., Meadows, R. P., Harlan, J. E., Yoon, H. S., Nettesheim, D., Chang, B. S., Thompson, C. B., Wong, S. L., Ng, S. L., and Fesik, S. W. (1996) *Nature* **381**(6580), 335-341

246. Kandasamy, K., Srinivasula, S. M., Alnemri, E. S., Thompson, C. B., Korsmeyer, S. J., Bryant, J. L., and Srivastava, R. K. (2003) *Cancer Res* **63**(7), 1712-1721

247. Bargou, R. C., Wagener, C., Bommert, K., Mapara, M. Y., Daniel, P. T., Arnold, W., Dietel, M., Guski, H., Feller, A., Royer, H. D., and Dorken, B. (1996) *J Clin Invest* **97**(11), 2651-2659

248. Beerheide, W., Tan, Y. J., Teng, E., Ting, A. E., Jedpiyawongse, A., and Srivatanakul, P. (2000) *Biochem Biophys Res Commun* **273**(1), 54-61

249. Pepper, C., Thomas, A., Hoy, T., and Bentley, P. (1999) *Br J Haematol* **104**(3), 581-588

250. Cory, S., and Adams, J. M. (2002) *Nat Rev Cancer* **2**(9), 647-656

251. Grinberg, M., Sarig, R., Zaltsman, Y., Frumkin, D., Grammatikakis, N., Reuveny, E., and Gross, A. (2002) *J Biol Chem* **277**(14), 12237-12245

252. Wei, M. C., Lindsten, T., Mootha, V. K., Weiler, S., Gross, A., Ashiya, M., Thompson, C. B., and Korsmeyer, S. J. (2000) *Genes Dev* **14**(16), 2060-2071

253. Panaretakis, T., Pokrovskaja, K., Shoshan, M. C., and Grander, D. (2002) *J Biol Chem* **277**(46), 44317-44326

254. Mandic, A., Viktorsson, K., Strandberg, L., Heiden, T., Hansson, J., Linder, S., and Shoshan, M. C. (2002) *Mol Cell Biol* **22**(9), 3003-3013

255. Bakhshi, A., Jensen, J. P., Goldman, P., Wright, J. J., McBride, O. W., Epstein, A. L., and Korsmeyer, S. J. (1985) *Cell* **41**(3), 899-906

256. Cleary, M. L., Smith, S. D., and Sklar, J. (1986) *Cell* **47**(1), 19-28

257. Tsujimoto, Y., Finger, L. R., Yunis, J., Nowell, P. C., and Croce, C. M. (1984) *Science* **226**(4678), 1097-1099

258. Hockenbery, D., Nunez, G., Milliman, C., Schreiber, R. D., and Korsmeyer, S. J. (1990) *Nature* **348**(6299), 334-336

259. Vaux, D. L., Cory, S., and Adams, J. M. (1988) *Nature* **335**(6189), 440-442

260. Jiang, M., and Milner, J. (2003) *Genes Dev* **17**(7), 832-837

261. Perez-Campo, R., Lopez-Torres, M., Cadenas, S., Rojas, C., and Barja, G. (1998) *J Comp Physiol [B]* **168**(3), 149-158

262. Sohal, R. S., and Allen, R. G. (1985) *Basic Life Sci* **35**, 75-104

263. Muller, F. L., Roberts, A. G., Bowman, M. K., and Kramer, D. M. (2003) *Biochemistry* **42**(21), 6493-6499

264. St-Pierre, J., Buckingham, J. A., Roebuck, S. J., and Brand, M. D. (2002) *J Biol Chem* **277**(47), 44784-44790

265. Turrens, J. F. (1997) *Biosci Rep* **17**(1), 3-8

266. Scheffler, I. E. (1999) *Mitochondria*, Wiley-Liss, New York

267. Miwa, S., and Brand, M. D. (2003) *Biochem Soc Trans* **31**(Pt 6), 1300-1301

268. Murphy, M. P., Echtay, K. S., Blaikie, F. H., Asin-Cayuela, J., Cocheme, H. M., Green, K., Buckingham, J. A., Taylor, E. R., Hurrell, F., Hughes, G., Miwa, S., Cooper, C. E., Svistunenko, D. A., Smith, R. A., and Brand, M. D. (2003) *J Biol Chem* **278**(49), 48534-48545

269. Buttke, T. M., and Sandstrom, P. A. (1994) *Immunol Today* **15**(1), 7-10

270. Halliwell, B., and Gutteridge, J. M. C. (1985) *Free radicals in biology and medicine*, Clarendon Press, Oxford

271. Crompton, M. (1999) *Biochem J* **341 (Pt 2)**, 233-249

272. Lennon, S. V., Martin, S. J., and Cotter, T. G. (1991) *Cell Prolif* **24**(2), 203-214

273. Kumar, D., Lou, H., and Singal, P. K. (2002) *Herz* **27**(7), 662-668

274. Mihara, S., Suzuki, N., Wakisaka, S., Suzuki, S., Sekita, N., Yamamoto, S., Saito, N., Hoshino, T., and Sakane, T. (1999) *J Clin Endocrinol Metab* **84**(4), 1378-1385

275. Russell, J. W., Golovoy, D., Vincent, A. M., Mahendru, P., Olzmann, J. A., Mentzer, A., and Feldman, E. L. (2002) *Faseb J* **16**(13), 1738-1748

276. Brookes, P. S., and Darley-Usmar, V. M. (2004) *Am J Physiol Heart Circ Physiol* **286**(1), H39-46

277. Castilho, R. F., Kowaltowski, A. J., Meinicke, A. R., Bechara, E. J., and Vercesi, A. E. (1995) *Free Radic Biol Med* **18**(3), 479-486

278. Packer, M. A., and Murphy, M. P. (1994) *FEBS Lett* **345**(2-3), 237-240

279. Halestrap, A. P., and Brennerb, C. (2003) *Curr Med Chem* **10**(16), 1507-1525

280. Grijalba, M. T., Vercesi, A. E., and Schreier, S. (1999) *Biochemistry* **38**(40), 13279-13287

281. Kowaltowski, A. J., Naia-da-Silva, E. S., Castilho, R. F., and Vercesi, A. E. (1998) *Arch Biochem Biophys* **359**(1), 77-81

282. Clarke, A. R., Purdie, C. A., Harrison, D. J., Morris, R. G., Bird, C. C., Hooper, M. L., and Wyllie, A. H. (1993) *Nature* **362**(6423), 849-852

283. Christ, M., Luu, B., Mejia, J. E., Moosbrugger, I., and Bischoff, P. (1993) *Immunology* **78**(3), 455-460

284. Schreck, R., Albermann, K., and Baeuerle, P. A. (1992) *Free Radic Res Commun* **17**(4), 221-237

285. Davis, W., Jr., Ronai, Z., and Tew, K. D. (2001) *J Pharmacol Exp Ther* **296**(1), 1-6

286. Chung, Y. M., Bae, Y. S., and Lee, S. Y. (2003) *Free Radic Biol Med* **34**(4), 434-442

287. Jacobson, M. D. (1996) *Trends Biochem Sci* **21**(3), 83-86

288. Brookes, P., and Darley-Usmar, V. M. (2002) *Free Radic Biol Med* **32**(4), 370-374

289. Brookes, P. S., Levonen, A. L., Shiva, S., Sarti, P., and Darley-Usmar, V. M. (2002) *Free Radic Biol Med* **33**(6), 755-764

290. Sauer, H., Wartenberg, M., and Hescheler, J. (2001) *Cell Physiol Biochem* **11**(4), 173-186

291. Halliwell, B., and Gutteridge, J. M. C. (1999) *Free radicals in biology and medicine*, 3rd Ed., Clarendon Press; Oxford University Press, Oxford, New York

292. Wu, G., Fang, Y. Z., Yang, S., Lupton, J. R., and Turner, N. D. (2004) *J Nutr* **134**(3), 489-492

Chapter 2:

A mechanism for P-glycoprotein mediated apoptosis as revealed by verapamil hypersensitivity

Joel Karwatsky, Maximilian C. Lincoln, and Elias Georges

Institute of Parasitology, McGill University, Quebec, Canada

Biochemistry. 2003 Oct 28; 42(42):12163-73.

Abstract

Selection of tumour cell lines with anti-cancer drugs has led to the appearance of multidrug resistant (MDR) subclones with P-glycoprotein 1 (P-gp1) expression that are cross resistant to several structurally and functionally dissimilar drugs. Interestingly, in the process of gaining resistance, MDR cells become hypersensitive, or develop collateral sensitivity to membrane-active agents, such as calcium channel blockers, steroids, and local anaesthetics. In this report, hypersensitivity to the calcium channel blocker verapamil was analysed in sensitive and resistant CHO cell lines. Our results show that treatment with verapamil preferentially induced apoptosis in MDR cells compared to drug sensitive cells. This effect was independent of p53 activity and could be inhibited by over-expression of the Bcl-2 gene. The induction of apoptosis by verapamil had a biphasic trend in which maximum cell death occurred at 10 μM, followed by improved cell survival at higher concentrations (50 μM). We correlated this effect to a similar biphasic trend in P-gp1 ATPase activation by verapamil in which low concentrations of verapamil (10 μM) activated ATPase, followed by inhibition at higher concentrations. To confirm the relationship between apoptosis and ATPase activity, we used two inhibitors of P-gp1 ATPase, PSC 833 and ivermectin. These ATPase inhibitors reduced hypersensitivity to verapamil in MDR cells. In addition, low concentrations of verapamil resulted in the production of reactive oxygen species (ROS) in MDR cells. Taken together, these results show that apoptosis was preferentially induced by P-gp1 expressing cells exposed to verapamil; an effect that was mediated by ROS produced in response the high ATP demand by P-gp1.

Introduction

The rise of multidrug resistant (MDR) tumour subclones has long been recognised as a major obstacle in clinical anti-cancer treatment. Although several mechanisms of drug resistance exist, the 170 kDa P-glycoprotein 1 (P-gp1) is one of the best-characterised causes of MDR. P-gp1 is an ATP-binding cassette (ABC) protein that causes energy-dependent efflux of many unrelated hydrophobic drugs from cancer cells [1,2]. Accordingly, much emphasis has been placed on identifying chemosensitizers, also called reversing agents. These are non-toxic compounds that interact with P-gp1 and inhibit its drug efflux function, thereby re-sensitising drug resistant cells [3]. Ironically, some MDR cells develop hypersensitivity to previously harmless drugs and chemosensitizers [4]. Hypersensitivity or "collateral sensitivity" in MDR cells has been observed with: calcium channel blockers [5,6], steroids [7], non-ionic detergents, and local anaesthetics [4,8]. The calcium channel blocker, verapamil is a classic chemosensitizer [9] that causes hypersensitivity in several MDR cell lines [5,6,10]. The MDR reversal effect of verapamil on P-gp1 is apparently independent of its ability to block calcium channels [5,11].

In addition to reversing drug resistance, verapamil induces a high level of ATP hydrolysis by P-gp1 [12]. Several reports have shown that the ATPase activity of P-gp1 is important for drug transport, although the mechanism by which ATP hydrolysis is coupled to drug transport is still unclear [13-15]. Unlike other ABC proteins, P-gp1 exhibits a high level of basal ATPase activity in the absence of drugs. The basal activity may be caused by transport of endogenous lipids or hydrophobic peptides [16,17]. ATPase activity that is uncoupled from substrate transport may also contribute to the basal activity [18]. Compounds that effect P-gp1 ATPase activity are classified into three categories. Class I compounds stimulate ATPase activity at low concentrations but inhibit activity at high concentrations. Class II compounds enhance ATPase activity as their concentration increases. Class III compounds inhibit basal and drug-stimulated ATPase activity [12,18-20]. Verapamil is a class I agent that increases ATPase to very high levels before inhibiting activity [19]. Other chemosensitizers such as cyclosporin A and the cyclosporin derivative PSC 833 are very effective class III ATPase inhibitors.

We report that the P-gp1 over-expressing Chinese hamster ovary (CHO) cell lines, CH^RC5 and CH^RB30, underwent heightened levels of apoptosis relative to the parental

AUXB1 and revertant I10 cells upon treatment with low concentrations of verapamil. Cell death was inhibited by the stable transfection of CH^RC5 with Bcl-2 and occurred independently of p53 activation. Verapamil-induced apoptosis was correlated to increased P-gp1 ATPase activation and elevated levels of reactive oxygen species (ROS). We used the ATPase inhibitors, PSC 833 and ivermectin to inhibit verapamil-induced ROS production, thereby reducing verapamil hypersensitivity. These observations suggest that the apoptotic pathway resulting from hypersensitivity to verapamil is mediated by ROS production via elevated oxidative phosphorylation.

Experimental Procedures

Reagents. All chemicals were of analytical grade and purchased from Sigma (Oakville, Ontario). PSC 833 was provided by Novartis (East Hanover, NJ). The Rc/RSV, LipofectAMINE, and G418 sulfate were purchased from Gibco-BRL (Burlington, Ontario). The ATPLite™ luminescence ATP detection system was obtained from PerkinElmer life sciences (Woodbridge, Ontario, Canada). Monoclonal anti-Bcl-2 (Ab-3) antibody was purchased from Calbiochem (San Diego, CA) and polyclonal anti-Bax (N-20) antibody was purchased from Santa Cruz Biotechnology (Santa Cruz, CA).

Cell Culture Conditions and Cell Lines. The CHO cell lines: AUXB1, CH^RC5, CH^RB30, and I10 were kindly provided by Dr. V. Ling of the British Columbia Cancer Institute, Vancouver, Canada and grown in alpha-minimal essential medium (α-MEM) supplemented with 10 % foetal calf serum (FCS) at 37 °C in the presence of 5 % CO_2. CH^RC5 was derived by clonal stepwise selected from the drug-sensitive parental line, AUXB1 [21]. CH^RB30 was derived from CH^RC5 by stepwise selection with colchicine. I10 is a drug-sensitive revertant cell line derived by a single step from CH^RC5 [22].

Dose-Response Assays. For dose-response assays, cells were added to 24-well plates at a concentration of 2000 cells per well (to produce single cell colonies) and incubated with α-MEM with 10 % FCS. After 24 h of growth, verapamil was added to the media. When the ATPase inhibitors PSC 833 and ivermectin were used concurrently with verapamil, cells were pre-incubated with inhibitor for 30 min before the addition of verapamil. The

cells were either incubated in verapamil for 24 h, after which the cells were washed and new media was added, or the cells were grown in verapamil continuously for 5 days. After a total of six days, surviving colonies were counted, stained with methylene blue dye, air dried, and solubilized in 0.1 % (v/v) SDS/PBS. The absorbance of the resulting solution was determined colorometrically at 510 nm in a multi-plate photospectrometer (Dynatech Laboratories, MR5000). Cell viability was expressed as a percentage of untreated control cells. Cell viability results represent the average of at least four independent experiments, each done in triplicate.

DNA Fragmentation Assay to Measure Apoptosis. AUXB1 and CH^RC5 cells were treated with verapamil, cisplatin (CDDP), the racemeric isomer R(+)-verapamil, or cycloheximide (CX). Fragmented genomic DNA was quantified 24 h after treatment. Briefly, adherent and non-adherent cells were pooled, washed 3 times in phosphate buffered saline (PBS), and resuspended in buffer A (0.15 M NaCl, 10 mM Tris pH 7.4, 2 mM $MgCl_2$, and 1 mM dithiothreitol). Nonidet P-40 (0.5 % (v/v)) was added to the mixture and the samples were left for 30 min on ice. After centrifugation at 16,000 × g for 5 min, the supernatant was discarded and the resulting pellet resuspended in buffer B (0.35 M NaCl, 10 mM Tris pH 7.4, 2 mM $MgCl_2$, and 1 mM dithiothreitol), and again left on ice for 30 min. Following a second centrifugation step at 16,000 × g, the supernatant was removed and extracted with a phenol-chloroform solution. The resulting aqueous solution containing fragmented genomic DNA was precipitated with an equal volume of ethanol. The DNA pellet was resuspended in Tris-EDTA and treated with DNAase-free RNAase A for 30 min at 37 °C prior to electrophoresis on a 1 % agarose gel.

Flow Cytometry Analysis to Assess Apoptosis. AUXB1 and CH^RC5 cells were treated with varying concentrations of CDDP, verapamil, or R(+)-verapamil for 24 h then harvested and washed with PBS. After centrifugation, all samples were resuspended drop-wise with vortexing in 2 mL of 70 % ice-cold ethanol followed by a 60 min incubation at 4 °C. The cells were washed once with PBS then incubated in PBS containing RNAase A (1 μg/mL) at 37 °C for 10 min. After centrifugation, the samples were resuspended in PBS with propidium iodide (PI, 50 μg/mL) and incubated overnight

in the dark at 4 °C. Fluorescence of PI-stained nuclei was read using a FACScan flow cytometer (Becton Dickinson, Mountain View, CA). The percentage of cells undergoing apoptosis was obtained through comparison of the relative proportions of diploid and subdiploid (apoptotic) nuclear DNA.

CAT Assay to Measure p53 Activity. p53 activity was measured by transfection with a PG-13 chloramphenicol acetyltransferase (CAT) construct, containing thirteen repeats of a ribosomal gene cluster sequence previously shown to interact with p53 as a promoter for the CAT gene [23]. Briefly, co-transfections of AUXB1 and CH^RC5 cells with 5 μg PG-13 CAT construct and 2 μg of RSV-galactosidase plasmid were carried out according to manufacturer's instructions using LipofectAMINE. After 24 h, the plates were treated with verapamil (10-50 μM) or 15 seconds of UV light (875 mJ/m^2). After another 48 h, all samples were harvested in CAT buffer A (40 mM Tris pH 7.5, 150 mM NaCl and 1 mM EDTA) and subjected to three repetitions of a freeze-thaw cycle prior to lysis. Samples were normalized with a galactosidase assay and incubated at 65 °C for 10 min. After centrifugation, the supernatants were incubated with 5 μL of CAT buffer B (N-butyril CoA (33.3 mg/mL), 5 μL [^{14}C]-chloramphenicol (50 Ci/mmol), and 25 mM Tris pH 7.5). After 2 h incubation at 37 °C, samples were extracted with ethyl acetate, separated by thin layer chromatography and subjected to autoradiography. TLC plates containing both substrate and the mono- and di-acetylated products were resuspended in scintillation cocktail. CAT activity was measured in counts per minute and expressed as a percentage of the UV control.

Western Blot of Endogenous P-gp1, Bax, and Bcl-2 Protein Levels. Western blot analysis was performed on 20-200 μg of total cell lysate and resolved on 10 % acrylamide gels using the Laemmli gel system [24]. Proteins separated by SDS-PAGE were then transferred to nitrocellulose membrane [25]. The membranes were probed with monoclonal anti-P-gp1 (C-219), monoclonal anti-Bcl-2 (Ab-3), or polyclonal anti-Bax (N-20) antibodies.

Transfection of Bcl-2 into CH^RC5 cells. CH^RC5 cells were seeded at 0.5×10^6 cells per well in 60 mm plates and transfected with an Rc/RSV vector containing a full-length gene

of human Bcl-2 cDNA (generously provided by Dr. G. Shore, Department of Biochemistry, McGill University) according to manufacturer's instructions using LipofectAMINE. Several colonies were isolated in the presence of 1 mg/ml of G418 sulfate. Single cell clones from G418 resistant colonies were immediately selected in 96-well plates and cultured continuously in G418. The expression of Bcl-2 in CH^RC5 transfectants (CH^RC5/Bcl-2) was determined by Western blot analysis using the monoclonal anti-Bcl-2 antibody as described above.

Viability of VRP-treated AUXB1, CH^RC5 and CH^RC5/Bcl-2 cells. All three cell lines were seeded at 0.5×10^6 cells in 60 mm plates and treated after 24 h with 10 μM verapamil, 50 μM CDDP, or left untreated. Forty-eight hours after treatment, cells were harvested, resuspended in equal volumes of PBS and the number of viable Trypan blue stained cells were counted for each sample. Cell viability is expressed as a percentage of untreated controls. Cell viability results represent the average of at least four independent experiments done in triplicate.

Hoechst Dye Staining for Apoptosis. AUXB1 and CH^RC5 cells were incubated with and without 10 μM verapamil for 36 h. Hoechst 33258 dye was then added at 1 μg/mL to the media. After 10 min incubation at 37 °C, the cells were observed under UV light for signs of apoptosis. Photographs were taken at 2000 × magnification (Nikon, Eclipse TE200, Montreal, Quebec).

Isolation of Purified Plasma Membranes. All steps were preformed at 4 °C. AUXB1 and CH^RC5 cells were washed with PBS before being resuspended in 10 mL lysis buffer (10 mM HEPES-Tris pH 7.4, 5 mM EDTA, 5 mM EGTA, and 2 mM dithiothreitol) containing protease inhibitors (2 mM PMSF, 10 μg/mL leupeptin, and 10 μg/mL pepstatin). Cells were lysed in a glass homogenizer (Kontes, Vineland, NJ, USA). Nuclei were sedimented by centrifugation at 300 × g for 10 min; mitochondria were then removed by centrifugation at 400 × g for 10 min. A final centrifugation at 45,000 × g for 60 min was used to sediment the plasma membrane fraction. The pellet was resuspended

in 1 mL of the lysis buffer and homogenized by aspiration ten times through a 27-gauge syringe. The membrane samples were stored at -80 °C.

P-gp1 ATPase Activity Assay. The P-gp1 ATPase activity was determined by quantifying the release of inorganic phosphate from ATP according to Litman et al. [19]. AUXB1 and CH^RC5 plasma membrane samples were diluted to 20 µg/mL in ice-cold ATPase assay medium (3 mM ATP, 100 mM KCl, 10 mM $MgCl_2$, 4 mM dithiothreitol, 100 mM Tris pH 8.0, 4 mM EGTA, 2 mM ouabain, and 10 mM NaN_3). Each series of experiments was conducted in a 96-well plate, with reaction volumes of 50 µL/well corresponding to 1 µg protein/well. Incubation with verapamil was started by transferring the plate from ice to 37 °C for 1 h, and terminated by the addition of 200 µL ice-cold stopping medium (0.2 % ammonium molybdate (w/v), 1.3 % sulfuric acid (v/v), 0.9 % SDS (w/v); 2.3 % trichloroacetic acid (w/v), and 1 % ascorbic acid (w/v)) to each well. After 75 min incubation at room temperature, the released phosphate was quantified colorimetrically in a micro-plate reader (Dynatech Laboratories, MR5000) at 630 nm. Plasma membranes were incubated with the ATPase inhibitors PSC 833 and ivermectin, for 30 min before the addition of verapamil. The results for P-gp1 ATPase activity were fitted using the following equation [19]:

$$V_{(S)} = \frac{K_1K_2V_0 + K_2V_1S + V_2S^2}{K_1K_2 + K_2S + S^2}$$

$V_{(s)}$ is the ATPase activity as a function of substrate concentration, V_0 is the basal activity, V_1 is the maximal enzyme activity, K_1 is the substrate concentration that produces half the maximal increment in ATPase activity, V_2 is the activity at infinite concentration of the modulator, and K_2 is the substrate concentration that produces half-maximal reduction in ATPase activity from the value V_1. Each condition was performed with three to six replicates a minimum of three times.

MTT Test for Superoxide Production. MTT [(3-(4, 5-dimethylthiazol-2-yl) 2, 5-diphenyl tetrazolium bromide] is a tetrazolium dye that can be reduced to its coloured formazan by

the ROS, superoxide ($O^{-}_{2}\cdot$) [26,27]. MTT was used to determine ROS production of AUXB1 and $CH^{R}C5$ cells. AUXB1 and $CH^{R}C5$ cells were seeded in 24-well plates at 1.5×10^5 and 1×10^5 cells per well, respectively. After 24 h, a solution containing verapamil was added to cells at final concentrations of 10, 25 and 75 μM, with 0.5 mg/mL MTT in PBS. The cells were incubated at 37 °C and readings were taken after 1.5 h. The media mixture was removed by aspiration and 250 μL of 10 % Triton-X100 in 0.01 N HCl was added to each well. The samples were then incubated at 37 °C until the reduced MTT was completely dissolved in solution. Samples were removed and their absorbance was quantified colourimetrically in a micro-plate reader at 570 nm. The amount of superoxide produced was determined relative to the OD of untreated controls. The status of cell survival was examined by Trypan blue staining to confirm that 1.5 h exposure to verapamil did not cause cell death.

Measurement of Total GSH. AUXB1 and $CH^{R}C5$ cells were seeded in 25 cm^2 flasks at a density of 6×10^5 and 4×10^5 cells per well, respectively. After 48 h, the cells were washed three times with ice cold PBS before scrapping. The cells were them collected in ice cold PBS and pelleted by centrifugation at 150 × g for 5 min at 4 °C. The cells were resuspended in 100 μL of 10 mM HCl and lysed by freeze/thawing in liquid nitrogen three times. After lysis, the sample was pelleted at 6000 × g for 5 min at 4 °C. Subsequently, 100 μL of supernatant was added to 400 μL of picric acid, vortexed, and centrifuged at 16,000 × g for 5 min at 4 °C and the supernatant was collected. In a cuvette, 700 μL of daily buffer (0.3 mM NADPH, 143 mM Na_2HPO_4, 6.3 mM Na_4-EDTA, pH 7.5), 100 μL DTNB (6 mM 5,5'dithiobis 2-nitrobenzoic acid), 143 mM Na_2HPO_4, 6.3 mM Na_4-EDTA, pH 7.5), and 150 μL water was warmed to 30 °C for 12 to 15 min. After warming, 40 μL of sample or standard (GSH), and 10 μL of GSSG reductase were added to the cuvette and mixed. The formation of yellow TNB was followed continuously on a spectrometer at 412 nm while the slope remained constant. The slope of each sample was compared to control to determine the percent change in GSH. The values obtained were the average of three experiments done in triplicate.

Measurement of Total Cellular ATP. AUXB1 and CH^RC5 cells were seeded in black 96-well plates at a density of 2×10^4 and 2.5×10^4 cells per well, respectively. After 24 h of growth, the cells were exposed to verapamil alone, or in conjunction with a 30 min pre-treatment of 2 μM PSC 833 or 4 μM invermectin. The ATPlite™ luminescence ATP detection assay system was used to monitor ATP levels. This monitoring system is based on firefly (*Photinus pyralis*) luciferase.

Results

Characterisation of Hypersensitivity to Verapamil in CHO Cell Lines. Hypersensitivity to verapamil has been previously demonstrated in several MDR cell lines that over express P-gp1 [4-6]. To explore the mechanisms involved in verapamil sensitivity, it was important to confirm this effect in cells expressing increasing levels of P-gp1 (figure 1A). Western blot analysis of the four CHO cells lines AUXB1, CH^RC5, I10, and CH^RB30 with the monoclonal antibody, C-219 confirmed that AUXB1 and I10 have undetectable levels of P-gp1. CH^RB30 had higher P-gp1 levels than CH^RC5. Clonal cell viability assays were conducted by exposing the four CHO cell lines with different levels of P-gp1 expression to verapamil for 24 h (figure 1B). AUXB1 was relatively unaffected by verapamil up to 50 μM, whereas verapamil reduced the survival of CH^RC5 by 40% at concentrations as low as 2 μM. Furthermore, the more highly resistant CH^RB30 cell line was exceptionally sensitive to verapamil (IC50 <1 μM). The disparity of survival between the different cell lines was most obvious at 10 μM verapamil. AUXB1 was unaffected at this concentration, whereas CH^RC5 and CH^RB30 survival was reduced to approximately 50 % and 2 %, respectively. The survival of non-MDR I10 cells was the least affected by verapamil toxicity. These results suggest that hypersensitivity to verapamil in MDR CHO cells correlates with P-gp1 expression. Remarkably, we repeatedly observed an interesting trend in the survival curve of CH^RC5 when cells were exposed to verapamil for 5 days (figure 1C) as opposed to 24 h (figure 1B). CH^RC5 had consistently poor survival between 1 and 10 μM verapamil followed by a moderate recovery above this concentration. In particular, CH^RC5 survival was several-fold higher at 50 μM verapamil than at 1.5 μM. This observation indicated that CH^RC5 hypersensitivity to verapamil was more pronounced at low concentrations.

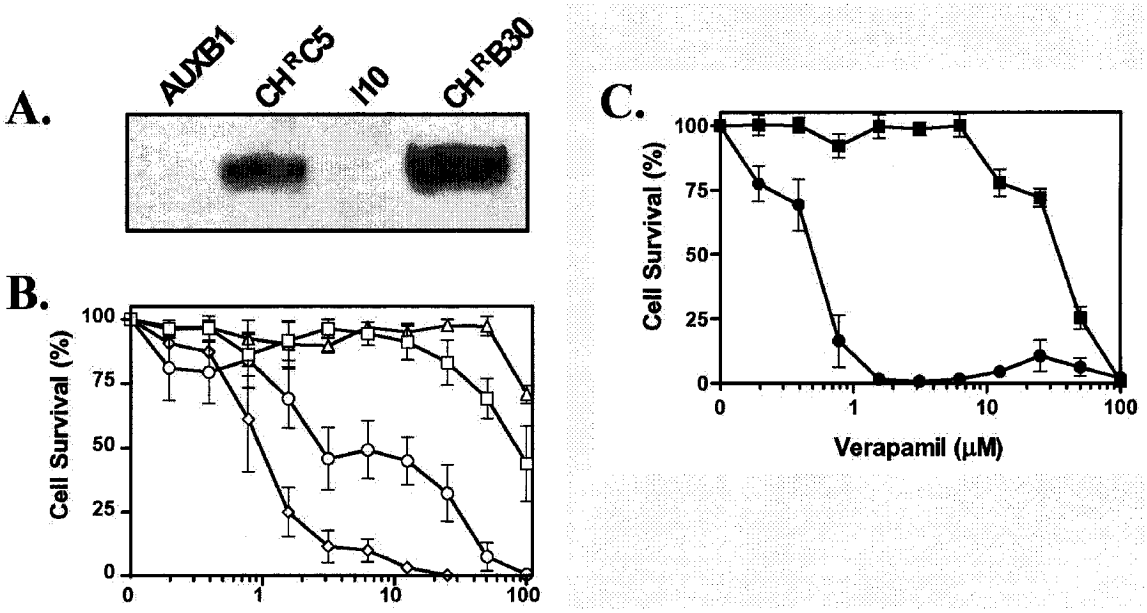

Figure 1

Western blot and verapamil dose response assays for sensitive and multidrug resistant CHO cells. (A) The relative amount of P-gp1 protein is shown by Western blot using the P-gp1 specific mAb, C-219, in the parental AUXB1 cells, the multidrug resistant CH^RC5 and CH^RB30 cells, and I10 (drug-sensitive revertant derived from CH^RC5). (B) AUXB1 (white squares), CH^RC5 (white circles), CH^RB30 (white diamonds), and I10 (white triangles) were exposed to increasing concentrations of verapamil for 24 h followed by 4 days of growth in drug-free conditions. The surviving colonies were stained with methylene blue and quantified by spectrophotometry. (C) AUXB1 (black squares) and CH^RC5 (black circles) were exposed to increasing verapamil concentrations for 5 days and survival was quantified as in (B).

Hypersensitivity to Verapamil and Apoptosis. In order to determine the mechanism that causes hypersensitivity, it was of interest to establish whether verapamil sensitivity was mediated by apoptosis or necrosis. For this purpose, DNA fragmentation was assessed in AUXB1 and CH^RC5 (figure 2A). Treatment of both cell lines with increasing concentrations of verapamil (10-50 μM) resulted in the appearance of an oligonucleosomal ladder characteristic of apoptosis in CH^RC5 but not AUXB1 cells. DNA laddering of CH^RC5 decreased in a dose-dependant manner up to 50 μM, consistent with increased survival seen at higher verapamil concentrations (figure 1C). Cisplatin

(CDDP), known to induce interstrand bulky adducts in DNA, was used as a positive control for apoptosis [28] in both AUXB1 and CH^RC5 cells (figure 2A).

Since apoptosis has been shown to require protein synthesis in some instances [28], the inhibition of protein synthesis by cycloheximide (CX) revealed a decrease in the levels of verapamil-induced apoptosis in CH^RC5 cells. A marked reduction in DNA laddering was apparent in verapamil or CDDP-treated CH^RC5 cells pre-incubated with CX (1 μg/mL) for 30-60 min. Therefore, both verapamil and CDDP-induced apoptosis in CH^RC5 cells required protein synthesis and can be blocked with CX. Similar results were also present for CDDP-treated AUXB1 cells pre-incubated with CX. To confirm the nature of cell death, the cellular nuclei were stained with Hoechst 33258. Representative photographs in figure 2B show the staining of condensed chromatin in CH^RC5 cells exposed to 10 μM verapamil. AUXB1 cells that were exposed to verapamil show little or no apoptosis (figure 2B). Moreover, FACScan analyses of propidium iodide stained nuclei from AUXB1 and CH^RC5 cells treated with either verapamil or CDDP are shown in figure 2C. The relative proportions of apoptotic, aneuploid cells, are summarized in figure 2C. Verapamil treatment preferentially induced an apoptotic, subdiploid peak in CH^RC5 but not AUXB1 cells, while CDDP had a similar effect on both cell lines. Consistent with results from the DNA fragmentation assay of figure 2A, CH^RC5 cells treated with verapamil showed a dose-dependent decrease in the number of aneuploid nuclei at concentrations above 10 μM. These results show that the cell death caused by verapamil in CH^RC5 occured by apoptosis alone. The highest levels of verapamil-induced apoptosis occurred at 10 μM. Again, the fact that the apoptotic effect of verapamil on CH^RC5 cells decreased at concentrations above 10 μM was consistently observed and supports the results of the cell survival assay in figure 1C.

Previous studies have shown that verapamil hypersensitivity in MDR cells is independent of its calcium blocking activities since verapamil is unable to alter accumulation of Ca^{2+} from extracellular stores in AUXB1 or CH^RC5 cells [5,29]. However, given the role of calcium levels in apoptosis, it was important to examine the effects of R(+)-verapamil (a non-active isomer of verapamil) on AUXB1 and CH^RC5 cells. Both DNA fragmentation and flow cytometry experiments showed that treatment of CH^RC5 cells with R(+)-verapamil resulted in apoptotic levels comparable to those induced by

racemic verapamil (data not shown). Therefore, the ability of verapamil to block calcium channels does not account for the apoptotic effect of the drug on CH^RC5 cells.

p53 Activity in Verapamil-Mediated Apoptosis. The tumour suppressor p53 can induce apoptosis in cells that have been incubated with DNA damaging agents [30]. Although verapamil has not previously been shown to be a DNA damaging agent, it is known to phosphorylate protein kinase C, an activator of p53 [31,32]. To determine if verapamil-induced apoptosis in CH^RC5 cells involves p53 activation, both AUXB1 and CH^RC5 cells were transiently transfected with the PG-13 construct and CAT activity was measured in response to increasing concentrations of verapamil. Figure 3 shows relative CAT activities for both cell lines. A dose-dependent increase in p53-induced CAT activity was present upon verapamil treatment of AUXB1 drug-sensitive cells. In contrast, treatment with 10 and 25 μM verapamil caused a decrease in p53-induced CAT activity in CH^RC5 cells, although higher concentrations of verapamil (50 μM) led to a small increase in p53-induced CAT activity. As a positive control, a 15 second exposure of cells to UV light caused a large increase in p53 CAT activity in both cell lines. The discrepancy seen in PG-13 CAT activity between AUXB1 and CH^RC5 cells in the presence of low concentrations of verapamil may be a consequence of the differential uptake of the drug between the two cell lines as verapamil is effluxed by P-gp1 [5]. Furthermore, p53 activation did not correspond with the apoptosis observed with verapamil treatment of AUXB1 or CH^RC5 cells (figures 1 and 2).

Endogenous Bax and Bcl-2 Expression. To further characterise the apoptotic components of verapamil-sensitive CH^RC5 cells, we examined the levels of Bax and Bcl-2. Both proteins are involved in the control of apoptosis. Bcl-2 expression is associated with inhibition of apoptosis, while Bax stimulates apoptosis. Figure 4 shows a Western blot of cell lysates from AUXB1 and CH^RC5 treated and untreated with 10 μM verapamil, probed with anti-Bcl-2 or anti-Bax antibodies. Treatment with 10 μM verapamil did not result in an increase in Bax levels above untreated controls in either AUXB1 or CH^RC5 cells. In contrast, AUXB1 but not CH^RC5 cells showed a slight increase in Bcl-2 above control levels when treated with verapamil.

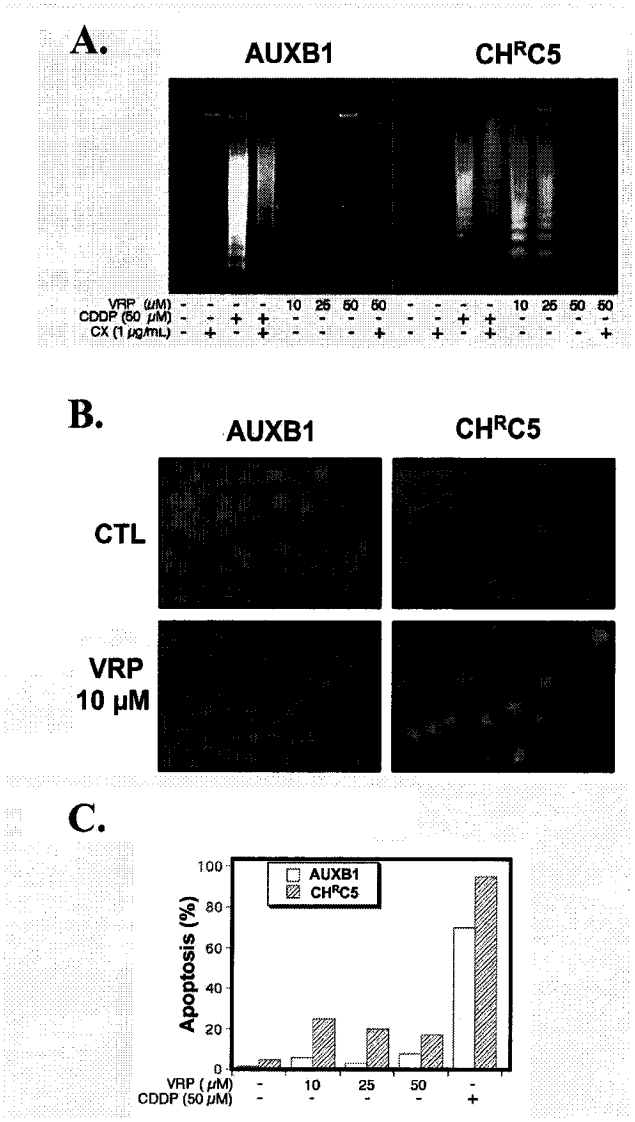

Figure 2.

Analysis of apoptosis by DNA laddering, nuclear staining, and flow cytometry in AUXB1 and CH^{R}C5 cells in response to verapamil. (A) DNA fragmentation was measured in AUXB1 and CH^{R}C5 cells treated with increasing concentrations of verapamil (VRP). 50 μM of Cisplatin (CDDP) was used as a positive control and 1 mg/mL cycloheximide (CX) was used to inhibit apoptosis. (B) Hoechst 33258 was added to determine the apoptotic state of AUXB1 and CH^{R}C5 cells grown with 10 μM verapamil and untreated. (C) Cells were treated for 24 h with the indicated concentrations of verapamil prior to quantification of apoptosis by flow cytometry. The cell number versus fluorescence is plotted for each treatment; concentrations for each drug appear in parentheses at the bottom of the graph.

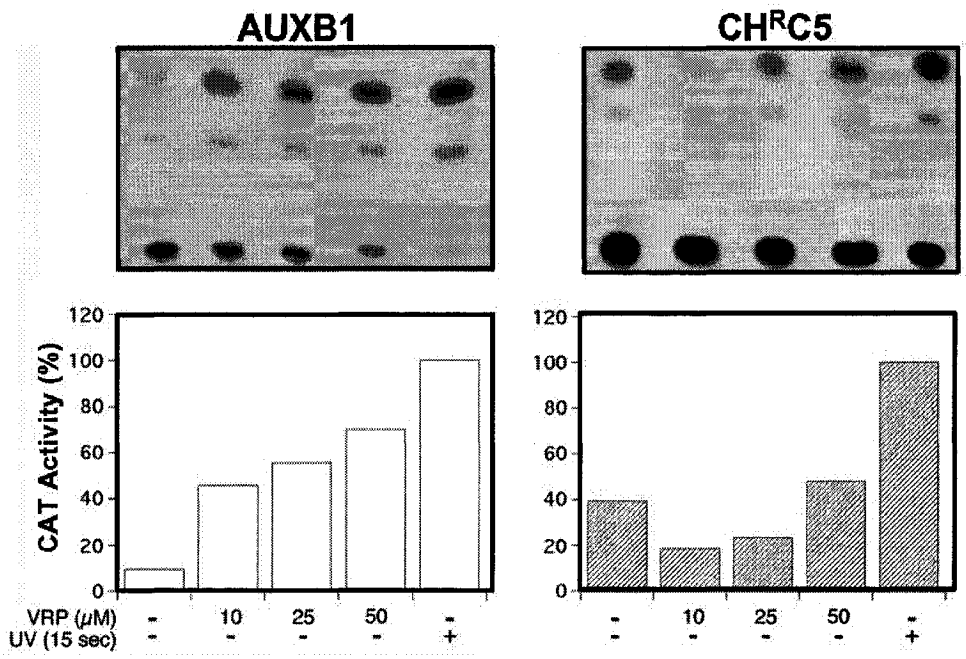

Figure 3

PG-13 CAT activity in AUXB1 and CH^{R}C5 cells treated with varying concentrations of verapamil. CAT activity was measured in AUXB1 and CH^{R}C5 cells 48 h after incubation with verapamil (VRP) at 10, 25 or 50 μM, or 15-second exposure to UV light (as indicated below). The corresponding bar graph depicts CAT activity in both AUXB1 and CH^{R}C5 cells under these conditions. Enzyme activity was calculated by scraping the radioactive material from each assay and determining the percentage of product from the entire radioactive material in each case. Results appear as a percentage of the CAT activity in the UV treatment.

Overexpression of Bcl-2 in CH^{R}C5 and Inhibition of Verapamil Hypersensitivity. Bcl-2 exerts its principle effects through stabilising mitochondria and preventing the release of cytochrome *c*. To further assess the pathway of verapamil-induced apoptosis, stable transfectants of CH^{R}C5 with full-length human specific Bcl-2 cDNA were generated. The resulting clone, CH^{R}C5/Bcl-2 expressed vastly increased levels of human specific Bcl-2 as seen by Western blot analysis with a human-specific anti-Bcl-2 mAb (figure 5A). CH^{R}C5/Bcl-2 cells treated for 48 h with 10 μM verapamil retained a heightened level of viability relative to CH^{R}C5 cells, as assessed by Trypan blue staining (figure 5B).

CDDP-treated CH^RC5/Bcl-2 cells similarly retained heightened cell viability relative to AUXB1 and CH^RC5 cells. To determine whether CH^RC5/Bcl-2 cells were protected from the toxicity of verapamil through suppression of apoptosis, a DNA fragmentation assay was carried out on AUXB1, CH^RC5 and CH^RC5/Bcl-2 cells treated for 24 h with either 10 μM verapamil or 50 μM CDDP (figure 5C). No oligonucleosomal laddering was present in verapamil or CDDP treated samples of CHRC5/Bcl-2 cells, demonstrating that apoptosis was diminished relative to CH^RC5 cells.

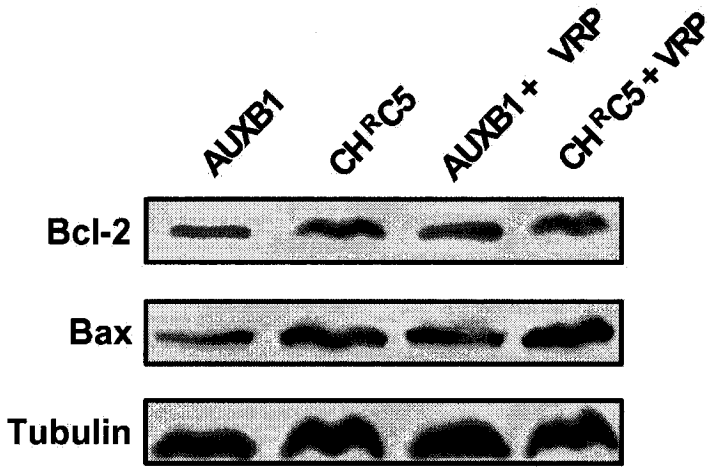

Figure 4

Endogenous Bcl-2 and Bax levels in AUXB1 and CHRC5 cells. Cell lysates from verapamil (VRP) treated (10 μM), or untreated AUXB1 and CHRC5 cells were resolved by SDS-PAGE and transferred to nitrocellulose membrane. The nitrocellulose membrane was probed with anti-serum against Bcl-2 or Bax. Tubulin expression served as control for loading.

Inhibition of P-gp1 ATPase Activity and Reduced Hypersensitivity to Verapamil. The DNA laddering and FACScan experiments (figure 2A and 2B) demonstrated the ability of verapamil to induce apoptosis. The cell survival experiments and apoptosis assays (figures 1 and 2) indicated that the P-gp1 expressing cells were most sensitive to verapamil at about 10 μM, with improved survival at higher concentrations. In addition to inducing cell death in P-gp1 expressing cells, verapamil is also one of the most potent

activators of P-gp1 ATPase activity [19]. Verapamil stimulates ATPase activity at low concentrations but inhibits the activity at high concentrations. This prompted us to test the response of P-gp1 ATPase to verapamil in AUXB1 and CH^RC5 cells. Figure 6A shows a representative profile of P-gp1 ATPase activity in AUXB1 and CH^RC5 plasma membranes exposed to increasing amounts of verapamil. The increase and subsequent decrease of ATP hydrolysis in CH^RC5 cells paralleled the apoptotic profile of these cells (as seen in figure 2). P-gp1 ATPase activity was not observed with AUXB1. Verapamil induced maximal ATPase activation at 10 μM in CH^RC5 cells. This concentration is comparable to the concentration of verapamil needed to induce apoptosis (figures 1 and 2). From this we deduced that the effect of verapamil on ATPase activation may be linked to its ability to cause apoptosis. To test this, it was necessary to find inhibitors of verapamil-induced ATP hydrolysis. Cyclosporin A and PSC 833 are known inhibitors of P-gp1 ATPase. Unfortunately, cyclosporin A is also known to inhibit apoptosis [33], leaving PSC 833. The ATPase activation by verapamil was almost completely reversed by 2 μM PSC 833 (figure 6B). In addition, we found that ivermectin was an effective inhibitor of P-gp1 ATPase activity. Figure 6C shows that 4 μM ivermectin effectively inhibits P-gp1 ATPase stimulation by verapamil. Analysis of the ATPase inhibition with a smaller scale Y-axis shows that PSC 833 is a more effective inhibitor than ivermectin (inset graphs of figures 6B and 6C). In fact, the characteristic biphasic ATPase activity produced by verapamil is still apparent with ivermectin.

To strengthen the correlation between apoptosis and P-gp1 ATPase, dose-response assays were conducted to see if CH^RC5 could be rescued from verapamil induced apoptosis using ATPase inhibitors. As previously demonstrated, figure 6D shows the effect of increasing amounts of verapamil on AUXB1 and CH^RC5. Cell survival was greatly reduced in CHRC5 relative to AUXB1. The ability of 2 μM PSC 833 to modulate verapamil toxicity is shown in figure 6E. The addition of PSC 833 almost completely inhibited the toxicity of verapamil, whereby the dose response of AUXB1 and CH^RC5 was almost identical. The difference in the survival of CH^RC5 cells exposed to verapamil in the presence or absence of PSC 833 is illustrated by comparing the dashed line (no PSC 833) to the solid line (2 μM PSC 833). Ivermectin was also able to alter the toxicity caused by verapamil in CH^RC5 cells (figure 6F). This effect is shown by comparing the

survival of CH^RC5 cells without ivermectin (dashed line) and with 4 μM ivermectin (solid line) in figure 6F. Interestingly, PSC 833 is a more potent ATPase inhibitor than ivermectin and reduced verapamil hypersensitivity more than ivermectin. These observations provided strong evidence that hypersensitivity to verapamil in MDR cells is directly associated with P-gp1 ATPase activation.

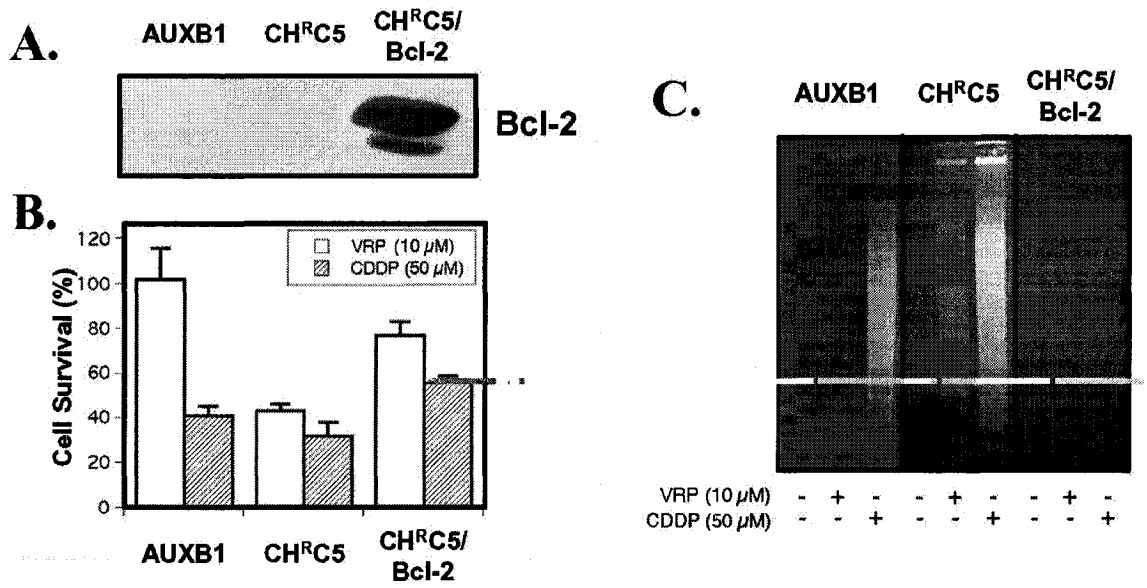

Figure 5

The effect of Bcl-2 overexpression on verapamil hypersensitivity in CH^RC5 cells. (A) Total cell lysates from AUXB1, CH^RC5 and CH^RC5/Bcl-2 cells were prepared for Western blotting and probed with human specific Bcl-2 mAb. (B) and (C) show cell viability and DNA laddering of AUXB1, CH^RC5, and CH^RC5/Bcl-2 cells following 48 h treatment with 10 μM verapamil (VRP) or 50 μM cisplatin (CDDP).

Production of Reactive Oxygen Species in CH^RC5 Cells by Verapamil. The correlation between ATP hydrolysis and apoptosis shown in figure 6 is very interesting and likely to be a function of P-gp1 activity. Possibly, apoptosis was initiated by the high ATP demand from P-gp1. One consequence of an elevated energy demand would be an increase in ATP synthesis by oxidative phosphorylation in mitochondria, which can lead to the production of reactive oxygen species (ROS). In order to determine if ROS production is elevated in AUXB1 and CH^RC5 cells exposed to verapamil, we measured

production of $O^{-}_{2}\cdot$ through the reduction of MTT dye [27] (figure 7A). A concentration of 10 μM verapamil was used to test ROS formation because it also induced high levels of ATPase activity as well as causing maximal killing of $CH^{R}C5$ cells. With the addition of 10 μM verapamil, the amount of superoxide in $CH^{R}C5$ cells was increased by almost 15 % (figure 7A). This indicates that verapamil selectively increases $O^{-}_{2}\cdot$ production in $CH^{R}C5$ but not AUXB1 cells. In addition, we observed that ROS production in $CH^{R}C5$ decreased at higher concentrations of verapamil (25 and 75 μM). Our observations were not affected by the inadvertent transport of MTT dye by P-gp1 because a previous study established that MTT accumulation is not affected by the presence of P-gp1 [34]. It was also determined that verapamil had no effect on MTT accumulation. PSC 833 was not included in the superoxide assay because PSC 833 non-specifically modified the MTT dye. Therefore, to determine the effect of PSC 833 on the oxidative state of cells, the total cellular glutathione (GSH) was measured (figure 7B). GSH is a tripeptide that plays a major role as an antioxidant in the elimination of ROS. It is also a substrate for scavenging ROS through GSH peroxidase and GSSG reductase [35]. The results indicate that verapamil reduced GSH levels in $CH^{R}C5$ cells by almost 25 %. PSC 833 was able to restore GSH levels to the same as control. No significant change in GSH was observed in AUXB1 with or without verapamil and PSC 833.

Reduction in Cellular ATP in $CH^{R}C5$ Cells by Verapamil. The ATPase activity of P-gp1 determined in the presence of verapamil, PSC 833, and ivermectin provided an indirect measure of cellular metabolism (figures 6D, 6E, and 6F). The two assays for ROS production also indicated the level of metabolic stress in $CH^{R}C5$ cells exposed to verapamil. By measuring the total cellular ATP levels in AUXB1 and $CH^{R}C5$ cells, we obtained a more direct view of the metabolic state of these cells when they were exposed to the above mentioned drugs. The most striking result was observed in $CH^{R}C5$ cells exposed to 10 μM verapamil. The amount of ATP in $CH^{R}C5$ exposed to verapamil was less than half of the untreated control cells. This effect can be linked to the increased hydrolysis of cellular ATP by P-gp1 due to verapamil stimulation. When these cells were co-incubated with 2 μM PSC 833, the level ATP in the cells returned to normal, probably

as a result of ATPase inhibition. Both verapamil and PSC 833 had no significant effect on the amount of ATP in AUXB1 cells.

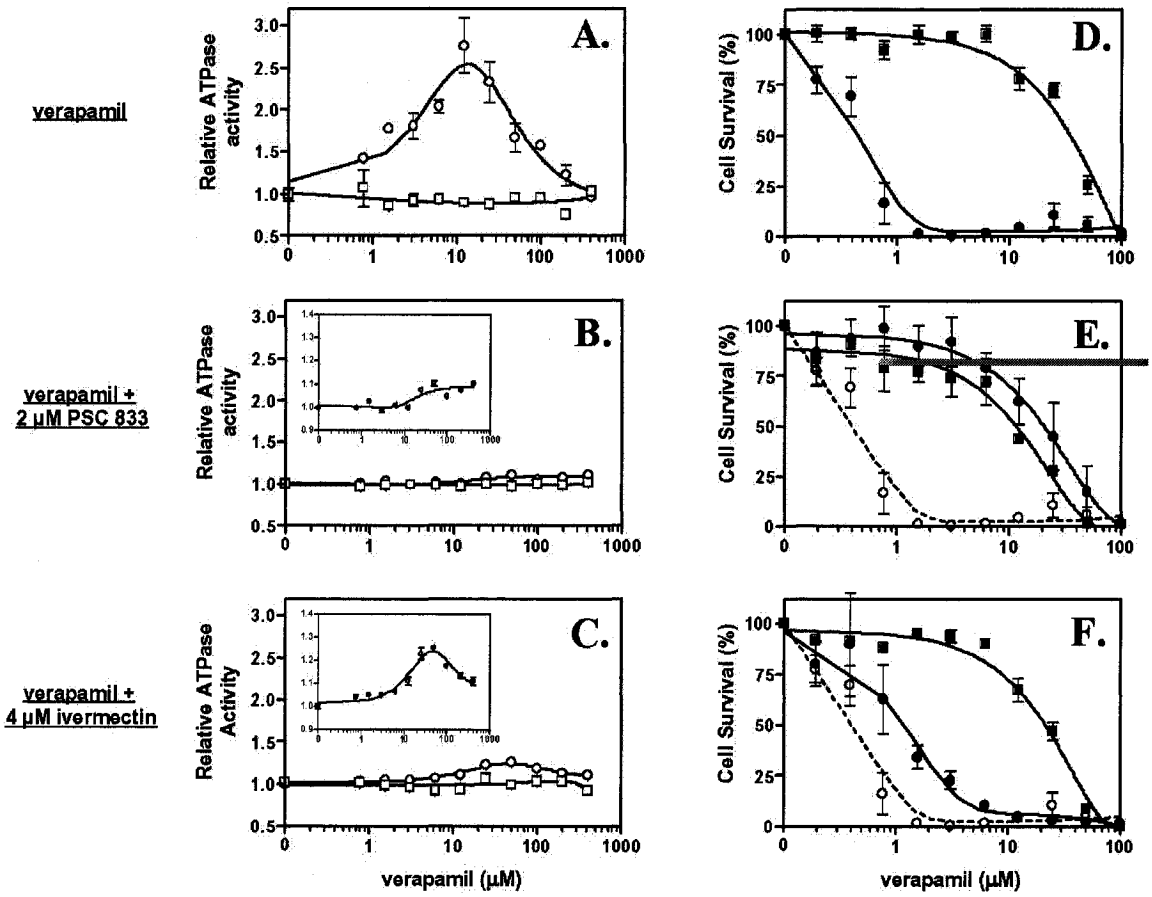

Figure 6

Effects of verapamil, PSC 833, and ivermectin on cell survival and P-gp1 ATPase in AUXB1 and CH^{R}C5. (A, B, and C) ATPase activity of AUXB1 (white squares) and CH^{R}C5 (white circles) was measured using purified plasma membranes exposed to increasing concentrations of verapamil. (B and C) ATPase activity was measured with an additional pre-treatment with 2 µM PSC 833 or 4 µM ivermectin. (D, E, and F) Survival of AUXB1 (black squares) and CH^{R}C5 (black circles) exposed to increasing concentrations of verapamil was determined by staining colonies with methylene blue and quantified by spectrophotometry. (E and F) Cell survival was determined with an additional pre-treatment with 2 µM PSC 833 or 4 µM ivermectin. For a comparison, the dashed line in (E and F) shows the survival curve of CH^{R}C5 with verapamil alone from (D). The results in panels B and C are plotted with a smaller scale Y-axis as inset-graphs.

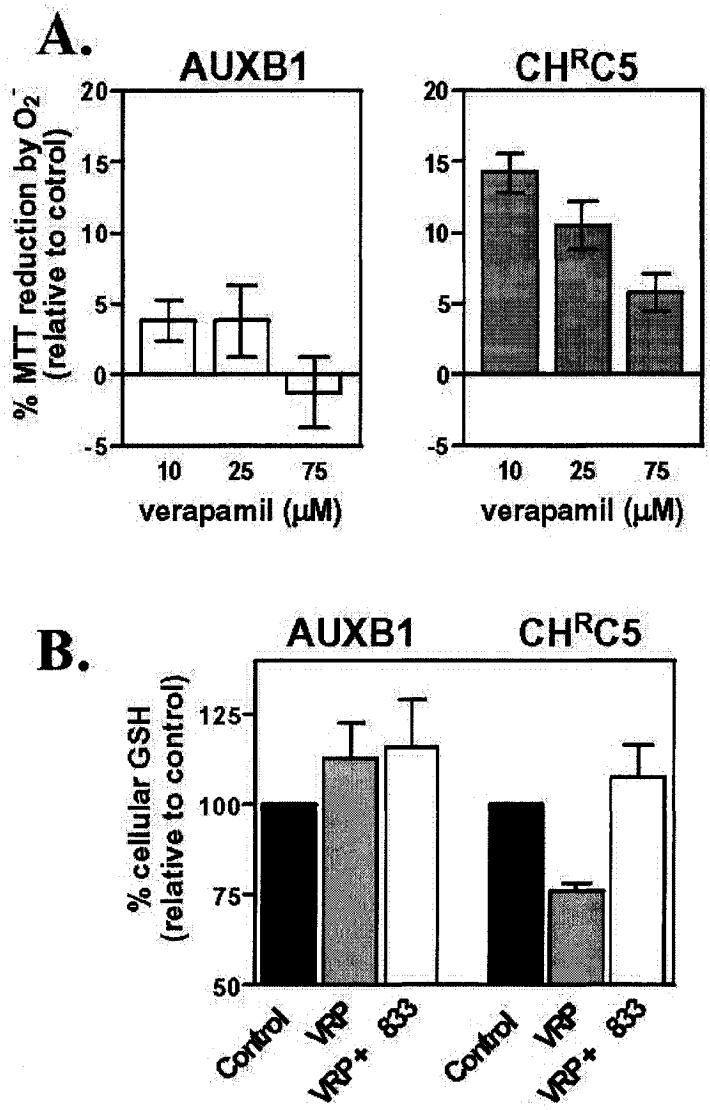

Figure 7

Superoxide production and GSH levels in AUXB1 and CH^{R}C5 exposed to verapamil and PSC 833. (A) MTT was used to measure superoxide ($O^-_2\cdot$) production in AUXB1 and CH^{R}C5 cells. Increasing amounts of verapamil (10, 25, 75 μM) was added to cells. The graphs show the percent change in MTT reduction relative to untreated controls. (B) The total cellular GSH was determined in AUXB1 and CH^{R}C5 cells. Untreated control cells are displayed as black bars, cells treated with 10 μM verapamil (VRP) are in grey, and cells treated with both 10 μM verapamil as well as 2 μM PSC 833 (VRP + 833) are in white.

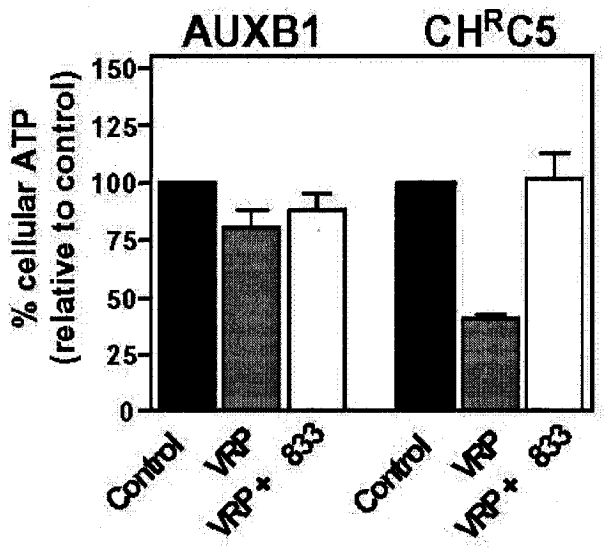

Figure 8

Total cellular ATP in AUXB1 and CH^{R}C5 exposed to verapamil and PSC 833. The total cellular ATP levels were determined using the ATPlite™ luminescence ATP detection assay system. Untreated control cells are displayed as black bars, cells treated with 10 μM verapamil (VRP) are in grey, and cells treated with both 10 μM verapamil as well as 2 μM PSC 833 (VRP + 833) are in white.

Discussion

The phenomenon of hypersensitivity or collateral sensitivity to verapamil in MDR cells has been widely reported [6,10,36-40]. To date, the mechanism and the role of P-gp1 in the development of hypersensitivity remain unclear. The findings in this study establish the first detailed mechanism of verapamil induced P-gp1-mediated hypersensitivity. Specifically, our results show that verapamil hypersensitivity correlates with P-gp1 expression as well as its effects on P-gp1 ATPase activity. Moreover, verapamil-triggered apoptosis in P-gp1 positive CH^{R}C5 cells was not mediated though modulation of calcium levels or the expression of apoptosis related proteins (Bcl-2 or Bax). However over-expression of Bcl-2 does reverse verapamil and cisplatin induced apoptosis in CH^{R}C5 cells. In addition, inhibition of P-gp1 ATPase by PSC 833 and ivermectin inhibits verapamil-induced apoptosis. These observations provide insight into the mechanism of collateral sensitivity to verapamil.

An outstanding question relating to the role of P-gp1-associated hypersensitivity is the observation that not all P-gp1 expressing cells display hypersensitive to verapamil. Our results suggest that other cellular changes, in addition to P-gp1 expression, appear to be required. Such changes include low redox capacity of MDR cells or high expression of pro-apoptotic proteins. Thus, tumour cells that overexpress P-gp1 together with high levels of anti-apoptotic proteins or high redox capacity are unlikely to show verapamil hypersensitivity. These results are consistent with a previous study which showed that hypersensitivity to verapamil in resistant CHO cells is proportional to P-gp1 expression, but only at very high resistance levels [10]. P-gp1 transfection of AUXB1 and E29 cells (with ~9-fold colchicine resistance) did not produce verapamil hypersensitivity. Further selection of the transfectants with colchicine raised resistance by 200-fold, after which the cells developed verapamil hypersensitivity. Therefore, the use of very intense selective pressure was required to overcome any protective mechanisms and induce collateral sensitivity. In contrast, another study demonstrated that NIH-3T3 cells develop verapamil hypersensitivity when transfected with lower levels of P-gp1 cDNA [37]. Our use of four CHO cell lines strengthens the observation that verapamil hypersensitivity is proportional to P-gp1 expression. The CH^RB30 cell line with higher P-gp1 expression than CH^RC5 displayed greater hypersensitivity to verapamil. Moreover, the I10 cell line, a single-step MDR revertant from CH^RC5, emphasizes the role of P-gp1 expression in this system because the only phenotypic difference between CH^RC5 and I10 is the presence of P-gp1 [22]. The dose-response assay showed that hypersensitivity to verapamil was completely abrogated in I10 cells, solely as a result of reduced P-gp1 expression. This indicates that P-gp1 may be the sole factor mediating verapamil hypersensitivity in the CHO cells we used.

The present study demonstrates that activation of P-gp1 ATPase by verapamil induces excessive metabolic stress leading to ROS-mediated apoptosis. The critical observation that allowed us to propose this mechanism was that P-gp1 expressing cells were more sensitive to low concentrations of verapamil (10 μM) than high concentrations (50 μM) (figures 1 and 2). This biphasic trend is demonstrated in the 5-day clonal cell viability assay with AUXB1 and CH^RC5 cells. This effect is also evident in several other assays of cell survival. DNA laddering, Hoechst dye staining, and FACScan analysis

show hypersensitivity to low concentrations of verapamil; they also indicated that the mechanism of cell death was apoptosis. Each assay consistently showed a biphasic trend in hypersensitivity to verapamil beginning with a decrease in CH^RC5 survival as the verapamil concentration was increased to 10 μM. At this point, survival began to improve as verapamil concentrations were increased to 50 μM. Finally, cell survival decreased to a fatal limit at approximately 100 μM. Interestingly, this unforeseen trend exposed a fascinating correlation between verapamil hypersensitivity and the activation of P-gp1 ATPase by verapamil.

Several explanations have been put forwards to explain the mechanism of hypersensitivity to verapamil. In one report, Stow and Warr [38] proposed that verapamil sensitivity occurs due to a mutation in P-gp1 during selection of MDR cells. The same group also put forward the possibility that high P-gp1 levels may destabilise the membrane thereby affecting survival [10]. We are proposing an alternate explanation based on P-gp1 ATPase activity.

It has been well documented that P-gp1 ATPase is particularly sensitive to activation by verapamil. Several drugs (e.g. vinblastine, paclitaxel and verapamil) stimulate ATPase activity at low concentrations but inhibit the activity at higher concentrations [12,15,19,41]. The similarity between ATPase activation and hypersensitivity is very striking. Not only were the biphasic curves for cell survival and ATPase activation very similar, but the verapamil concentration that caused maximum hypersensitivity (10 μM) also resulted in the highest level of ATPase activation. To further strengthen the link between P-pg1 ATPase and cell survival, we reasoned that by inhibiting verapamil induced ATPase activity it would be possible to abrogate hypersensitivity to verapamil. Indeed, PSC 833 and ivermectin were able to reduce verapamil-induced ATPase stimulation as well as hypersensitivity in P-gp1 expressing cells. In addition, the more effective ATPase inhibitor, PSC 833, reduced collateral sensitivity to verapamil more effectively than ivermectin, the less potent ATPase inhibitor. The correlation between the degree of ATPase inhibition and modulation of cell survival provides convincing evidence that hypersensitivity to verapamil in P-gp1 expressing cells is directly linked to the stimulation of P-gp1 ATPase.

It was of interest to determine how P-gp1 ATPase stimulation by verapamil could cause apopsosis. ATP synthesis in eukaryotic cells is accomplished via glycolysis and mitochondrial oxidative phosphorylation. We believe that the second source provided ATP to P-gp1 ATPase for several reasons. A recent report shows that P-gp1 is dependent primarily on ATP produced in mitochondria by F sub 1-ATPase and F sub 0-ATPase in the vinblastine-resistant leukaemic cell line, CEM/VLB0.1 [42]. Furthermore, it was shown that the P-gp1 expressing K/DAU600 and CEM/VLB100 cell lines have a more active electron transport chain (ETC) than their drug–sensitive parental cell lines, whereas glycolytic metabolism between resistant and sensitive cell lines remained consistent [43]. One consequence of having ATP generated by the ETC in mitochondria, rather than glycolysis, is the generation of toxic ROS known to cause apoptosis [44,45].

The production of ATP through the coupling of electron transport and oxidative phosphorylation in mitochondria is normally very efficient (95 to 99 %). When this process is uncoupled, electrons are lost and reduce oxygen to $O^{-}_{2}\cdot$. This radical can then go on to form other more destructive ROS such as hydrogen peroxide (H_2O_2) and the highly reactive hydroxyl radical ($OH\cdot$) [46]. These can initiate apoptosis in a variety of ways. ROS cause apoptosis by reacting with, and damaging, biomolecules such as lipids and DNA [47-49]. ROS-mediated apoptosis sometimes requires p53 activation which does not appear to play a role in our system (figure 3). ROS can also lead to mitochondrial permeability transition, which causes the release of apoptogenic factors such as cytochrome *c* and the apoptosis inducing factor (AIF); a process that is inhibited by Bcl-2 [33,50]. Since we showed that verapamil hypersensitivity is inhibited by Bcl-2 (figure 5), we believe that apoptosis in our system is mediated by a mitochondrial pathway.

We propose that cells with high P-gp1 expression exist in a state of heightened oxidative stress due to a highly active ETC. This situation is exaggerated when verapamil creates an even greater need for ATP by stimulating P-gp1 ATPase. We used two assays to show that hypersensitivity in P-gp1 expressing $CH^{R}C5$ cells was accompanied by an increase in ROS. When $CH^{R}C5$ cells were exposed to 10 μM verapamil, their $O^{-}_{2}\cdot$ levels increased by approximately 15 %, compared to 2 % for AUXB1 (figure 7A). Furthermore, increasing the concentration of verapamil above 10 μM resulted in decreased $O^{-}_{2}\cdot$ levels. This trend is similar to the reduction in apoptosis and ATPase

activity observed with the addition of increasing concentration of verapamil. We also examined the overall oxidative status of these cells by measuring the amount of GSH, a critical ROS scavenger in most cells [35]. GSH levels were almost 25 % lower in CH^RC5 exposed to verapamil compared to AUXB1 and untreated CH^RC5 cells. This indicated that the pool of available GSH had been reduced in CH^RC5, possibly due to higher than normal ROS production. These observations all point to greater metabolic stress in MDR cells exposed to verapamil.

Finally, in an attempt to gain a more direct measure of the metabolic state of CH^RC5 cells exposed to 10 μM verapamil, we measure total cellular ATP relative to untreated controls. These observations confirmed that the stimulation of P-gp1 ATPase activity resulted in a reduction in the pool of cellular ATP by more than 50 % (figure 8). This effect has previously been observed in the MDR human ovarian carcinoma cells, 2780AD, exposed to verpamil [51]. This study found that 2780AD exposed to 8 μM verapamil had a reduction in the ATP:ADP ratio by about 50 % relative to drug-sensitive parental cells, A2780. Moreover, we found that cellular ATP levels could be restored with 2 μM PSC 833. This evidence confirms that the metabolic state of MDR cells is directly altered by verapamil and PSC 833.

This report presents evidence that verapamil hypersensitivity in MDR cells is associated with high levels of P-gp1 expression. In addition, we outlined pathway in cells with high P-gp1 expression that leads to apoptosis. This pathway begins with an elevated ATP demand caused by verapamil, resulting in an overactive ETC which produces ROS and depletes cellular GSH, finally ending in apoptosis (see figure 9). This new understanding of the mechanism of hypersensitivity in MDR cells could lead to a novel approach in the treatment of P-gp1 positive tumours. At present, the response of P-gp1 ATPase to a diverse set of drugs has been characterised and several of these compounds also produce a similar pattern of collateral sensitivity (Appendix 1). Some of the less-toxic drugs could be used to control the oxidative state of cancer cells, thereby targeting multidrug resistant tumours. Finally, we present evidence for the first time that PSC 833 can prevent apoptosis by a mechanism that is independent of its commonly accepted pro-apoptotic effects [52-54].

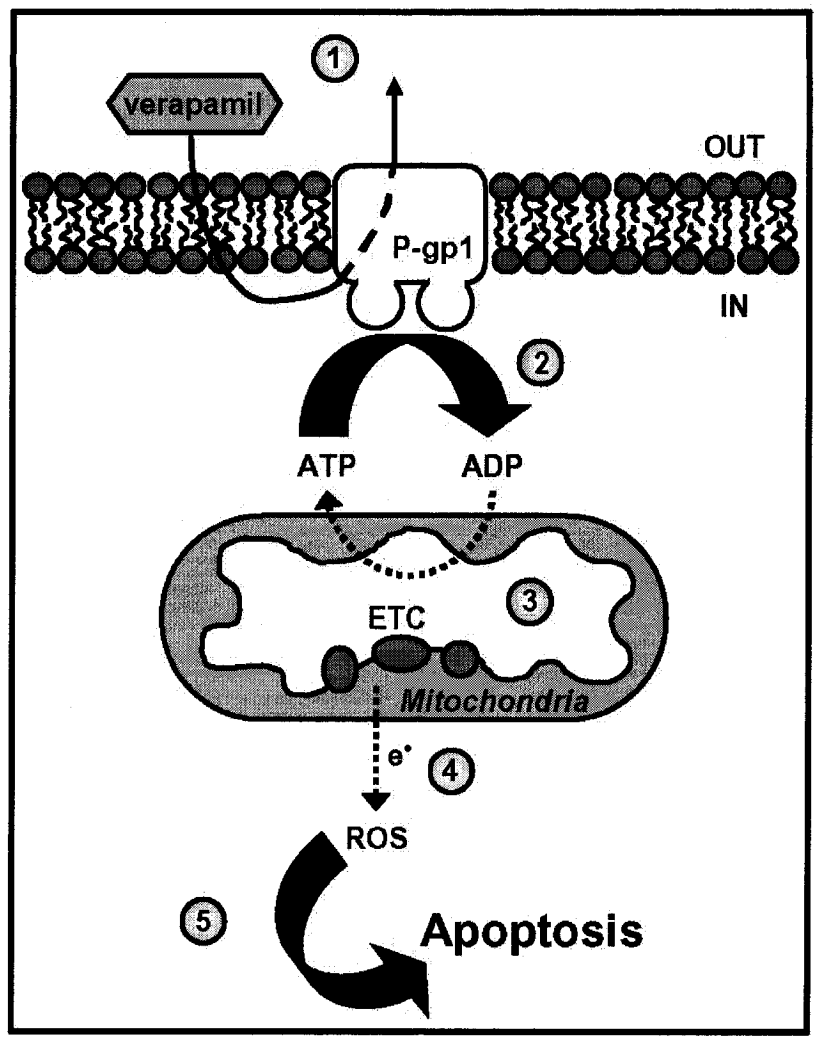

Figure 9

Proposed mechanism of verapamil collateral sensitivity in P-gp1 expressing cells. Verapamil crosses the cellular membrane and interacts with P-gp1, which transports verapamil back into the extracellular environment (1). The interaction with verapamil causes elevated levels of ATP hydrolysis by P-gp1 (2). This creates a high demand for ATP which is generated from oxidative phosphorylation in the mitochondria (3). As a result of the high ATP demand, electrons are lost from the electron transport chain (ETC), causing the production of higher than normal levels of ROS (4). The high concentration of ROS causes apoptosis by damaging lipids and DNA, or by initiating the cytocrome *c* apoptotic pathway (5).

Acknowledgments

The authors would like to thank Mrs. Zhi Liu and Ms. Francoise L'Heureux for their technical assistance in this study. Dr. G. J. Matlashewski (Department of Microbiology and Immunology, McGill University, Canada) generously provided the PG-13 CAT construct. We offer many thanks to our colleagues for their careful reading this manuscript. This work is supported by a grant from the Canadian Institute of Health Research (CIHR) to EG. ML is a recipient of the Max Stern Fellowship for McGill University.

References

1. Endicott, J. A., and Ling, V. (1989) *Annu Rev Biochem* 58, 137-171
2. Gottesman, M. M., and Pastan, I. (1993) *Annu Rev Biochem* 62, 385-427
3. Georges, E., Sharom, F. J., and Ling, V. (1990) *Adv Pharmacol* 21, 185-220
4. Bech-Hansen, N. T., Till, J. E., and Ling, V. (1976) *J Cell Physiol* 88(1), 23-31
5. Cano-Gauci, D. F., and Riordan, J. R. (1987) *Biochem Pharmacol* 36(13), 2115-2123
6. Warr, J. R., Anderson, M., and Fergusson, J. (1988) *Cancer Res* 48(16), 4477-4483
7. Barancik, M., Docolomansky, P., Slezak, J., and Breier, A. (1993) *Neoplasma* 40(1), 21-25
8. Riehm, H., and Biedler, J. L. (1972) *Cancer Res* 32(6), 1195-1200
9. Tsuruo, T., Iida, H., Tsukagoshi, S., and Sakurai, Y. (1982) *Cancer Res* 42(11), 4730-4733
10. Warr, J. R., Quinn, D., Elend, M., and Fenton, J. A. (1995) *Cancer Lett* 98(1), 115-120
11. Naito, M., Hamada, H., and Tsuruo, T. (1988) *J Biol Chem* 263(24), 11887-11891
12. Shapiro, A. B., and Ling, V. (1994) *J Biol Chem* 269(5), 3745-3754
13. Ambudkar, S. V., Lelong, I. H., Zhang, J., and Cardarelli, C. (1998) *Methods Enzymol* 292, 492-504
14. Shapiro, A. B., and Ling, V. (1995) *J Biol Chem* 270(27), 16167-16175
15. Sharom, F. J., Yu, X., and Doige, C. A. (1993) *J Biol Chem* 268(32), 24197-24202

16. Ruetz, S., and Gros, P. (1994) *Cell* 77(7), 1071-1081
17. Sharom, F. J., Yu, X., Chu, J. W., and Doige, C. A. (1995) *Biochem J* 308 (Pt 2), 381-390
18. Ambudkar, S. V., Dey, S., Hrycyna, C. A., Ramachandra, M., Pastan, I., and Gottesman, M. M. (1999) *Annu Rev Pharmacol Toxicol* 39, 361-398
19. Litman, T., Zeuthen, T., Skovsgaard, T., and Stein, W. D. (1997) *Biochim Biophys Acta* 1361(2), 159-168
20. Watanabe, T., Kokubu, N., Charnick, S. B., Naito, M., Tsuruo, T., and Cohen, D. (1997) *Br J Pharmacol* 122(2), 241-248
21. Ling, V., and Thompson, L. H. (1974) *J Cell Physiol* 83(1), 103-116
22. Ling, V. (1975) *Can J Genet Cytol* 17(4), 503-515
23. Kern, S. E., Pietenpol, J. A., Thiagalingam, S., Seymour, A., Kinzler, K. W., and Vogelstein, B. (1992) *Science* 256(5058), 827-830
24. Laemmli, U. K. (1970) *Nature* 227(259), 680-685
25. Towbin, H., Staehelin, T., and Gordon, J. (1979) *Proc Natl Acad Sci U S A* 76(9), 4350-4354
26. Burdon, R. H., Gill, V., and Rice-Evans, C. (1993) *Free Radic Res Commun* 18(6), 369-380
27. Madesh, M., and Balasubramanian, K. A. (1998) *Indian J Biochem Biophys* 35(3), 184-188
28. Barry, M. A., Behnke, C. A., and Eastman, A. (1990) *Biochem Pharmacol* 40(10), 2353-2362
29. Lee, S. C., Deutsch, C., and Beck, W. T. (1988) *Proc Natl Acad Sci U S A* 85(6), 2019-2023
30. Canman, C. E., and Kastan, M. B. (1995) *Semin Cancer Biol* 6(1), 17-25
31. Baudier, J., Delphin, C., Grunwald, D., Khochbin, S., and Lawrence, J. J. (1992) *Proc Natl Acad Sci U S A* 89(23), 11627-11631
32. Massheimer, V., and de Boland, A. R. (1992) *Biochem J* 281 (Pt 2), 349-352
33. Kroemer, G., Zamzami, N., and Susin, S. A. (1997) *Immunol Today* 18(1), 44-51
34. Marks, D. C., Belov, L., Davey, M. W., Davey, R. A., and Kidman, A. D. (1992) *Leuk Res* 16(12), 1165-1173

35. Meister, A. (1988) *J Biol Chem* 263(33), 17205-17208
36. Cano-Gauci, D. F., Seibert, F. S., Safa, A. R., and Riordan, J. R. (1995) *Biochem Biophys Res Commun* 209(2), 497-505
37. Croop, J. M., Guild, B. C., Gros, P., and Housman, D. E. (1987) *Cancer Res* 47(22), 5982-5988
38. Stow, M. W., and Warr, J. R. (1991) *Biochim Biophys Acta* 1092(1), 7-14
39. Stow, M. W., and Warr, J. R. (1993) *FEBS Lett* 320(2), 87-91
40. Vickers, S. E., Stow, M. W., and Warr, J. R. (1993) *Cell Biol Int* 17(5), 477-485
41. al-Shawi, M. K., and Senior, A. E. (1993) *J Biol Chem* 268(6), 4197-4206
42. Jia, L., Allen, P. D., Macey, M. G., Grahn, M. F., Newland, A. C., and Kelsey, S. M. (1997) *Br J Haematol* 98(3), 686-698
43. Jia, L., Kelsey, S. M., Grahn, M. F., Jiang, X. R., and Newland, A. C. (1996) *Blood* 87(6), 2401-2410
44. Chandra, J., Samali, A., and Orrenius, S. (2000) *Free Radic Biol Med* 29(3-4), 323-333
45. Lennon, S. V., Martin, S. J., and Cotter, T. G. (1991) *Cell Prolif* 24(2), 203-214
46. Richter, C., Gogvadze, V., Laffranchi, R., Schlapbach, R., Schweizer, M., Suter, M., Walter, P., and Yaffee, M. (1995) *Biochim Biophys Acta* 1271(1), 67-74
47. Christ, M., Luu, B., Mejia, J. E., Moosbrugger, I., and Bischoff, P. (1993) *Immunology* 78(3), 455-460
48. Maltzman, W., and Czyzyk, L. (1984) *Mol Cell Biol* 4(9), 1689-1694
49. Schreck, R., Albermann, K., and Baeuerle, P. A. (1992) *Free Radic Res Commun* 17(4), 221-237
50. Susin, S. A., Zamzami, N., Castedo, M., Hirsch, T., Marchetti, P., Macho, A., Daugas, E., Geuskens, M., and Kroemer, G. (1996) *J Exp Med* 184(4), 1331-1341
51. Broxterman, H. J., Pinedo, H. M., Schuurhuis, G. J., and Lankelma, J. (1990) *Br J Cancer* 62(1), 85-88
52. Bezombes, C., Maestre, N., Laurent, G., Levade, T., Bettaieb, A., and Jaffrezou, J. P. (1998) *FASEB J* 12(1), 101-109
53. Come, M. G., Bettaieb, A., Skladanowski, A., Larsen, A. K., and Laurent, G. (1999) *Int J Cancer* 81(4), 580-587

54. Lehne, G., and Rugstad, H. E. (1998) *Br J Cancer* 78(5), 593-600

Connecting Statement 1

Chapter 2 included a study that focused on the biochemistry of P-gp1, the first ABC transporter associated with the multidrug resistance phenotype. Specifically, a mechanism was proposed to explain the phenomenon of collateral sensitivity to verapamil. This facet of P-gp1 biochemistry is not directly associated with its drug transport function but still has a significant impact on the understanding of cellular biochemistry of the protein. After Pgp-1, MRP1 is the most studied multidrug transporter. Chapter 3 examines a facet of MRP1 biochemistry that is also not directly associated with its ability to transport anti-cancer drugs. This study investigates the interactions between MRP1 and one of its most important endogenous substrates, GSH.

Chapter 3

Binding of a photoaffinity analog of glutathione to MRP1 (ABCC1) within two cytoplasmic regions (L0 and L1) as well as transmembrane domains 10-11 and 16-17

Joel Karwatsky ϕ, Roni Daoud ϕ, Jie Cai§, Philippe Gros §, and Elias Georges ϕ¶

ϕInstitute of Parasitology and §Department of Biochemistry, McGill University, Quebec, Canada

Biochemistry. 2003 Mar 25; 42(11):3286-94.

Abstract

MRP1 (or ABCC1) is an ABC membrane protein that transports a wide range of natural products as well as glutathione (GSH)-, glucuronate-, and sulfate-conjugated metabolites. In addition, free GSH is required for MRP1 to transport several chemotherapeutic drugs. However, the mechanisms regulating the influence of GSH on MRP1 are poorly understood, and the locations of GSH binding sites within MRP1 have yet to be determined. To address these issues we have synthesized a [^{125}I] labelled azido-derivative of GSH (IAAGSH) to photoaffinity label MRP1. Our results revealed that IAAGSH labelled MRP1 with high specificity, and binding was inhibited by MRP1 substrates leukotriene C_4 and MK571. Interestingly, verapamil and vincristine enhanced IAAGSH photolabelling of MRP1, in agreement with observations that both drugs enhance GSH transport. We observed GSH to be the best inhibitor of photoaffinity labelling, as compared to oxidized glutathione (GSSG) and four different GSH alkyl-derivatives. These observations indicate that IAAGSH interacted with MRP1 in a similar manner as unmodified GSH. Moreover, using eight MRP1-HA variants, each containing hemagglutinin A (HA) epitopes inserted at different sites in MRP1, we mapped the GSH binding sites in MRP1. Our GSH analog photoaffinity labelled four MRP1 polypeptides that were located within two cytoplasmic domains in linkers sequences (L0 and L1) as well as transmembrane domains 10-11 and 16-17. Taken together, this study provides the first evidence that GSH interacts directly with MRP1 and provides the most precise information to date on the location of GSH binding sites in MRP1.

Introduction

Several types of cancer respond to initial drug treatment, but develop resistance upon further therapy (e.g., lymphoma and breast cancer) [1]. The emergence of drug resistance usually prevents treatment from being curative. A more critical problem arises when cancers develop multidrug resistance (MDR), which is characterized by resistance to a diverse group of chemically unrelated drugs. *In vitro* selection of tumour cell lines for resistance to anti-cancer drugs causes the over-expression of large integral membrane proteins such as P-glycoprotein1 (P-gp1) or the multidrug resistance protein 1 (MRP1 or ABCC1) [2,3]. Both P-gp1 and MRP1 function as broad-specificity drug pumps that bind and transport drugs against a concentration gradient using ATP hydrolysis as an energy source [4,5].

P-gp1 and MRP1 are both members of the ATP-binding cassette (ABC) superfamily of transport proteins. Although they share only 15% amino acid identity [2], both P-gp1 and MRP1 confer resistance to many natural product anti-cancer drugs including methotrexate, epipodophyllotoxins, vinca alkaloids, and certain anthracyclines [6-8]. Despite their similar resistance profiles, several key differences exist. Unlike P-gp1, the preferred substrates of MRP1 are organic anions, including drugs conjugated to: glutathione, sulfate, or glucuronate [9-12]. In addition, considerable evidence indicates that GSH is required for MRP1 to transport unmodified drugs such as vincristine and daunorubicin [13-15]. GSH may also be co-transported with some of these compounds [16]. Potential physiological substrates of MRP1 may include: glucuronidate- and sulfate-conjugated bile salts, oxidized glutathione (GSSG), as well as the GSH-conjugates leukotriene C_4 (LTC_4) and prostaglandin A_2 [9-11,17]. In contrast, these conjugated organic anions are poor substrates for P-gp1.

Typically, members of the ABC superfamily are made up of one or more core regions. Each core region contains six transmembrane α-helices comprising a membrane-spanning domain (MSD) and a nucleotide-binding domain (NBD). P-gp1 contains two such core regions connected by an intracellular linker domain, with both the N- and C-terminals located in the cytoplasm [18,19]. The topology of MRP1 is similar to P-gp1, although it has an additional modification at the N-terminal. MRP1 has a group of five transmembrane (TM) sequences at its N-terminal (MSD0) connected through an

intracellular linker domain (L0) to a P-gp1-like core. Therefore, the predicted topological organization of MRP1 is: MSD0-L0-MSD1-NBD1-L1-MSD2-NBD2 [20,21].

Several MRP1-specific photoreactive drugs have been used to show direct binding between MRP1 and unmodified natural product drugs [22-26]. More recently, photoaffinity labelling studies have identified specific drug-binding regions in MRP1 using two iodinated azido derivatives, these include *N*-(hydrocinchonidin-8'-yl)-4-azido-2-hydroxybenzamide (IACI), a quinoline-based drug [22], as well as iodoaryl azido-rhodamine 123 (IAARh123) [23]. These compounds photoaffinity label proteolytic MRP1 fragments within the TM domains 10-11 and 16-17 [27]. LTC_4 can also photoaffinity label sites in both the N- and C-terminal halves of MRP1 [28], however it is not clear if LTC_4 binds to the same regions as the azido-derivatives. None of these studies with azido-drug derivatives indicate that GSH is required for MRP1-drug interactions. However, GSH was shown to be required for MRP1 photoaffinity labelling with an azido-derivative of agosterol-A [29].

Unlike other MRP1 substrates, GSH appears to play a role in facilitating the transport process, possibly by conjugation or co-transport with other molecules. However, at present little is known about how GSH and MRP1 interact despite the critical role GSH plays in transporting MRP1 substrates. The most familiar role of GSH in cells is as an antioxidant. GSH detoxifies reactive oxygen species by acting as a substrate for GSH transferase and GSSG reductase [30]. In this study, we aimed to assess whether or not GSH interacts directly with MRP1 and, if so, to identify the regions of MRP1 involved in GSH binding. To address these questions we synthesized a radiolabelled, iodinated azido-derivative of GSH (IAAGSH) to photoaffinity label MRP1. Our results show that IAAGSH interacted with MRP1 specifically and at physiologically relevant sites. Furthermore, several IAAGSH binding sites were identified by photoaffinity labelling proteolytic fragments of eight MRP1 variants containing hemagglutinin A (HA) epitopes inserted at different positions [27,31,32]. This approach localized IAAGSH binding sites to TM 10-11 and TM 16-17, as well as to two novel cytoplasmic linker regions (L0 and L1). This information provides the most precise location of GSH binding sites within MRP1 to date.

Experimental Procedures

Materials. Protein A Sepharose CL-4B and carrier-free Na[^{125}I] (100 mCi/ml) were purchased from Amersham Biosciences (Baie d'Urfe, Quebec). MK571 was kindly provided by Dr. A.W. Ford-Hutchinson (Merk-Frost Centre for Therapeutic Research, Quebec [33]). LTC_4 was purchased from Cayman Chemical Co. (Ann Arbor, Michigan). The monoclonal anti-hemagglutinin A antibody 16B12 (anti-HA) was purchased from Berkeley Antibody Co. (Richmond, California). The QCRL1 murine hybridoma was obtained from ATCC (Nanassas, Virginia). The MRPr1 mAb was purchased from Kamiya Biomedical Company (Seattle, Washington). Trypsin (sequencing grade and TPKC treated) was procured from Roche Diagnostics, (Laval, Quebec). NHS-ASA and ImmunoPure™ immobilized protein G was purchased from PIERCE (Rockford, Illinois). All other chemicals were of the highest possible quality.

Cell culture and plasma membrane preparation. HeLa cells were cultured in α-MEM media containing 10 % fetal bovine serum (Hyclone) as previously described [31,32]. HeLa cells transfected with MRP1-HA variants had a stable expression of MRP1 containing one or more copies of the HA epitope (YPYDVPDYAS) inserted after amino acids: 1, 163, 271, 574, 653, 938, 1001, or 1222 from the N-terminus [31,32]. For plasma membrane preparations, cells were detached with trypsin-EDTA and washed with phosphate-buffered saline, pH 7.4 (PBS). The cell pellet was then resuspended in hypotonic buffer (1 mM $MgCl_2$, 10 mM KCl, and 10 mM Tris-HCl, pH 7.4) containing protease inhibitors (2 μg/mL leupeptin, 2 μg/mL aprotinin, and 1 μg/mL pepstatin A, 1 mM PMSF). Cells were lysed in a Dounce homogenizer and centrifuged at 10,000 × g for 5 min followed by a second centrifugation at 100 000 × g for 1 h. The final pellet was resuspended in PM buffer (5 mM Tris-HCl with 250 mM sucrose, pH 7.4) and stored at -70 °C. Protein concentrations were determined by the Lowry method [34].

Synthesis of ASA-GSH. All reactions were carried out in the dark. The synthesis of a photoreactive analog of GSH (Iodo-azido-GSH) was done as previously described [35] with some modifications. Briefly, 10 mg GSH was dissolved in 75 μL ddH_2O and diluted to 500 μL with dry dimethylformamide (DMF). NHS-ASA (5.5 mg) was dissolved in 250 μL

DMF and mixed with an equal volume of GSH. Triethylamine (20 µL) was added to the latter reactants and allowed to incubate for 48 h at room temperature with rotation. The reaction was terminated and the resulting mixture was separated on high-pressure liquid chromatography using a reverse phase C18 column from Grace Vydac (Hesperia, California). Separation was achieved using 0.025 M Ammonium Acetate pH 5.5 and an acetonitrile mobile gradient as previously described [35]. Purified ASA-GSH was characterized by mass spectrometry, dried, and stored at –70 °C.

Iodination of ASA-GSH. ASA-GSH (30 µg) was dissolved in 10 µL of PBS and mixed with 100 µL of 3 % chloramine T prepared in Buffer I (10 mM Na_2HPO_4, pH 8.5) along with 2 mCi of carrier-free Na[^{125}I] (100 mCi/ml). The reaction proceeded for 5 min at room temperature and was stopped with 100 µL of 5 % Na-metabisulfate in Buffer I. The sample was then loaded on a C18 SepPak column that was previously washed with 100 % methanol followed by Buffer I. The column was then washed 10 times with 5 mL aliquots of Buffer I to remove free iodine. IAAGSH was eluted from the column with 5 mL of 100 % methanol then dried down to 50-100 µL by aspiration with N_2. Finally, the iodinated sample was resuspended in PBS.

Photoaffinity labelling and SDS-PAGE. For photoaffinity labelling, IAAGSH was added to 20-100 µg aliquots of plasma membrane in PM buffer (5 mM Tris-HCL with 250 mM sucrose, pH 7.4) and incubated at room temperature for 30 min, in the dark. Samples were further incubated on ice for 10 min followed by UV irradiation at 254 nm for 10 min, as previously described [35]. Photoaffinity labelled samples underwent proteolytic digestion and immunoprecipitation [36] as described below, or were directly resolved by SDS-PAGE. Protein samples were resolved on SDS-PAGE exclusively using the Fairbanks system [37]. Coomassie blue staining was used to detect all proteins in plasma membrane samples. Alternatively, gels with radiolabelled proteins were dried and exposed on Kodak BIOMAX™ MS film at –65 °C.

Western blotting. For immunodectection of P-gp1, 20 µg of enriched plasma membranes were resolved on SDS-PAGE and transferred to nitrocellulose membrane by using a wet

electroblotting technique as outlined in Towbin *et al.* [38]. The nitrocellulose membrane was blocked in PBS with 5 % skim milk and incubated with C219 mAb overnight at 4 °C [36]. After incubation, membranes were washed and incubated for 2 h with 1:3000 (v/v) goat anti-mouse antibody conjugated to horseradish peroxidase. SuperSignal™ chemoluminescent (Pierce, Rockford, IL) substrate was used to detect mAb binding

Proteolytic digestion and immunoprecipitation. Photoaffinity labelled plasma membrane samples (100 µg) were digested with increasing concentrations of trypsin at 37 °C for 40 min. The digestion was stopped by placing the samples on ice and adding 80 µL of Buffer A (1 % SDS, 50 mM Tris-HCl, pH 7.4) with protease inhibitors (10 µg/mL leupeptin, pepstatin, aprotinin, and 1 mM PMSF). Samples were left on ice for 15 min before the addition of 320 µl of Buffer B (1.25 % Triton X-100, 190 mM NaCl, and 0.05 M Tris-HCl, pH 7.4). The digested peptides were immunoprecipitated as previously described [36]. Briefly, samples were incubated overnight with protein A Sepharose beads conjugated to anti-HA or QCRL1 mAb in an end-over-end rotator. After incubation, samples were washed 5 times with Buffer C (0.05 % Triton X-100, 0.03 % SDS, 150 mM NaCl, 5 mg/mL BSA, and 0.05 M Tris-HCl, pH 7.4) and once with buffer D (150 M NaCl and 0.05 M Tris-HCl, pH 7.4). For immunoprecipitation with MRPr1 mAb, each labelled plasma membrane sample was first pre-cleared with 50 µL ImmunoPure™ immobilized protein G for 30 min then incubated overnight with 2 µg of MRPr1 mAb. Following incubation, 50 µL ImmunoPure™ immobilized protein G was added to each sample and incubated for 30 min at room temperature and 2 h at 4 °C. The samples were then washed 6 times with immunoprecipitation buffer (20 mM sodium phosphate, pH 7.5, 500 mM NaCl, 0.1 % SDS, 1 % NP-40, 0.5 % sodium deoxycholate and 0.02 % NaN_3). Finally, the samples were resolved on SDS-PAGE.

Results

To investigate the interactions between MRP1 and GSH, we have synthesized a radiolabelled, photoreactive analogue of GSH, IAAGSH (figure 1).

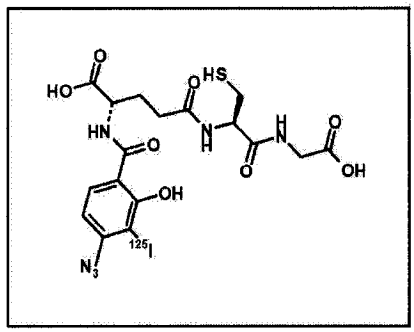

Figure 1.

The chemical structure of radioactive Iodoaryl-azido glutathione (IAAGSH).

Membrane-enriched fractions from HeLa and HeLa/MRP1 transfected cells were photoaffinity labelled with IAAGSH and resolved by SDS-PAGE (figure 2). Lanes 1 and 2 (figure 2A) show photoaffinity labelling of a 190 kDa protein in membranes from HeLa/MRP1 but not HeLa cells. While multiple bands were observed, suggesting the presence of other photoaffinity labelled proteins in HeLa and HeLa/MRP1 membranes, the 190 KDa band is the only band that is selectively labelled in Hela/MRP1 transfected cells. The other labelled proteins likely represent other GSH binding proteins that interact with GSH or IAAGSH. This was not unexpected because GSH interacts with a diverse group of transferases and reductases, including glutathione S-transferases [30]. To confirm the identity of the 190 kDa photoaffinity labelled protein, HeLa and HeLa/MRP1 membranes were photoaffinity labelled with IAAGSH and immunoprecipitated with MRP1-specific mAb, MRPr1, or an irrelevant IgG2a antibody. The results of figure 2A (Lanes 3 and 4) show a 190 kDa photoaffinity labelled protein immunoprecipitated from Hela/MRP1 but not from HeLa photoaffinity labelled plasma membranes. Similar immunoprecipitation with an irrelevant IgG2a did not result in the immunoprecipitation of a 190 kDa protein (data not shown). Together, the molecular mass and binding to MRPr1 mAb, as well as the results in figure 2A (lanes 1-4), confirm the identity of the 190 kDa photolabelled protein to be MRP1. As indicated above, several other proteins from HeLa and HeLa/MRP1 enriched plasma membranes were shown to interact with IAAGSH. Consequently, it was of interest to know if the photoaffinity labelling of MRP1 in HeLa/MRP1 transfectants was exclusively due to the overexpression of MRP1 protein. To address this possibility, total membrane proteins from HeLa and Hela/MRP1 cells were resolved by SDS-PAGE and

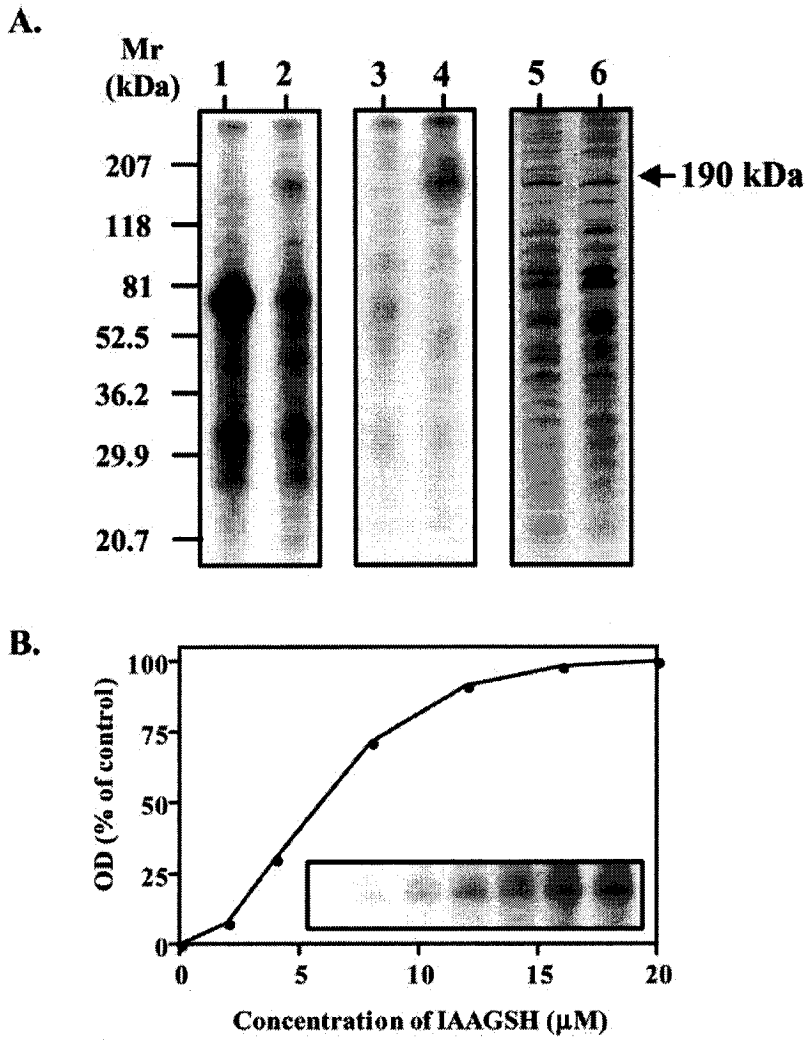

Figure 2

Photoaffinity labelling of HeLa and HeLa-MRP1 with IAAGSH. Plasma membranes (25-50 μg) were incubated with 0.2 μM of IAAGSH and exposed to UV light at 4 °C. Proteins from HeLa and HeLa-MRP1 were resolved on SDS-PAGE (lanes 1 and 2, respectively). Lanes 3 and 4 show an immunoprecipitation of IAAGSH photolabelled HeLa and HeLa-MRP1 membrane proteins with MRP1-specific mAb (MRPr1). Lanes 5 and 6 show the staining of membrane proteins from HeLa and HeLa-MRP1 with Coomassie Blue. The graph in Panel B, demonstrates the saturable photoaffinity labelling of MRP1 with increasing amounts of IAAGSH: 2, 4, 8, 12, 16, and 20 μM (seen in the inset). Lanes 1-4 of panel A and the insert in panel B are autoradiographic images.

stained with Coomassie blue. As demonstrated in lanes 5 and 6 of figure 2A, MRP1 is barely detectable relative to other more highly expressed proteins. Therefore, the labelling of MRP1 by IAAGSH is due to a specific interaction between the IAAGSH and MRP1, and not because of high expression of MRP1. To demonstrate the specificity of IAAGSH toward MRP1, we examined the photoaffinity labelling of MRP1 with increasing amounts of IAAGSH (2-20 μM). Figure 2B shows that MRP1 photoaffinity labelling became saturated at 16 μM of IAAGSH. Incidentally, the band representing labelled MRP1 first appeared at 4 μM of IAAGSH, in contrast to results contained in figure 2A which show MRP1protein labelled with 0.2 μM of IAAGSH. However, in order to prevent saturation of the autoradiography film at high concentrations of IAAGSH (10-20 μM) it was necessary to reduce film exposure time for results shown in figure 2B. Taken together, the results in figure 2 demonstrate that IAAGSH specifically photoaffinity labelled MRP1.

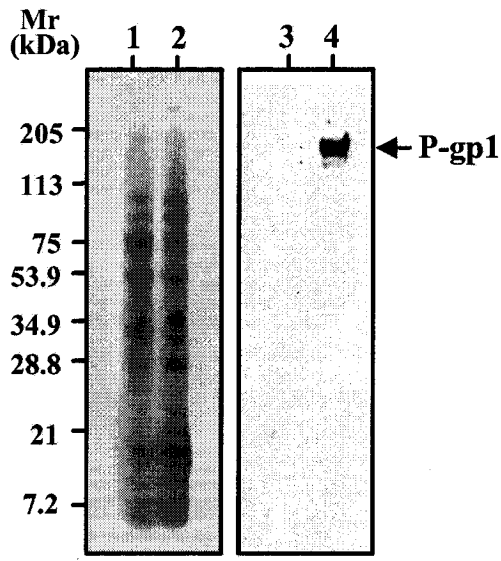

Figure 3

Photoaffinity labelling and Western blot of CEM and CEM/VLB1.0 membranes with IAAGSH. Plasma membranes (25-50 μg) were incubated with 0.2 μM of IAAGSH and exposed to UV light at 4 °C. Proteins from CEM and P-gp1 expressing cells CEM/VLB1.0 (lanes 1 and 2, respectively) were resolved on SDS PAGE. Lanes 3 and 4 show a western blot of plasma membrane from the same cells (CEM and CEM/VLB1.0, respectively) with the P-gp1 specific C219 mAb.

To further investigate the specificity of IAAGSH towards MRP1 and to determine if P-gp1 also interacts with IAAGSH, plasma membranes from human MDR cells (CEM/VL$^{1.0}$), which overexpress P-gp1 at high levels, were photoaffinity labelled with IAAGSH. Western blot analysis with Pgp1 specific mAb (C129) confirmed high expression levels of P-gp1 in CEM/VLB$^{1.0}$ drug resistant, but not in the CEM parental drug sensitive cells (lanes 3 and 4, figure 3). Importantly, the absence of a 170 kDa band in lane 2 indicates that IAAGSH failed to interact with and photolabel P-gp1 in CEM/VLB$^{1.0}$ membranes.

Earlier studies using inside-out membrane vesicles [16,28,39] have indicated that GSH can modulate MRP1-mediated transport of certain anti-cancer drugs. Thus, it was of interest to examine the ability of known MRP1 substrates to interfere with the binding of MRP1 to IAAGSH. Figure 4 shows the effect of increasing concentrations of etoposide (VP16), MK571 (LTD_4 antagonist), doxorubicin (DOX), LTC_4, vincristine (VCR), and verapamil (VRP) on MRP1 binding to IAAGSH. The most effective competitors were MK571 and LTC_4. The presence of 10-fold molar excess of MK571 reduced IAAGSH photolabelling of MRP1 by more than 50 %, and 100-fold excess almost completely inhibited photolabelling. LTC_4 was a more potent inhibitor of IAAGSH photolabelling. It reduced IAAGSH labelling of MRP1 by approximately 50 % when it was added in 1- and 10-fold molar excesses. VP-16 and doxorubicin, both substrates of MRP1, were the least effective competitors, having no significant effect even at 100-fold molar excess of IAAGSH. These results indicate that IAAGSH interacts with similar or overlapping binding sites as known MRP1 substrates. Interestingly, vincristine and verapamil enhanced the photoaffinity labelling of MRP1 by IAAGSH. Vincristine enhanced photolabelling up to about 150 % of control (IAAGSH alone) at 1- and 10-fold molar excess, while at 100-fold excess vincristine more than doubled IAAGSH labelling of MRP1. Verapamil was even more effective at increasing MPR1 labelling by IAAGSH. Ten-fold molar excess of verapamil increased labelling to approximately 300 % of control, and 100-fold excess increased binding to almost 500 % of control.

To ascertain the binding characteristics of IAAGSH to MRP1, photoaffinity labelling of MRP1 in membranes from HeLa/MRP1 cells was conducted in the presence of increasing concentrations of reduced glutathione (GSH), oxidized glutathione (GSSG), and

several alkyl-GSH derivatives: S-methylglutathione (Meth-GSH), S-ethylglutathione (Eth-GSH), S-hexylglutathione (Hex-GSH), and S-Octylglutathione (Oct-GSH). The results in figure 5 show that unmodified GSH inhibited IAAGSH labelling far more effectively than GSSG or any of the alkyl-derivatives. When GSH was added at 500-fold molar excess of IAAGSH, photoaffinity labelling was completely abolished. Moreover, as little as 5-fold molar excess of GSH reduced IAAGSH labelling by half. GSSG was the next most effective inhibitor of IAAGSH photolabelling. Both Methyl-GSH and Ethyl-GSH caused a moderate inhibition on IAAGSH labelling relative to GSH by causing a 20 to 25 % reduction at 500-fold molar excess (figure 5). The two most hydrophobic GSH alkyl-derivatives, Hexyl-GSH and Octyl-GSH, caused an increase of approximately 20 and 25 %, respectively, in IAAGSH photolabelling at 50-fold molar excess. Taken together, the results in figure 5 confirm the specificity of IAAGSH towards MRP1-GSH binding domain(s) and provide the first direct evidence for GSH and MRP1binding.

Using several variants of MRP1, we have previously identified two regions in MRP1 encoding binding sites for structurally diverse drugs. Each variant contains one or more HA epitopes inserted at eight different sites in MRP1 (figure 6). These binding regions were localized to two peptide fragments with sizes of 6.5 and 7 kDa, encoding amino acid sequences from TM 10-11 and 16-17, respectively [27]. Given the above results, it was of interest to determine if the binding domains of IAAGSH are the same or if they overlap these previously identified drug-binding domains. The results in figure 6 describe the IAAGSH photoaffinity labelling of plasma membranes from each cell line transfected with the different MRP1 variants containing HA-epitopes. Each MRP1-variant was digested separately with increasing concentrations of trypsin (1:800 to 1:25). The digested peptide fragments were immunoprecipitated with anti-HA mAb and resolved by SDS-PAGE. The resulting polypeptide bands contained a HA-epitope and a cross-linked IAAGSH.

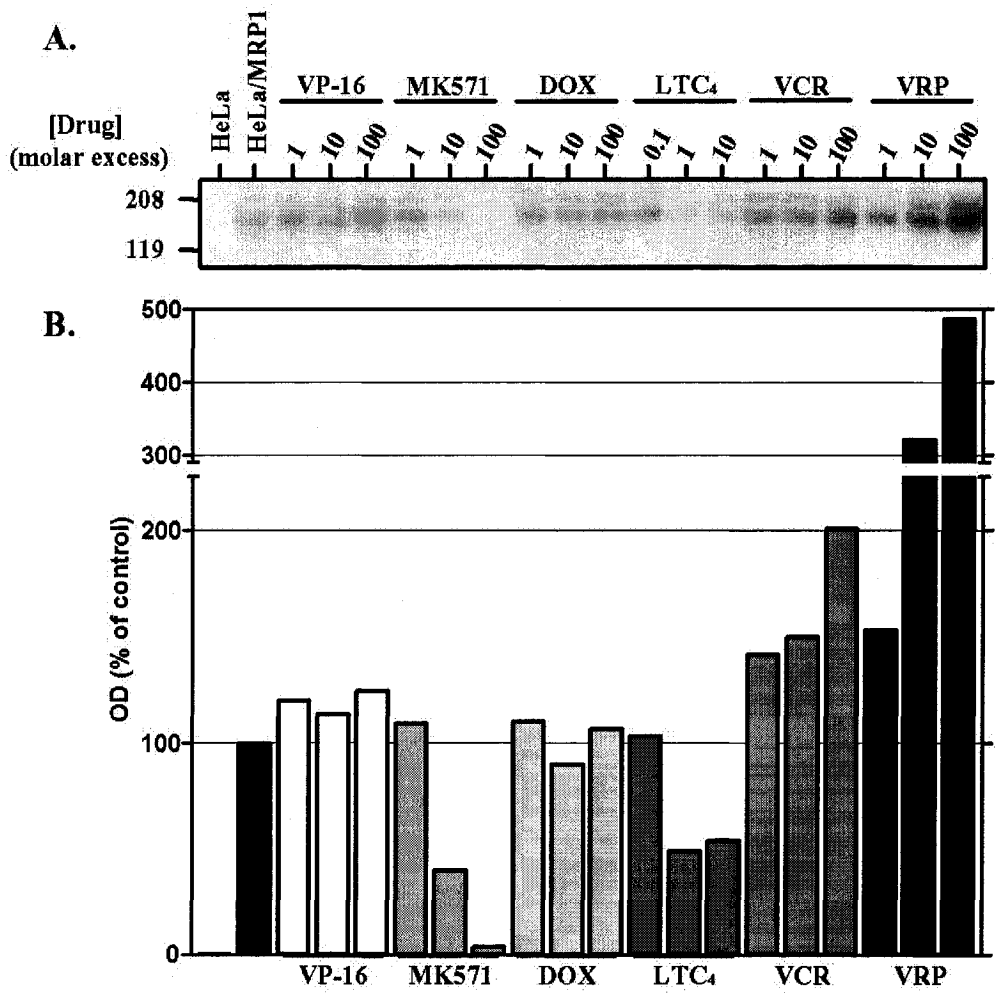

Figure 4

Effect of several drugs on photoaffinity labelling of MRP1 by IAAGSH. HeLa or HeLa/MRP1 plasma membranes were photoaffinity labelled with 2 μM IAAGSH in the absence or presence of: etoposide (VP-16), MK571, doxorubicin (DOX), Leucotriene C_4 (LTC_4), vincristine (VCR), and verapamil (VRP). LTC4 was added in: 0.1, 1, and 10 molar excess of IAAGSH. All other drugs were added in: 1, 10, and 100 molar excess of IAAGSH. Panel B demonstrates the relative change in photolabelling of MRP1 with IAAGSH in the presence of the same drugs. Plasma membranes were immunoprecipitated with hemagglutinin A (HA) mAb. These results are representative of at least three individual experiments.

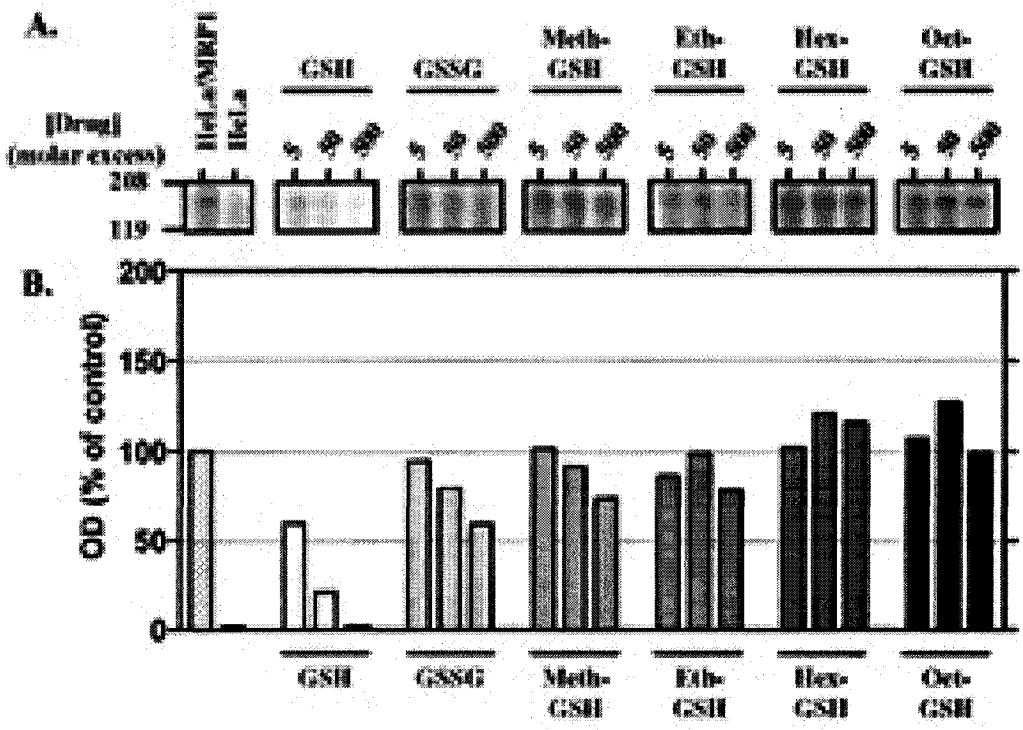

Figure 5

Effect of GSH and its derivatives on the photoaffinity labelling of MRP1 by IAAGSH. Panel A shows HeLa or HeLa/MRP1 plasma membranes photoaffinity labelled with 2 μM IAAGSH in the absence or presence of increasing molar excess (5, 50, and 500) of: reduced glutathione (GSH), oxidized glutathione (GSSG), S-Methylglutathione (Meth-GSH), S-Ethylglutathione (Eth-GSH), S-Hexylglutathione (Hex-GSH), and S-Octylglutathione (Oct-GSH). Panel B demonstrates the relative decrease in photolabelling of MRP1 with IAAGSH in the presence of the same compounds. These results are representative of at least three individual experiments.

The digestion pattern of each photoaffinity labelled MRP1-variant is displayed in figure 6. A topological diagram of MRP1 and connecting arrows indicate the position of the inserted HA epitopes in each MRP1 variant. The tryptic peptide fragments from MRP1-variant 4 (HA epitope inserted after the fourth amino acid) are visible in figure 6A. In addition to full length MRP1 (190kDa), a 111 kDa fragment was resolved. This fragment corresponds to one of two peptides that results from digestion at a known trypsin-sensitive site located in the linker domain, L1 [40].

MRP1-variants: 163, 271, and 574 (figures 6B, 6C, and 6D, respectively) share two common peptides fragments, the previously mentioned 111 kDa band as well as a 65 kDa fragment. In addition, MRP1-variant 271 also has a photoaffinity labelled 24 kDa peptide. Based on its apparent molecular mass and the known trypsin cutting sites, the 24 kDa peptide is made up of approximately 216 amino acid residues and must be located somewhere between Asp^{171} (within TM 5) and Lys^{357} (before TM 6). Close examination of the mobility of the 24 kDa peptide on SDS-PAGE shows a broad band that could suggest the presence of several polypeptides of various lengths.

Analysis of the trypsin digest of MRP1-variant 574 can be seen in panel D of figure 6. This digested variant produced three large fragments: 111, 130, and 65 kDa. The 111 and 65 kDa fragments correspond to the same ones indicated above. A faintly visible 130 kDa peptide (not highlighted in the figure) corresponds to a cleavage of MRP1 at the linker domain L0, the second trypsin-sensitive site [40]. In addition, two other fragments with approximate molecular masses of 18 and 6.5 kDa became visible with a higher trypsin concentration (1/25). The appearance of these fragments correlates with the digestion pattern previously observed with IAARh123-labelled MRP1 [27]. The 6.5 kDa fragment corresponds to the smallest polypeptide containing the HA-epitope (574) between two trypsin sites Ser^{542} and Arg^{593}: ^{542}SAYLSAVGTFTWVCTPFLVAL-CTFAVYVTIDEN[**HA**]NILDAQTAFVSLALFNILR^{593}. The calculated molecular mass of this polypeptide, including the 10 amino acids of the HA-epitope, is 6.9 kDa. The underlined regions represent the predicted TM 10 and TM 11. The MRP1 HA-variants: 653, 938, and 1001 (figures 7E, 7F, and 7G respectively) produced a 31 kDa proteolytic fragment. This shows that IAAGSH photoaffinity labels a region of MRP1 between MSD1 and MSD2. The predicted molecular weight of the primary sequence from amino acid 653 to 1001 is approximately 38 kDa; indicating that this fragment migrated lower than expected, and is represented by the 31 kDa band. A more precise location for IAAGSH labelling in this region was apparent in the highly digested MRP1-variant 938; in addition to the 31 kDa band, 24 and 18 kDa fragments could also be resolved. By comparing the 18 kDa band with MRP1 topology and trypsin cutting sites it was possible to localise IAAGSH photoaffinity labelling of MRP1 to a region after NBD1 but before TM 12 of MSD2. We know that this fragment does not extend into MSD2 because no lysine or arginine residues

are located from the start of MSD2 up to position 1001, the location of the next MRP1 HA-variant.

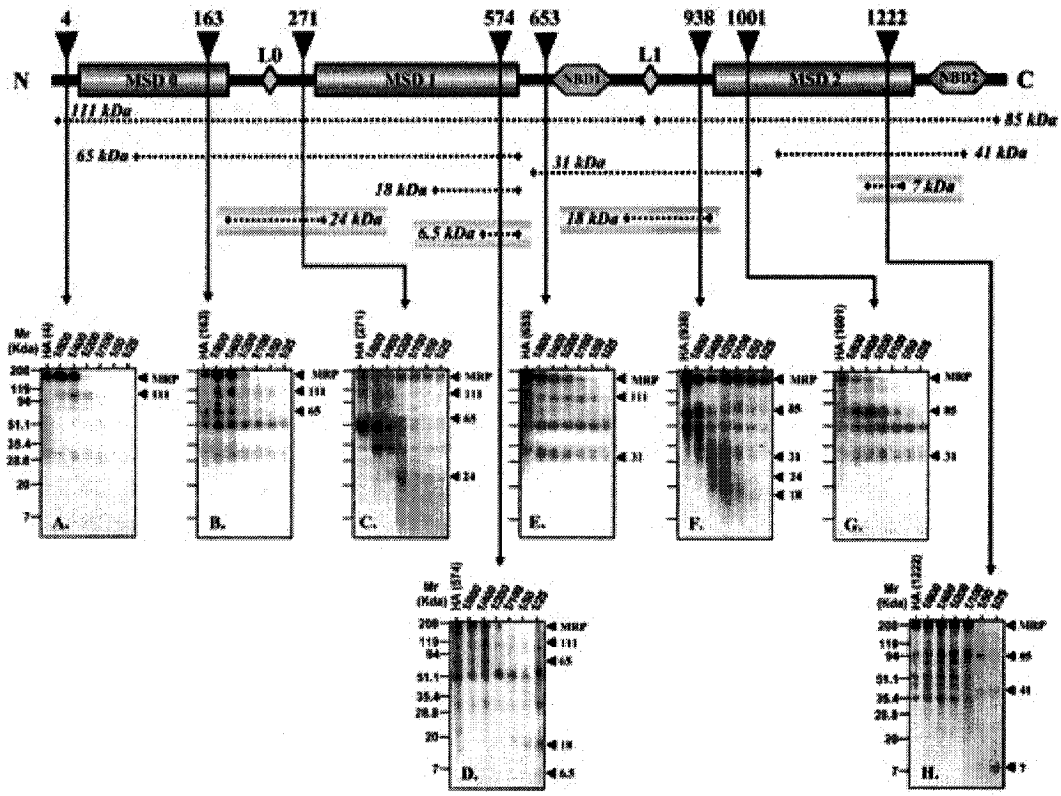

Figure 6

Immunoprecipitation of the tryptic digest of IAAGSH-labelled MRP1-HA variants. The image at the top represents the topology of MRP1 and the arrows correspond to the locations of HA-epitope insertions. Directly below, in panels A through H, are the resulting labelled and immunoprecipitated peptides derived from the digested plasma membranes containing the eight different full length MRP1 HA-variants. The horizontal dashed lines represent all of the peptides that are resolved by SDS-PAGE on Panels A through H. The vertical solid arrows connect the particular MRP1 HA-variant in the top panel diagram to its SDS-PAGE digest analysis, and cross horizontal dashed lines representing the peptide fragments observed in said panel. All plasma membranes were photoaffinity labelled with 4 μM IAAGSH. Each sample was digested with increasing concentrations of trypsin, from 1/800 to 1/25 (w/w : protein/trypsin).

The HA-epitopes of MRP1-variants 938, 1001, and 1222 (figures 6F, 6G, and 6H respectively) are located to the C-terminal side of L1. As a result, their digestion pattern did not include the 111 kDa fragment found in the five other variants. Instead, an 85 kDa labelled polypeptide was immunoprecipitated, which correlates to the C-terminal fragment produced from the L1 trypsin sensitive site [22,23]. Digestion of MRP1-variant 938 produced two previously discussed fragments, 130 and 85 kDa, whereas only the 85 kDa peptide was visible in variant 1001. Alternatively, the digestion of MRP1-variant 1222 produced three polypeptides: 85, 41, and 7 kDa. The two smaller polypeptides are unique to variant 1222. These fragments map IAAGSH photoaffinity labelling to a region at, or near to the photolabelling site of IAARh123 in MRP1 [27]. The 7 kDa polypeptide is the smallest photoaffinity labelled fragment that can be immunoprecipitated from the tryptic digest of MRP1-variant 1222. We believe that this band corresponds to the smallest possible trypsin-derived fragment that contains an HA-epitope at position 1222 in MRP1. Photoaffinity labelling of the 7 kDa peptide occurs within the following amino acid sequence: ^{1203}LECVGNCIVLFAALFAVISR[**HA-HA**]HSLSAGLVGLSVSYSLQVTT-YLNWLVR^{1249}, in which the underlined regions represent the putative TM 16 and TM 17. The calculated molecular mass of this polypeptide, including the two HA-epitopes, is 7.4 kDa.

In summary, the trypsin digestions shown in figure 6 indicate that IAAGSH photoaffinity labelled four distinct regions in MRP1. Two of these regions are located within putative transmembrane domains (MSD1 and MSD2) and correspond to TM 10-11 and TM 16-17. These sites are identical to those found for IAARh123. Remarkably, the peptide mapping in figure 6 also demonstrates that IAAGSH also interacts with two previously unidentified regions corresponding to L0 and L1. These sites are particularly novel because their proposed location is within the cellular cytoplasm.

To confirm the presence of photolabelling sites within the two cytoplasmic regions L0 and L1, we preformed peptide mapping experiments using two MRP1-specific mAb within these regions, MRPr1 and QCRL1 that are located close to the HA epitopes of MRP1-variants 271 and 938 (figure 7). The epitopes of MRPr1 and QCRL1 are found within amino acids 238-247 and 918-924, respectively [41]. The results obtained from immunoprecipitation with MRPr1 were similar to the MRP1-variant 271. The 111 and 65

kDa products of the L1 trypsin sensitive site were visible, as well as the smaller 24 kDa peptide (figure 7A). At higher concentration of trypsin (1/12.5 and 1/3.125, protein/trypsin), an even smaller peptide was visible at approximately 18 kDa. Immunoprecipitation of peptides with QCRL1 also confirmed the digestion pattern of MRP1-variant 938 (figure 7B). The 85 kDa fragment is visible which is characteristic of MRP1-variants that contain an HA-epitope inserted after L1. The smaller 18 kDa band is not visible.

It should be pointed out that several IAAGSH-labelled polypeptides were immunoprecipitated and their bands were visible in the digestion of all eight clones. These polypeptides were located in the undigested sample and did not increase in intensity with increasing concentrations of trypsin; hence are not products of MRP1 digestion. We have determined the approximate size of two non-specific labelled peptides: 34 and 50 kDa. Previous analysis [27] determined that the 50 kDa fragment may originate from the foetal bovine serum used to culture the cell lines. In addition, two photoaffinity labelled polypeptide of the same size are found in undigested HeLa cell plasma membrane (figure 2).

Discussion

Unlike Pgp1-mediated drug transport, MRP1 activity is often associated with binding or transport of reduced or oxidized glutathione and several MRP1-substrates are exclusively transported when they are conjugated to GSH [13-15,17]. Moreover, there is evidence that GSH is co-transported with unmodified drugs such as vincristine [14,16,42]. In this study, an iodinated photoreactive analog of GSH (IAAGSH) was synthesized and used to characterize interactions between GSH and MRP1, and identify binding domains. Our results show that there is a direct and specific interaction between MRP1 and IAAGSH. Moreover, MRP1 photolabelling by IAAGSH was specifically inhibited with unmodified GSH and to a lesser extent with GSSG and GSH alkyl-derivatives. These results indicate that the binding characteristics of IAAGSH are very similar to GSH compared to GSSG and the alkyl-derivatives. The fact that GSSG also caused noticeable competition is expected since it too is a substrate of MRP1 [43]. We also tested the effect of other known MRP1 substrates on IAAGSH photoaffinity labelling. Surprisingly, both verapamil and, to a lesser extent, vincristine caused an increase in IAAGSH photoaffinity labelling of MRP1.

These results are interesting since it was previously demonstrated that verapamil inhibits LTC_4 transport into inside-out MRP1-enriched membrane vesicles by enhancing the transport of GSH [44]. Vincristine also stimulates ATP-dependent transport of GSH in a similar manner [14]. These studies suggest that verapamil and vincristine mediate GSH transport via a process of co-transport. Our labelling results correlate well with these transport studies and indicate that verapamil and vincristine enhance GSH binding to MRP1 as a preliminary step to co-transport.

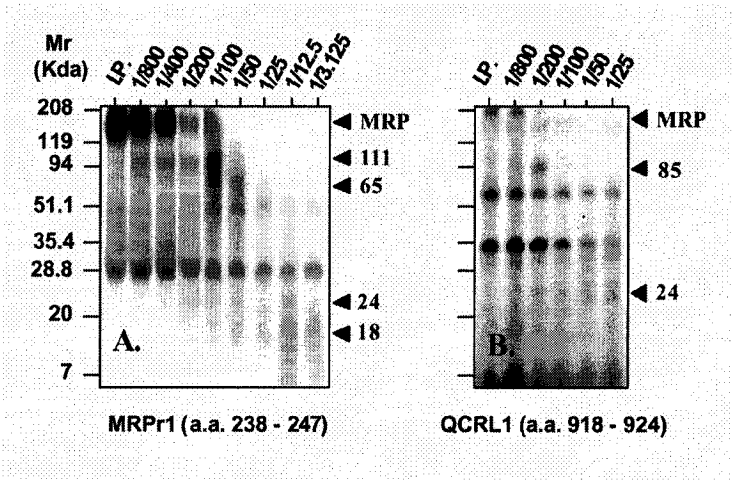

Figure 7

Immunoprecipitation of the tryptic digest of IAAGSH-labelled MRP1 with two MRP1-specific mAbs, MRPr1 and QCRL1. The epitopes in MRP1 that are targeted by MRPr1 and QCRL1 are 238–247 and 918–924, respectively. Panels A and B are the resulting labelled and immunoprecipitated peptides derived from the digested plasma membranes of HeLa cells transfected with MRP1 resolved by SDS-PAGE. All plasma membranes were photoaffinity labelled with 4 μM IAAGSH. The samples were digested with increasing concentrations of trypsin from 1/800 to 1/3.125 (w/w : protein/trypsin).

As opposed to verapamil and vincristine, the physiological MRP1 substrate LTC_4 inhibited IAAGSH photoaffinity labelling. Unlike verapamil and vincristine, LTC_4 is directly conjugated to GSH and is transported independent of free GSH. This indicates that IAAGSH and LTC_4 share the same or overlapping binding domains. Perhaps the efficient

inhibition of IAAGSH binding occurred because the LTC_4 molecule contains a GSH component capable of competing for as GSH-specific binding site.

Previous attempts to map the binding sites of MRP1 used a quinoline-based drug (IACI) and a Rhodamine 123 analog (IAARh123). Using these compounds, two binding regions were identified within MRP1: TM 10-11 and TM 16-17 [27]. The present report showed that IAAGSH photolabelled these same regions, in addition to two novel sites. These newly identified sites are located in the large cytoplasmic regions on the N-terminal sides of both MSD1 and MSD2. The first region on the N-terminal half of MRP1 is located in or near to the cytoplasmic region connecting MSD0 to the rest of the protein, and has been named L0 (~130 amino acids) [41]. Several studies attempting to localize binding sites in MRP1 have found L0 to be important. Using an azido-derivative of the polyhydroxylated sterol acetate (AG-A), Ren *et al.* [29] observed that photoaffinity labelling of the C-terminal half of MRP1 requires the L0 domain. They also observed that a double mutation involving Trp^{261} and Lys^{267} within L0 decreases labelling by ~3-fold [29]. In addition, Gao *et al.* [7] showed that a truncated MRP1 mutant lacking MSD0 but still containing L0 behaved like wild-type MRP1 in vesicle uptake and nucleotide trapping experiments. Similarly, Bakos *et al.* [45] demonstrated that truncated MRP1 lacking MSD0 but retaining the majority of the predicted L0 domain retained considerable LTC_4 transport activity [45]. Finally, a photoaffinity labelling study using [^{3}H]LTC_4 indicates that all or part of L0 between amino acids 204 and 281 is essential for LTC_4 binding [28]. Taken together, these studies show importance of L0 in the activity of MRP1 and support our observations that IAAGSH photolabels a region within L0. This was demonstrated from the labelling of a 24 kDa peptide in MRP1-variant 271. Proteolysis and immunoprecipitation with the MRP1-specific mAb, MRPr1, confirmed this observation by demonstrating that IAAGSH labels MRP1 the same 24 kDa fragment in addition to a smaller 18 kDa peptide. Based on the size of the 18 kDa fragment, GSH binding must occur within L0.

A second IAAGSH-labelling region on the C-terminal half of MRP1 is located after NBD1 but before TM 12, encompassing the L1 region. This labelled portion of MRP1 is symmetrical orientation relative to the L0 region. Both binding regions are cytoplasmic and are located on the N-terminal side of a six-pass membrane-spanning domain. Since IAAGSH binds to these regions, while IACI and IAARh123 do not, we suggest that these

two cytoplasmic regions form GSH-specific binding sites. They may form autonomous binding sites or they may act cooperatively to make a binding pocket in the properly folded protein. Cooperative interactions between the N- and C-terminal halves of MRP1 are required for high affinity LTC_4 binding [28] favouring the possibility that these cytoplasmic binding sites form a single GSH-binding pocket. Similarly, the two transmembrane regions that are labelled, TM10-11 and TM16-17 may represent a single drug binding pocket that has an affinity for drugs such as IAARh123 and IACI, as well as IAAGSH.

A recent study examined the labelling of MRP1 with a photoactive derivative of GSH, [^{35}S]azidophenacyl-GSH [46]. This study found that the photoactive GSH derivative also labels both halves of MRP1. In contrast to our findings, this study found that L0 is not photolabelled, although it is required for binding. Several possibilities may explain this discrepancy with our observations. Perhaps azidophenacyl-GSH is modified at the thiol-group of GSH rather than the amino-group, as in IAAGSH. Modification at a different portion of GSH group could influence the binding affinity of the compound. It may also be possible that the peptide comprising amino acids 1-280 of MRP1 is difficult to resolve with a more weakly radioactive [^{35}S] compound.

Numerous observations give credence to the existence of a GSH-binding site located in the cytoplasmic portion of MRP1. As a hydrophilic molecule, the pool of cellular GSH is found within the cytoplasm, and is thus readily accessible for binding to the cytoplasmic portions of MRP1. Furthermore, we observed that hydrophobic alkyl-derivatives with a higher number of hydrocarbon additions (from Met- to Oct-GSH) appear to cause very little inhibition of IAAGSH photoaffinity labelling of MRP1 (figure 5). This correlates with our observation that the GSH binding site is located within the cytoplasm, in which the alkyl derivatives would not be freely soluble. Conversely, GSH also interacts with the transmembrane drug-binding sites, located in TM 10-11 and 16-17. Despite its polar nature, it is not totally unexpected that GSH can interact with the hydrophobic transmembrane domains; many anionic and polar substrates are known to be substrates of MRP1 [38]. The interaction of IAAGSH with TM 10-11 and TM 16-17 is consistent with our findings that increasing concentrations of GSH and GSSG can compete from binding of IAARh123 to TM 10-11 and TM 16-17 [27] (Appendix 1).

In summary, the findings of this study contribute important information about the interactions between GSH and MRP1, in addition to emphasising the value of photoaffinity labelling studies in general. Firstly, IAAGSH behaves in a very similar manner as native GSH. This was initially demonstrated by the ability of IAAGSH to specifically photolabel MRP1. This binding specificity was supported by the ability of unmodified GSH to compete and reduce binding of IAAGSH more effectively than other GSH-analogs. Furthermore, the observation that verapamil and vincristine increased IAAGSH binding presents a strong correlation between GSH binding and its subsequent transport by MRP1. We show that IAAGSH photolabels TM 10-11 and TM 16-17, indicating that it can interact with the same sites as exogenous drugs. We also present evidence that IAAGSH has two novel cytoplasmic binding sites located on the N-terminal sides of MSD1 and MSD2 (L0 and L1), possibly GSH-specific binding sites. This data provides the most precise evidence to date on the location of GSH binding sites in MRP1, and adds significant insight to our understanding of how MRP1 interacts with anti-cancer drugs and one of its physiological substrates.

References

1. Lehnert, M. (1996) *Eur J Cancer* 32A(6), 912-920
2. Cole, S. P., Bhardwaj, G., Gerlach, J. H., Mackie, J. E., Grant, C. E., Almquist, K. C., Stewart, A. J., Kurz, E. U., Duncan, A. M., and Deeley, R. G. (1992) *Science* 258(5088), 1650-1654
3. Ling, V. (1975) *Can J Genet Cytol* 17(4), 503-515
4. Borst, P., and Schinkel, A. H. (1997) *Trends Genet* 13(6), 217-222
5. Germann, U. A. (1996) *Eur J Cancer* 32A(6), 927-944
6. Cole, S. P., Sparks, K. E., Fraser, K., Loe, D. W., Grant, C. E., Wilson, G. M., and Deeley, R. G. (1994) *Cancer Res* 54(22), 5902-5910
7. Gao, M., Yamazaki, M., Loe, D. W., Westlake, C. J., Grant, C. E., Cole, S. P., and Deeley, R. G. (1998) *J Biol Chem* 273(17), 10733-10740
8. Hooijberg, J. H., Broxterman, H. J., Kool, M., Assaraf, Y. G., Peters, G. J., Noordhuis, P., Scheper, R. J., Borst, P., Pinedo, H. M., and Jansen, G. (1999) *Cancer Res* 59(11), 2532-2535

9. Evers, R., Cnubben, N. H., Wijnholds, J., van Deemter, L., van Bladeren, P. J., and Borst, P. (1997) *FEBS Lett* 419(1), 112-116

10. Jedlitschky, G., Leier, I., Buchholz, U., Barnouin, K., Kurz, G., and Keppler, D. (1996) *Cancer Res* 56(5), 988-994

11. Leier, I., Jedlitschky, G., Buchholz, U., Cole, S. P., Deeley, R. G., and Keppler, D. (1994) *J Biol Chem* 269(45), 27807-27810

12. Loe, D. W., Stewart, R. K., Massey, T. E., Deeley, R. G., and Cole, S. P. (1997) *Mol Pharmacol* 51(6), 1034-1041

13. Loe, D. W., Almquist, K. C., Deeley, R. G., and Cole, S. P. (1996) *J Biol Chem* 271(16), 9675-9682

14. Loe, D. W., Deeley, R. G., and Cole, S. P. (1998) *Cancer Res* 58(22), 5130-5136

15. Renes, J., de Vries, E. G., Nienhuis, E. F., Jansen, P. L., and Muller, M. (1999) *Br J Pharmacol* 126(3), 681-688

16. Rappa, G., Lorico, A., Flavell, R. A., and Sartorelli, A. C. (1997) *Cancer Res* 57(23), 5232-5237

17. Leier, I., Jedlitschky, G., Buchholz, U., Center, M., Cole, S. P., Deeley, R. G., and Keppler, D. (1996) *Biochem J* 314 (Pt 2), 433-437

18. Loo, T. W., and Clarke, D. M. (1995) *J Biol Chem* 270(2), 843-848

19. Rosenberg, M. F., Callaghan, R., Ford, R. C., and Higgins, C. F. (1997) *J Biol Chem* 272(16), 10685-10694

20. Bakos, E., Hegedus, T., Hollo, Z., Welker, E., Tusnady, G. E., Zaman, G. J., Flens, M. J., Varadi, A., and Sarkadi, B. (1996) *J Biol Chem* 271(21), 12322-12326

21. Hipfner, D. R., Almquist, K. C., Leslie, E. M., Gerlach, J. H., Grant, C. E., Deeley, R. G., and Cole, S. P. (1997) *J Biol Chem* 272(38), 23623-23630

22. Daoud, R., Desneves, J., Deady, L. W., Tilley, L., Scheper, R. J., Gros, P., and Georges, E. (2000) *Biochemistry* 39(20), 6094-6102

23. Daoud, R., Kast, C., Gros, P., and Georges, E. (2000) *Biochemistry* 39(50), 15344-15352

24. Vezmar, M., Deady, L. W., Tilley, L., and Georges, E. (1997) *Biochem Biophys Res Commun* 241(1), 104-111

25. Vezmar, M., and Georges, E. (1998) *Biochem Pharmacol* 56(6), 733-742

26. Vezmar, M., and Georges, E. (2000) *Biochem Pharmacol* 59(10), 1245-1252
27. Daoud, R., Julien, M., Gros, P., and Georges, E. (2001) *J Biol Chem* 276(15), 12324-12330
28. Qian, Y. M., Qiu, W., Gao, M., Westlake, C. J., Cole, S. P., and Deeley, R. G. (2001) *J Biol Chem* 276(42), 38636-38644
29. Ren, X. Q., Furukawa, T., Aoki, S., Nakajima, T., Sumizawa, T., Haraguchi, M., Chen, Z. S., Kobayashi, M., and Akiyama, S. (2001) *J Biol Chem* 276(25), 23197-23206
30. Meister, A. (1988) *J Biol Chem* 263(33), 17205-17208
31. Kast, C., and Gros, P. (1997) *J Biol Chem* 272(42), 26479-26487
32. Kast, C., and Gros, P. (1998) *Biochemistry* 37(8), 2305-2313
33. Jones, T. R., Zamboni, R., Belley, M., Champion, E., Charette, L., Ford-Hutchinson, A. W., Frenette, R., Gauthier, J. Y., Leger, S., Masson, P., and et al. (1989) *Can J Physiol Pharmacol* 67(1), 17-28
34. Lowry, O. H., Rosebrough, N. J., Farr, A. L., and Randall, R. J. (1951) *J Biol Chem* 193(1), 265-275
35. Nare, B., Prichard, R. K., and Georges, E. (1994) *Mol Pharmacol* 45(6), 1145-1152
36. Georges, E., Zhang, J. T., and Ling, V. (1991) *J Cell Physiol* 148(3), 479-484
37. Fairbanks, G., Steck, T. L., and Wallach, D. F. (1971) *Biochemistry* 10(13), 2606-2617
38. Towbin, H., Staehelin, T., and Gordon, J. (1979) *Proc Natl Acad Sci U S A* 76(9), 4350-4354
39. Bagrij, T., Klokouzas, A., Hladky, S. B., and Barrand, M. A. (2001) *Biochem Pharmacol* 62(2), 199-206
40. Hipfner, D. R., Almquist, K. C., Stride, B. D., Deeley, R. G., and Cole, S. P. (1996) *Cancer Res* 56(14), 3307-3314
41. Hipfner, D. R., Deeley, R. G., and Cole, S. P. (1999) *Biochim Biophys Acta* 1461(2), 359-376
42. Mao, Q., Deeley, R. G., and Cole, S. P. (2000) *J Biol Chem* 275(44), 34166-34172
43. Jedlitschky, G., Leier, I., Buchholz, U., Center, M., and Keppler, D. (1994) *Cancer Res* 54(18), 4833-4836

44. Loe, D. W., Deeley, R. G., and Cole, S. P. (2000) *J Pharmacol Exp Ther* 293(2), 530-538

45. Bakos, E., Evers, R., Szakacs, G., Tusnady, G. E., Welker, E., Szabo, K., de Haas, M., van Deemter, L., Borst, P., Varadi, A., and Sarkadi, B. (1998) *J Biol Chem* 273(48), 32167-32175

46. Qian, Y. M., Grant, C. E., Westlake, C. J., Zhang, D. W., Lander, P. A., Shepard, R. L., Dantzig, A. H., Cole, S. P., and Deeley, R. G. (2002) *J Biol Chem* 277(38), 35225-35231

Connecting Statement 2

Chapter 3 presented a detailed investigation of the interaction between MRP1 and a photoreactive analog of its endogenous substrate GSH, IAAGSH. This study demonstrated that IAAGSH photolabels MRP1 with a high degree of specificity and shares many binding characteristics with unmodified GSH. Furthermore, several photolabelling sites were elucidated, with two previously identified "drug sites" in TM 10-11 and TM 16-17, as well as two novel "GSH sites" in the cytoplasmic L0 and L1 linker regions. Given these results with an endogenous substrate of MRP1, it was of interest to investigate the highest affinity endogenous substrate, LTC_4. To this end, a photoreactive derivative of LTC_4 was generated. The study in chapter 4 examined the binding characteristics of the photoreactive derivative, $IAALTC_4$.

Chapter 4

The leucotriene C_4 binding sites in MRP1 (ABCC1) include the first membrane multiple spanning domain

Joel Karwatsky ϕ, Mara Leimanis ϕ, Jie Cai§, Philippe Gros §, and Elias Georges ϕ¶

ϕInstitute of Parasitology and §Department of Biochemistry, McGill University, Quebec, Canada

Biochemistry. 2005 Jan 11; 44(1):340-51.

Abstract

The Multiple Drug Resistance Protein (MRP1 or ABCC1) transports anti-cancer drugs and normal cell metabolites. Leucotriene C_4 (LTC_4) is one of the highest affinity substrates of MRP1. In this study, we have synthesised and characterized a novel photoreactive azido-analog of LTC_4 ($AALTC_4$). The specificity of $AALTC_4$ binding to MRP1 was confirmed using an LTC_4-specific monoclonal antibody. Moreover, binding with radio-iodinated [^{125}I]$AALTC_4$ (or $IAALTC_4$) to MRP1 was dramatically competed with unmodified LTC_4, and to a lesser degree by reduced glutathione (GSH). The MRP1 substrates MK571, verapamil, and vincristine also inhibited $IAALTC_4$ binding to MRP1. Using $AALTC_4$ together with a panel of epitope-specific and LTC_4-specific monoclonal antibodies, we identified LTC_4 binding sites in MRP1. Western blotting of large tryptic fragments of MRP1 with three well-characterised epitope specific mAbs (MRPr1, QCRL1, and MRPm6) showed LTC_4 binding in both the N- and C-terminal halves of MRP1. Furthermore, a peptide corresponding to the N-terminal membrane-spanning domain of MRP1 (MSD0) was photoaffinity labelled by $AALTC_4$, indicating that MSD0 contains an LTC_4 binding site. Higher resolution mapping of additional LTC_4 binding sites was obtained using eight MRP1 variants with each containing hemaglutanin A (HA) epitopes at different sites (at amino acid: 4, 163, 271, 574, 653, 938, 1001, or 1222). MRP1-variants were photoaffinity labelled with $IAALTC_4$ and digested with trypsin to isolate specific regions of MRP1 that interact with LTC_4. These results confirmed that sequences in MSD0 interact with $IAALTC_4$. Other regions that were photoaffinity labelled by $IAALTC_4$ include TM 10-11, TM 16-17, and TM 12, shown previously to encode MRP1 drug binding site(s). Together, our results show a high-resolution map of LTC_4 binding domains in MRP1 and provide the first direct evidence for LTC_4 binding within MSD0.

Introduction

Chemotherapy is commonly used in the treatment of malignant tumours in cancer patients. Unfortunately, treatment of patients with anti-cancer drugs often fails due to the rise of chemo-resistant tumours. Using *in vitro* tumour model systems, several proteins have been identified to cause resistance to multiple anti-cancer drugs. P-glycoprotein (P-gp1 or ABCB1) was the first protein identified and shown to efflux anti-cancer drugs [1]. This transmembrane protein was shown to bind and transport a diverse group of compounds, thereby conferring multidrug resistance (MDR) [2,3]. A decade after its discovery, several MDR cell lines were identified that did not over-express P-gp1 [4,5]. These cells expressed another membrane protein termed the multidrug resistance-associated protein (MRP1 or ABCC1 [6]). Both P-gp1 and MRP1 function as broad-specificity drug pumps that bind and transport drugs against a concentration gradient using ATP hydrolysis [7,8]. P-gp1 and MRP1 confer resistance to natural product drugs including epipodophyllotoxins, vinca alkaloids, and certain anthracyclines [9-11]. Unlike P-gp1, the substrates of MRP1 include a range of amphiphilic organic anions. Many of its substrates are conjugated with glutathione (GSH), glucuronate or sulfate [12]. Moreover, several of the conjugated and non-conjugated compounds such as aflatoxin B_1 and vincristine display a dependence on GSH for their transport [13,14]. The clinically relevant non-conjugated anti-metabolite, methotrexate, is also directly transported by MRP1 [11]. The discovery of MRP1 substrates have largely been found due to their ability to inhibit the transport of LTC_4, one of the highest affinity MRP1 substrates [13]. LTC_4, along with other cysteinyl leukotrienes, is a mediator of immediate hypersensitivity reactions, acting as a potent agonist of bronchoconstriction and vascular permeability [15,16]. Studies with *mrp1*$^{-/-}$ mice have shown LTC_4 to be an important natural substrate of MRP1 due to their impaired LTC_4–mediated inflammatory response [17]. Another study showed that dendritic cell mobilization and trafficking into lymphatic vessels is reduced in *mrp1*$^{-/-}$ mice; this effect was restored by exogenously adding LTC_4 [18]. These studies have proved a valuable *in situ* tool to confirm that LTC_4 is a natural substrate of MRP1.

MRP1 has 17 predicted transmembrane (TM) helices and two nucleotide binding domains (NBD) that hydrolyze ATP [19-21]. The TM regions are divided into three core membrane multiple spanning domains (MSD). The first (MSD0) encodes 5 TM helices,

while the two others (MSD1 and MSD2) contain 6 TM helices each. Although a region equivalent to MSD0 does not exist in P-gp1, the organization of MSD1 and MSD2 is similar to the topology of P-gp1. The third cytoplasmic loop (CL3) in MRP1 connects MSD0 to the P-gp1-like core of MSD1 and MSD2, and is termed linker domain 0 (L0). Two protease hypersensitive sites exist in MRP1, one in L0 and the other in the NBD1/MSD2 linker (L1). These trypsin sites can generate protein fragments capable of associating to form a functional transporter. The predicted topological organization of MRP1 from the NH_2-terminus to the COOH-terminus of the protein proceeds as follows: MSD0-*L0*-MSD1-NBD1-*L1*-MSD2-NBD2 [20,21]. Recently, we have examined the substrate binding sites in MRP1 using radiolabelled photoreactive substrates of MRP1. The compounds have widely differing structures and interact with MRP1 in functionally diverse ways. These include two quinoline analogs (IAAQ and IACI), a modified analog of the fluorescent rhodamine 123 (IAARh123), and an analog of glutathione (IAAGSH). Interestingly, each of these compounds reacts with TM 10-11 and TM 16-17 in MSD1 and MSD2, respectively [22,23]. Subsequent amino acid replacement studies have also identified these regions as potential substrate binding sites [24-28], in addition to other domains in MRP1 which appear to affect primarily drug transport or MRP1-mediated MDR [29-32]. Indeed, studies using [^{3}H]LTC_4 have been shown to photoaffinity label MRP1 [13,33-36], however the low labelling efficiency has limited its use. In this study, we synthesized a radiolabelled photoreactive analog of LTC_4 ([^{125}I]iodoaryl azido-leucotriene C_4 or $IAALTC_4$) in an effort to obtain a high resolution map of its binding domains in MRP1. Our findings revealed that $IAALTC_4$ interacts specifically with MRP1 at physiologically relevant binding sites. The location of LTC_4 binding occurred within TM 10-11 and TM 16-17, in addition to TM 12 of MRP1. Interestingly, we found that $IAALTC_4$ interacted with and photolabelled the MSD0 domain of MRP1.

Experimental Procedures

Materials. Protein A Sepharose CL-4B and carrier-free Na^{125}Iodine (100 mCi/ml) were purchased from Amersham Pharmacia Biotech (Baie d'Urfe, QC, Canada). ImmunoPure immobilized protein G, Trypsin (sequencing grade and TPKC treated), and NHS-ASA were purchased from Pierce (Rockford, IL, USA). Leukotriene C_4 (LTC_4) was purchased

from Biomol (Cedarlane Laboratories, Limited, Hornby, ON, Canada). The monoclonal anti-hemagglutinin A monoclonal antibody (mAb) 16B12 (anti-HA) was purchased from Berkeley Antibody Co. (Richmond, CA, USA). Leukotriene C4/D4/E4 Ab-1 mAb was obtained from NeoMarkers (Medicorp, QC, Canada). Anti-MRP1, clone MRPm6, MRPr1, and QCRL1 mAbs were acquired from Kamiya Biomedical Company (Seattle, WA, USA). Protease inhibitor cocktail for mammalian tissues was purchased from Sigma (Saint Louis, MI, USA). All other chemicals were of the highest possible quality.

Cell culture and Plasma membrane Preparation. HeLa cells were cultured in α-MEM media containing 10% fetal bovine serum (Hyclone). HeLa cells transfected with MRP1-HA variants had a stable expression of MRP1 containing one or more copies of the hemagglutinin A (HA) epitope (YPYDVPDYAS) inserted after amino acids: 1, 163, 271, 574, 653, 938, 1001, or 1222 from the N-terminus [37,38]. For plasma membrane preparations, cells were detached with trypsin-EDTA and washed with phosphate-buffered saline, pH 7.4 (PBS). The cell pellet was then resuspended in hypotonic buffer (1 mM $MgCl_2$, 10 mM KCl, 10 mM Tris-HCl, pH 7.4) containing protease inhibitors. Cells were lysed in a Dounce homogenizer and centrifuged at 10 000 × g for 5 min followed by a second centrifugation at 100 000 × g for 1 h. The final pellet was resuspended in buffer M (5 mM Tris-HCl, 250 mM sucrose, pH 7.4) and stored at -70 °C. Protein concentrations were determined by the Lowry method [39].

Synthesis of AALTC$_4$. The synthesis of a photoreactive analog of LTC_4, aryl azido-LTC_4 ($AALTC_4$) was done as previously described [40] with some modifications. All manipulation was preformed in dark-room conditions. Briefly, 200 µg of LTC_4 (dissolved in methanol/ammonium acetate buffer, 65:35, pH 5.6) was dried. The full amount was dissolved in 200 µl of dimethylformamide (DMF), followed by the addition of 0.02 % (v:v) triethylamine. Finally, NHS-ASA (dissolved in DMF) was added to produce a final reaction containing 0.8 mM LTC_4, 3.2 mM NHS-ASA, and 0.01 % triethylamine in 400 µl, pH 8-9. The reactants were allowed to incubate for 48 h at room temperature with rotation. The reaction was terminated and the resulting mixture was separated on high-performance liquid chromatography using a reverse phase C18 column

from Grace Vydac (Hesperia, California). Separation was achieved using a 90 min gradient of 0-100 % acetonitrile in 0.025 M ammonium acetate buffer, pH 5.5. Purified $AALTC_4$ was characterized by mass spectrometry then dried, and stored at –70 °C.

Iodination of $AALTC_4$. $AALTC_4$ was dissolved in 10 µL of methanol/ammonium acetate buffer, 65:35, pH 5.6 and mixed with 100 µL of 3 µg/µL chloramine T prepared in sodium phosphate buffer (10 mM, pH 8.5) along with 5 mCi of carrier-free Na[^{125}I] (100 mCi/mL). The reaction proceeded for 5 min at room temperature and was stopped with 100 µL of 5 % Na-metabisulfite in sodium phosphate buffer. The sample was then loaded on a C18 SepPak column that was pre-equilibrated with 100% methanol, followed methanol/sodium phosphate buffer (10:90). After injection of the reaction into the column, it was washed 10-20 times with 5 mL aliquots of methanol/sodium phosphate buffer (10:90) to remove free iodine. $IAALTC_4$ was eluted from the column with 5 mL of 100 % methanol then dried. The iodinated sample was resuspended in 100-200 µL methanol/ammonium acetate buffer, 65:35, pH 5.6.

Plasma membrane and vesicle preparation. Plasma membranes were prepared as follows. Cells were centrifuged for 45 min at 100,000 × g, 4 °C. The pellet was resuspended in a hypotonic lysis buffer containing 10 mM KCL, 1.5 mM $MgCl_2$–$6H_2O$, 10 mM Tris-HCl, pH 7.4, and protease inhibitors. The cells were homogenized with 200 strokes using a tight-fitting Dounce homogenizer and centrifuged for 10 min at 10,000 × g, 4 °C. The supernatant was removed at set aside while the pellet was resuspended in TS buffer (50 M Tris-HCl, 250 mM sucrose, pH 7.4) and homogenized with another 200 strokes; the suspension was centrifuged for 10 min at 10,000 × g, 4 °C. The supernatant was combined with the supernatant from the first centrifugation, and centrifuged for 45 min at 100,000 × g, 4 °C. The pellet was resuspended in TS buffer. For vesicle preparation, the final pellet in was passed through a 27-G needle 30 times. The protein concentration was determined using the Lowry method [39]. The plasma membranes and vesicles were snap-frozen in liquid nitrogen at stored at -70 °C.

Photoaffinity labelling and SDS-PAGE. For photoaffinity labelling, $IAALTC_4$ (0.1-1 μM) was added to 20-40 μL aliquots of plasma membrane (20-100 μg) in TS buffer and incubated at room temperature for 30 min, in the dark. Samples were further incubated on ice for 10 min followed by UV irradiation at 254 nm for 10 min, as previously described [40]. Photolabelled samples underwent proteolytic digestion and immunoprecipitation [41] as described below. Protein samples were resolved on SDS-PAGE exclusively using the Fairbanks system [42]. Coomassie blue staining was used to detect all proteins in plasma membrane samples. Alternatively, gels with radiolabelled proteins were dried and exposed on Kodak BIOMAX MS film at –70 °C.

Proteolytic digestion and immunoprecipitation. Photoaffinity labelled plasma membrane samples (100 μg) were digested with increasing concentrations of trypsin at 37 °C for 40 min. The digestion was stopped by placing the samples on ice and adding 80 μL of I.P. buffer A (1 % SDS, 50 mM Tris-HCl, pH 7.4) with protease inhibitors. Samples were left on ice for 15 min before the addition of 320 μl of I.P. buffer B (1.25 % Triton X-100, 190 mM NaCl, 0.05 M Tris-HCl, pH 7.4). The digested peptides were immunoprecipitated as previously described [41]. Briefly, samples were incubated overnight with protein A Sepharose beads conjugated to anti-HA mAb. After incubation, samples were washed 5 times with I.P. buffer C (0.05 % Triton X-100, 0.03 % SDS, 150 mM NaCl, 5 mg/ml BSA, 0.05 M Tris-HCl, pH 7.4) and once with I.P. buffer D (150 M NaCl, 0.05 M Tris-HCl, pH 7.4). For immunoprecipitation with the MRPr1 mAb, plasma membrane samples were pre-cleared with 50 μL of ImmunoPure immobilized protein G for 30 min. The protein G beads were removed and the samples were incubated overnight with 2 μg of the mAb. After incubation, 50 μL of ImmunoPure immobilized protein G was added to each sample and incubated for 30 min at room temperature and 2 h at 4 °C. The samples were then washed 5 times with I.P. buffer C and once with I.P. buffer D and resolved by SDS-PAGE.

N-glycosidase F (PNGase F) digestion of digested polypeptides. Deglycosylation of MRP1 or proteolytic fragments was performed as previously described [43]. Briefly, after the immunoprecipitation washes, purified MRP1 was denatured by adding 10 μL of 0.1

M 2-ME/0.1 % SDS to the immobilized protein A or G pellets and heating for 5 min at 65 °C. The denatured MRP1 was transferred to a fresh tube and the following components were added in order: 3 µL 0.5 M Tris-Cl (pH 8.6), 5 µL H_2O, 2 µL 10 % Triton X-100, and 5 µL 1 U/ml PNGase F. The samples were then incubated overnight at 37 °C in the presence of protease inhibitors and resolved by SDS-PAGE.

Western Blotting. For immunodetection of MRP1, 20 µg of enriched plasma membranes were resolved on SDS-PAGE and transferred to nitrocellulose membrane by using a wet electroblotting technique as outlined in Towbin *et al.* [44]. The nitrocellulose membrane was blocked in PBS with 5 % skim milk and incubated with: MRPr1, QCRL1, MRPm6, and anti-LTC_4 mAbs for 2 h at room temperature. After incubation, membranes were washed and incubated for 2 h with 1:3000 (v/v) goat anti-mouse or anti-rat antibodies conjugated to horseradish peroxidase. SuperSignal West Pico or Femto chemoluminescent substrate (Pierce, Rockford, IL) was used to detect mAb binding.

Vesicle transport of IAALTC$_4$ and [^{3}H]LTC$_4$. Transport of $IAALTC_4$ and [^{3}H]LTC_4 into membrane vesicles were determined by rapid filtration as described with modifications [13]. The membrane vesicles were diluted in TS buffer and passed through a 27-G needle 5 times. Transport assays were carried out at 23 °C in a buffer containing 1 mM ATP, 10 mM $MgCl_2$, 10 mM phosphocreatine, 0.1 U/µL creatine kinase, and 50 nM [^{3}H]LTC_4 or $IAALTC_4$, in TS buffer. At specific time intervals, aliquots were removed and added to 1 ml of ice-cold TS buffer. Each sample was then placed filtered through 0.22 µm nitrocellulose filters on a vacuum manifold. The filters were washed three times with 3 ml of cold TS buffer, solubilized, and the radioactivity was determined. All data was corrected for the amount of [^{3}H]LTC_4 or $IAALTC_4$ that bound nonspecifically to the filters in the absence of membrane vesicles.

Results

In an effort to isolate LTC_4 substrate binding sites in MRP1, we synthesized a photoreactive analog of LTC_4, aryl azido-LTC_4 ($AALTC_4$) (figure 1) and characterized its modification by mass spectrometry.

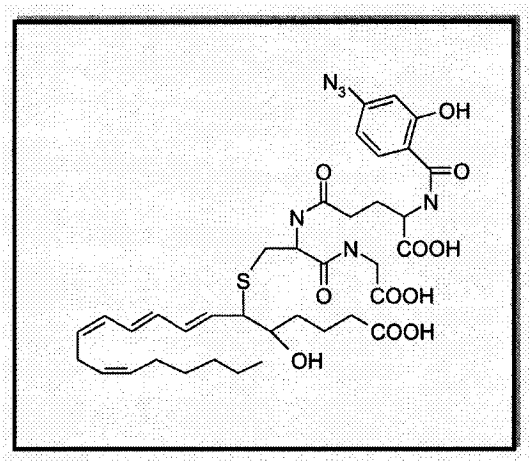

Figure 1

The chemical structure of aryla azido-leucotriene C_4 ($AALTC_4$).

Figure 2A shows $AALTC_4$ photoaffinity labelled plasma membranes from HeLa and MRP1-transfected HeLa cells immunoprecipitated with an MRP1-specific mAb (MRP1r1), and then probed with an LTC_4-specific mAb (lanes 1 and 2, respectively). The specificity of the photoreactive analog ($AALTC_4$) towards MRP1 is illustrated by the observation that the LTC_4-specific mAb reacted with a 190 kDa protein in plasma membranes from MRP1-transfected but not HeLa plasma membranes. The results of this Western blot also confirm the integrity of the photoreactive analog ($AALTC_4$) as it is recognized by an anti-LTC_4 mAb which binds native LTC_4. Indeed, previous efforts to identify LTC_4 binding domains using [^{3}H]LTC_4, have been of limited success largely due to the low efficiency of photolabelling of MRP1 with LTC_4 and time required to obtain a reasonably detectable signal. Thus, $AALTC_4$ was further iodinated ($IAALTC_4$) and used to photoaffinity label plasma membranes prepared from HeLa and MRP1-transfected HeLa cells (figure 2A, lanes 3 and 4, respectively). Specific photolabelling of a ~190 kDa protein can be seen in MRP1-transfected but not in un-transfected cells. Furthermore, the results in figure 2A (lanes 5 and 6) show immunoprecipitated samples with the MRP1-specific mAb, MRPr1. A radiolabelled polypeptide with a molecular mass of ~190 kDa was found only in lane 6 of figure 2A, demonstrating that $IAALTC_4$ specifically photoaffinity labelled MRP1. Membrane proteins from HeLa and MRP1-transfected HeLa cells were visualized with Coomassie blue (figure 2A, lanes 7 and 8, respectively). Since there was no detectable increase in expression of a 190 kDa protein,

it can be inferred that specific photolabelling of MRP1 by $IAALTC_4$ is not exclusively caused by over-expression. The specificity of $IAALTC_4$ to MRP1 was further confirmed when increasing concentrations of $IAALTC_4$ were used to saturate the binding site(s). Figure 2B shows that the intensity of photoaffinity labelling of MRP1 levels-off as the concentration of $IAALTC_4$ is increased from 0.0625 to 1 μM. This saturation of photolabelling indicates that the LTC_4 analog interacted with a physiologically relevant site within MRP1 and is consistent with the high affinity of LTC_4 towards MRP1.

To determine whether $IAALTC_4$ interacts with the same binding sites as other MRP1 substrates, MRP1-enriched plasma membranes were photolabelled in the presence of various MRP1 substrates. Figure 3A shows the effect of increasing concentrations of three endogenous substrates on MRP1 labelling: LTC_4, GSH and GSSG. The addition of very low concentrations of LTC_4 showed significant binding competition of $IAALTC_4$ to MRP1. In fact, 0.1 (or 10 % of the total $IAALTC_4$ concentration) produced a small, yet significant, reduction in photolabelling. Furthermore, at 0.5 molar excess (or 50 %), LTC_4 reduced photolabelling by more than 60 %. Interestingly, GSH produced a similar decrease as seen with LTC_4, although at a significantly higher molar concentration (100 μM). In contrast, 10 μM GSSG, also a substrate of MRP1 [45], had no effect, while 100 μM GSSG caused a slight increase in MRP1 photolabelling with $IAALTC_4$ (~25 %).

It was also of interest to examine the photolabelling of MRP1 in the presence of several exogenous substrates of MRP1: MK571, verapamil and vincristine (figure 3B). Each of the compounds are transported or co-transported by MRP1 [46-49]. All three drugs caused a moderate decrease in the intensity of MRP1 labelling at a molar concentration of 10 μM. At 100 μM, MK571 reduced the photolabelling of MRP1 by more than 80%. This observation is consistent with a previous finding that MK571 acts as a competitor in the photolabelling of MRP1 by $[^3H]LTC_4$ [34]. Binding competition was less effective with both verapamil and vincristine at 100 μM, with each causing approximate 50 % competition. This is consistent with the higher affinity of MRP1 for MK571 compared to verapamil or vincristine [46-50]. These findings show that $IAALTC_4$ photolabels a binding site that overlaps, or interacts with known substrates of MRP1.

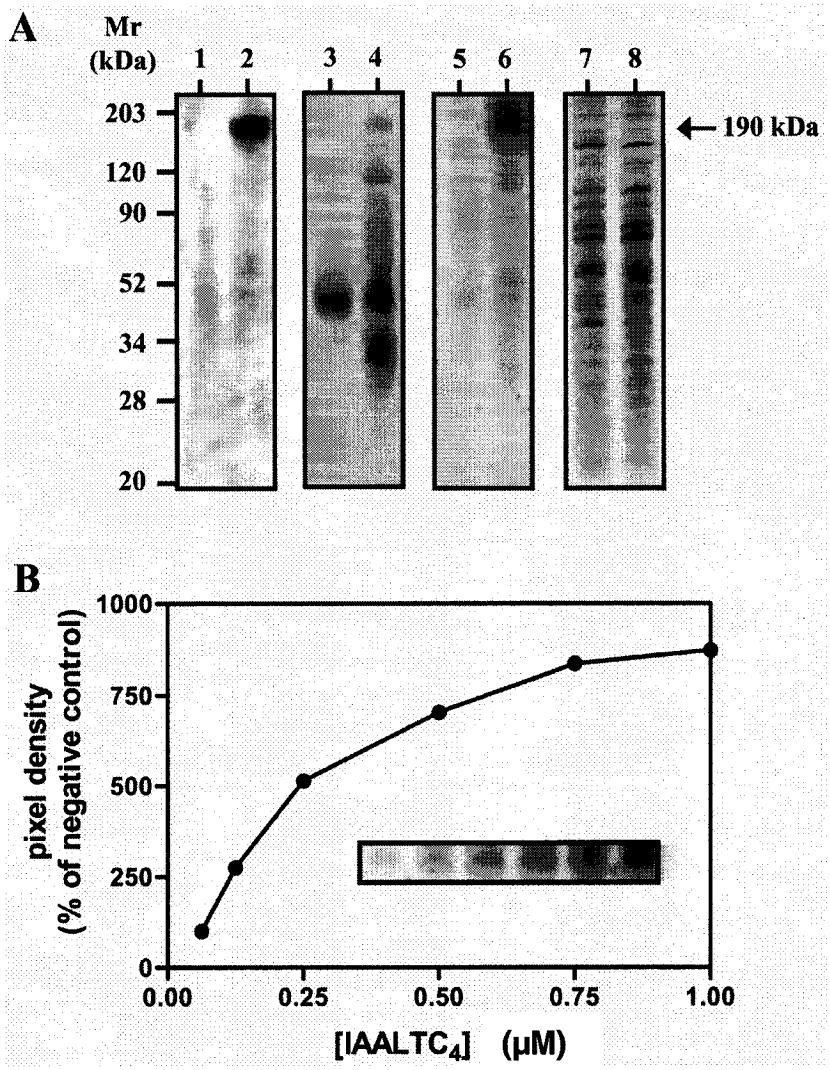

Figure 2

Western blot and Photolabelling of HeLa and MRP1-enriched HeLa plasma membranes. Western blot analysis using an anti-LTC_4 mAb was used to detect $AALTC_4$ photolabelling in HeLa and HeLa-MRP1 membranes which were previously immunoprecipitated with an MRP1-specific mAb (MRPr1) (lanes 1 and 2, respectively). Lanes 3 and 4 show $IAALTC_4$-photolabelled HeLa and HeLa-MRP1 membrane proteins. Lanes 5 and 6 show an immunoprecipitation of $IAALTC_4$ photolabelled HeLa and HeLa-MRP1 membrane proteins with MRPr1. Lanes 7 and 8 show the staining of membrane proteins from HeLa and HeLa-MRP1 with Coomassie Blue. The graph in Panel B, demonstrates the saturable photoaffinity labelling of MRP1 with increasing amounts of $IAALTC_4$.

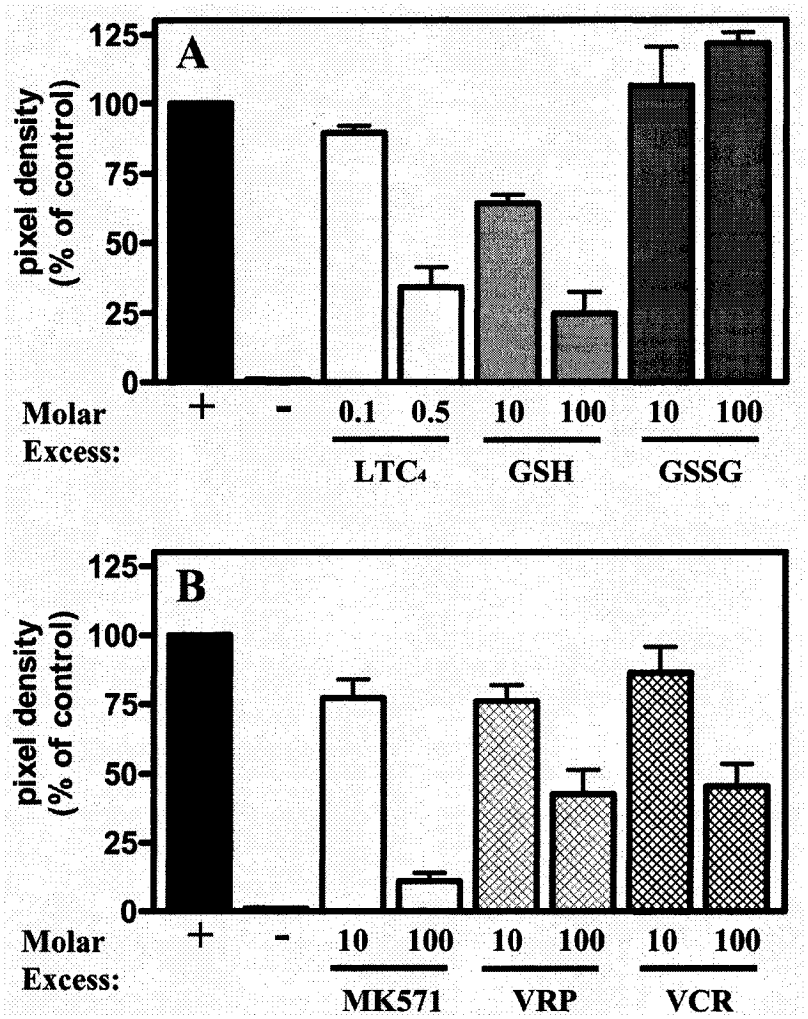

Figure 3

Effect of several drugs on MRP1 photolabelling. Panel A shows the change in photolabelling of MRP1 with IAALTC$_4$ in the presence of several endogenous compounds: LTC$_4$, GSH, and GSSG. Panel B shows photolabelling in the presence of exogenous drugs: MK517, verapamil (VRP) and vincristine (VCR). Plasma membranes were immunoprecipitated with hemagglutinin A (HA) mAb. The intensity of photolabelling is expressed relative to MRP1 photolabelled with IAALTC$_4$ alone. All samples were photolabelled and immunoprecipitated with an MRP1-specific mAb. Each condition was repeated at least three times in duplicate.

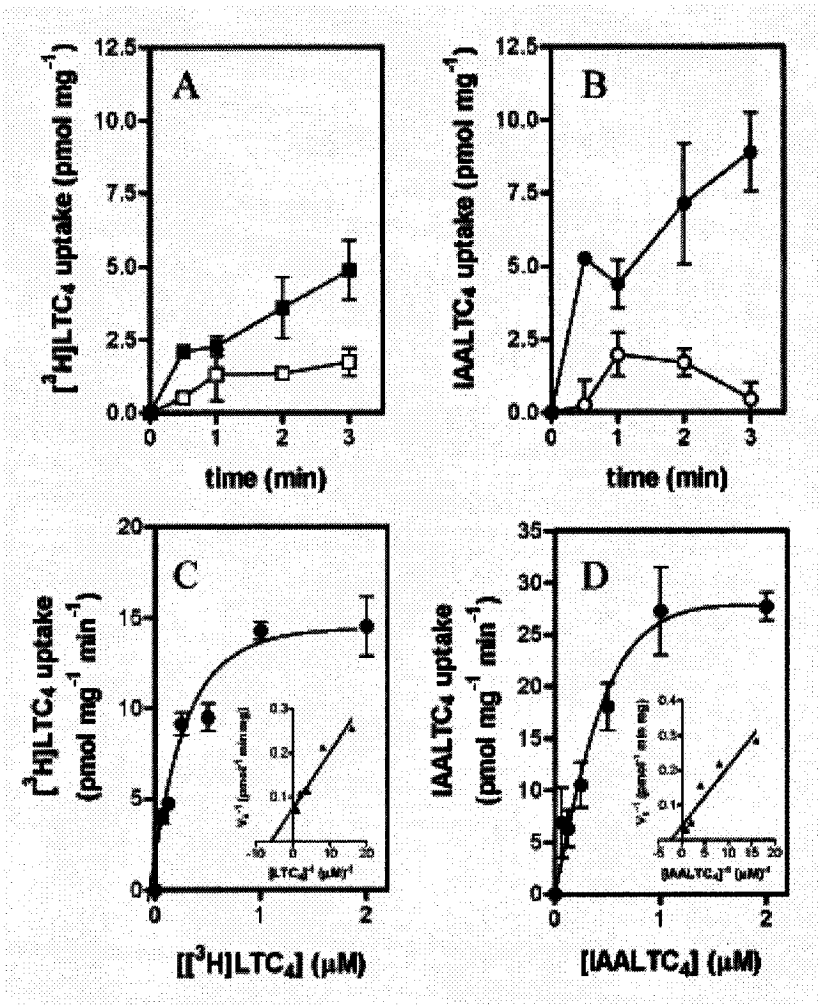

Figure 4

Uptake of [^{3}H]LTC$_4$ and IAALTC$_4$ into membrane vesicles. The uptake of 50 nM [^{3}H]LTC$_4$ and IAALTC$_4$ into membrane vesicles is shown in Panels A and B, respectively. The uptake of each compound was measured from 0 to 3 min. Open symbols represent uptake in vesicles derived from HeLa cells; closed symbols show uptake in vesicles from MRP1-transfected HeLa cells. Panels C and D show uptake of [^{3}H]LTC$_4$ and IAALTC$_4$, respectively, into vesicles from MRP1-transfected HeLa cells at various concentrations (0.0625 to 2 μM) for 2 min at 23 °C. The kinetic parameters, K_m and V_{max}, were determined from determined from regression analysis of the Lineweaver-Burk transformation of the data (insets).

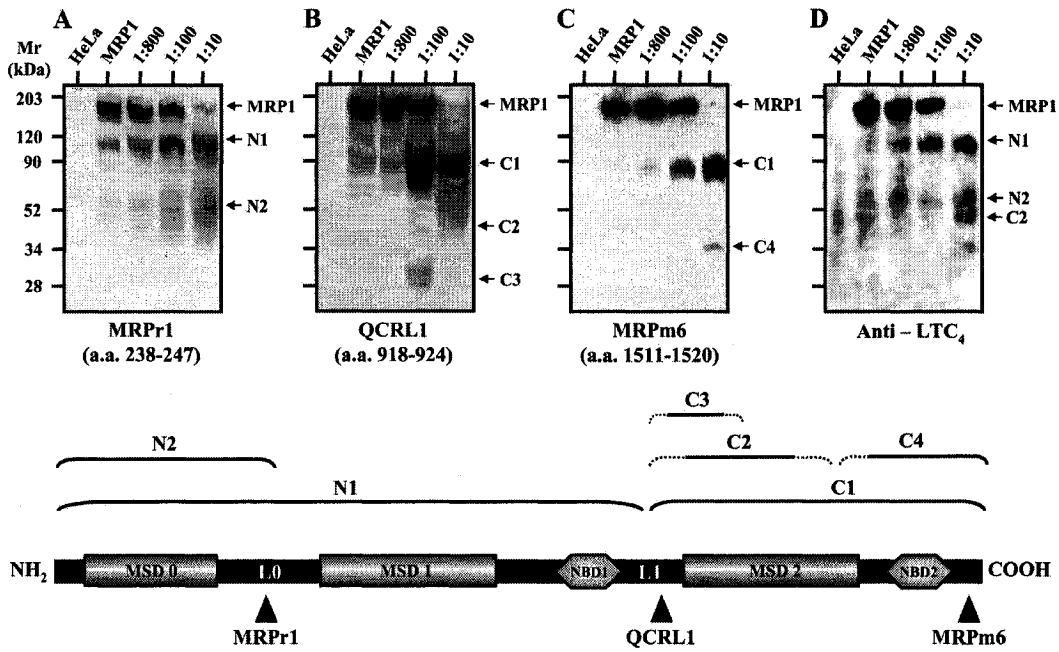

Figure 5

Western blot analyses of MRP1 peptides generated by limited trypsin proteolysis. MRP1 from transfected HeLa cells was digested with increasing concentrations of trypsin (trypsin:protein). The proteolitic fragments were detected by Western blot using three MRP1 specific monoclonal antibodies: MRPr1, QCRL1, and MRPm6 (panels A to C, respectively). MRP1 was also photolabelled with $AALTC_4$, digested, and probed with an anti-LTC_4 antibody (panel D). For clarification, the epitope for each antibody is indicated on a topological illustration of MRP1. The size and location of each peptide are also shown

To determine if $IAALTC_4$ is transported by MRP1 in an ATP-dependent manner, its transport was measured using inside-out membrane vesicles prepared from HeLa and MRP1-transfected HeLa cells. Since transport of [^{3}H]LTC_4 into vesicles has been extensively studied, it was of interest to investigate $IAALTC_4$ transport and compare it to [^{3}H]LTC_4. Figure 4A shows the time-dependant uptake of [^{3}H]LTC_4 into vesicles. This graph shows a correlation between LTC_4 transport and levels of MRP1 expression, whereby vesicles from MRP1-transfected cells show higher uptake than the HeLa vesicles. The levels of [^{3}H]LTC_4 uptake did not exceed 6 pmol mg^{-1} after 3 minutes which is relatively low compared to previous studies using vesicles isolated from H69/AR

cells which have a very high level of MRP1 expression (35). A similar difference due to the level of MRP1 expression was seen in the uptake of IAALTC$_4$ although the maximum uptake at 3 min did not exceed 10 pmol mg^{-1} (figure 4B). The higher uptake of IAALTC$_4$ compared to [^{3}H]LTC$_4$ indicated that IAALTC$_4$ may have a higher transport rate than native LTC$_4$. To resolve this, the rates of uptake for IAALTC$_4$ at several concentrations were measured to compare K_m and V_{max} for transport in membrane vesicles (figure 4C). It is apparent that vesicular uptake becomes saturated above 1 μM IAALTC$_4$. The Lineweaver-Burk double reciprocal plot of a single experiment produced an apparent K_m of 0.42 μM and a V_{max} of 25.25 pmol mg^{-1} min^{-1} (inset of figure 4C). The average K_m and V_{max} values for three experiments were 0.26 ± 0.17 μM and 24.00 ± 4.78 pmol mg^{-1} min^{-1}. As a comparison, we measured the same kinetic parameters with [^{3}H]LTC$_4$, obtaining a K_m of 0.17 ± 0.053 μM and a V_{max} of 13.7 ± 1.07 pmol mg^{-1} min^{-1} (figure 4D).

The primary goal of this study was to identify the photolabelling sites of LTC$_4$ in MRP1. To do so, we made use of the well established MRP1 trypsin digestion profile together with an anti-LTC$_4$ specific mAb to initially identify the large fragments of MRP1 that interacted with LTC$_4$. The identity of MRP1 trypsin digestion patterns was confirmed using MRP1 epitope-specific mAbs (e.g. the mAb MRPr1 epitope is between amino acids 238-247 [51], QCRL1 recognizes amino acids 918-924 [52], and MRPm6 recognizes amino acids 1511-1520 [51]). The most visible product of digestion and immuno-blotting with the MRPr1 mAb is a polypeptide of 120 kDa (figure 5A). This fragment has previously been identified under similar conditions and corresponds to the NH_2-proximal half of MRP1 [21]. The trypsin sensitive site that generates this fragment is well documented and found within the L1 cytoplasmic loop [52]. Although this fragment was detected in the absence of trypsin, its intensity was dramatically increased as the concentration of trypsin was increased. The 120 kDa polypeptide has previously been labelled as N1 [21]. In addition to N1, a second polypeptide is visible with a broad molecular mass of 45-55 kDa; this fragment has been named N2 [21]. N2 corresponds to a fragment that extends from the amino terminal to a digestion site within the L0 cytoplasmic linker region within CL3 [20]. Two other antibodies, QCRL1 and MRPm6, react with regions on the COOH-proximal side of the L1 trypsin sensitive site. QCRL1 reacts with an epitope in the L1 cytoplasmic loop of MRP1. Digestion and Western

blotting with QCRL1 produced a 111 kDa fragment named C1. This fragment extends from the L1 trypsin sensitive site to the carboxyl terminal of MRP1 (figure 5B). In addition, two other polypeptides were generated at 1:100 and 1:10. The larger one, at approximately 42 kDa, we named C2. A smaller 29 kDa band is also visible at 1:100. Both C2 and C3 were not detected in a previous study using similar conditions [21]; perhaps a greater amount of plasma membrane was used per sample in the current study. In fact, we could not detect either the C2 or C3 fragments with less than 25 μg (data not shown). The MRPm6 antibody reacts with an epitope in the cytoplasmic loop on the COOH-proximal side of MSD2. It was also able to detect the C1 fragment with increasing trypsin concentrations (figure 5C). In addition, MRPm6 detected a 35 kDa polypeptide at the highest trypsin concentration (1:10) (named C4). An illustration of the various MRP1 tryptic fragments and their position relative to MRP1 topology is shown directly below figures 5A to 5C. Using the tryptic profile of MRP1, we determined which peptides were photolabelled by non-iodinated $AALTC_4$ using an LTC_4-specific mAb. Figure 5D shows MRP1-enriched membranes photolabelled and digested before immuno-blotting. The N1 fragment was the most clearly visible polypeptide in the Western blot. This band indicates that $AALTC_4$ photolabelled the NH_2-terminal portion of MRP1. Additional polypeptides were visible at the highest concentration of trypsin (1:10). These bands correspond to N2 and C2. This further localizes the binding of $AALTC_4$ to the regions encompassed by N2 and C2, namely MSD0-L0 and MSD2, respectively. Although these bands are less distinct than those seen in figures 5A to 5C, their resolution is impressive considering that very low amounts of $AALTC_4$ were used to photolabel MRP1.

We have previously localized the binding sites of several photoreactive drugs using MRP1 proteins with HA epitopes inserted at eight different sites, after amino acids 4, 163, 271, 574, 653, 938, 1001, or 1222 [22,23]. Figure 6 shows results obtained using these eight different MRP1-HA variants photolabelled with $IAALTC_4$ and digested with increasing concentrations of trypsin. Proteolytic fragments containing the HA-epitope were immunoprecipitated with an HA-specific mAb and $IAALTC_4$ photolabelled fragments were identified. The topological illustration of MRP1 located below figure 6 indicates the position of each HA epitope as well as the potential location of known trypsin fragments based on the MRP1 primary amino acid sequence. Figure 6A and 6B

shows two proteolytic peptides from MRP1-variants 4 and 163, whereby the largest fragment corresponds to the 111 kDa or N1 fragment identified in figure 5A. The other polypeptide that was photolabelled by $IAALTC_4$ corresponds to the 50-60 kDa or N2 fragment, visible at higher concentrations of trypsin (1:100 and 1:10). The appearance of the N1 and N2 fragments indicates that a photolabelling site is found in the NH_2-proximal portion of MRP1 as well as MSD0. In addition to the N1 and N2 fragments, an 18 kDa polypeptide is visible in MRP1-variant 163 (figure 6B). This further localizes the photolabelling site to the COOH-proximal side of the N2 fragment. The N2 fragment was not visible in the MRP1-variant 271 because the trypsin site is located on the N-terminal side of this epitope. Only the N1 fragment was produced at trypsin concentrations of 1:800 and 1:100 with MRP1-variant 271 (figure 6C). MRP1-variant 574 yielded a larger spectrum of photolabelled polypeptides in addition to the N1 fragment (figure 6D). Digestion of this MRP1-variant at the highest trypsin concentration (1:10) generated three bands with the approximate sizes of: 22, 18 and 6.5 kDa. The appearance of these bands correlates with fragments identified with other photoreactive drugs: IACI, IAARh123, and IAAGSH [22,23]. Consequently, the sequence of the 6.5 kDa fragment has previously been determined as: ^{542}SAYLSAVGT-FTWVCTPFLVALCTFAVYVTIDEN-**[HA][HA]**NILDAQTAFVSLALFNILR^{593}. The underlined portion of the linear amino acid sequence corresponds to the proposed TM 10 and TM 11. The mass of this fragment is calculated to be 6.9 kDa which is identical to the size of the peptide in figure 6D. The position of the HA epitopes and the size of the smallest peptide limits the region of photolabelling to TM 10-11. A 52-55 kDa polypeptide was also visible in the digested MRP1-variant 574. This polypeptide corresponds to a previously identified fragment named N3 [21]. The N3 fragment is a polypeptide bordered by the L0 and L1 trypsin sensitive sites. We believe that $IAALTC_4$ photolabels the N3 fragment because the size of the polypeptide and the position of the HA epitope correlates with the characteristics of N3. The N3-like fragment was also clearly photolabelled with $IAALTC_4$ in MRP1-variant 653.

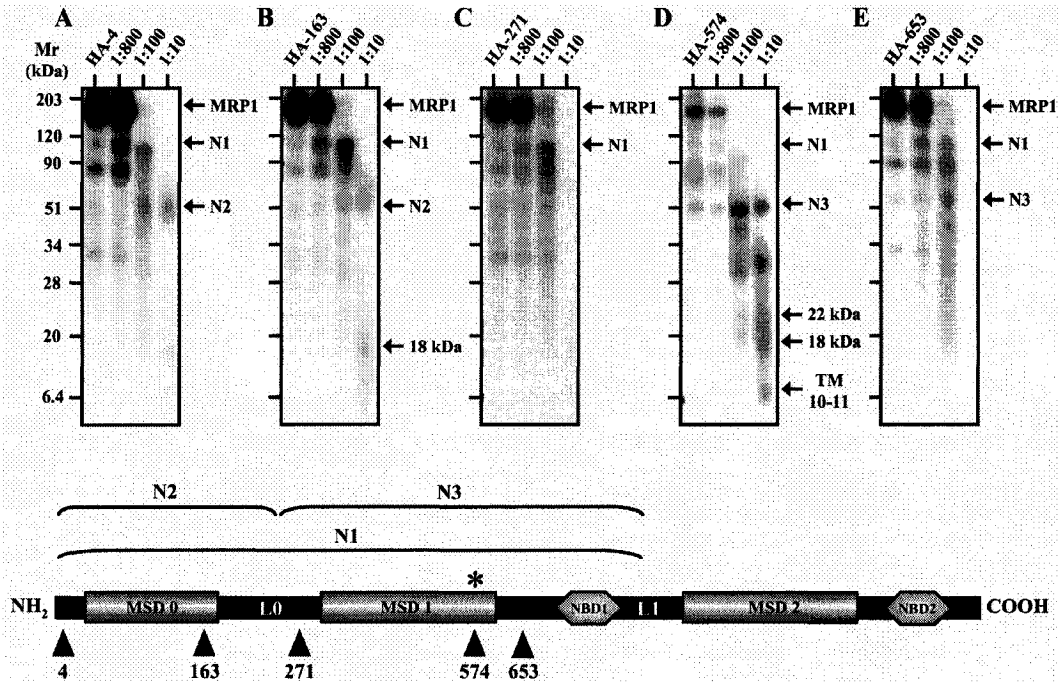

Figure 6

Photolabelling and digestion of N-terminal MRP1-HA variants. Six different MRP1 HA-variants (4, 163, 271, 574, and 653) were photolabelled with IAALTC$_4$, digested with trypsin (trypsin:protein), and immunoprecipitated with an anti-HA antibody. The location of each HA epitope is indicated on a topological illustration of MRP1. The size and location of peptides are also shown; the asterisk (*) indicates the location of a localized photolabelling site.

The results from MRP1-variants 938, 1001, and 1222 are shown in figures 7A, 7B, and 7C, respectively. An 85 kDa polypeptide is visible in the digestion pattern of all three MRP1-variants in figure 7. This band corresponds to the C1 fragment that was characterized by Western blot (figures 5B and 5C). C1 is generated at a trypsin concentration of 1:800 and 1:100 in these three MRP1-variants. This confirms that IAALTC$_4$ photolabelled the COOH-proximal half of MRP1. In addition, a 38 kDa fragment was photolabelled in MRP1-variants 938, 1001, and 1222. This corresponds to the mass of the smallest trypsin fragment that encompasses the MRP1 amino acid sequence between 938 and 1222 (including the mass of HA epitopes). The size of this band corresponds to the C2 fragment identified in figure 5B. Moreover, the C3 fragment

identified in figure 5B was also photolabelled in MRP1-variants 938 and 1001 (figures 7A and 7B). Interestingly, digestion of MRP1-variant 1001 produced three previously unidentified photolabelled polypeptides with molecular masses of 15, 10, and 6 kDa. The following sequence is the smallest tryptic fragment that contains the HA epitope at position 1001: ^{969}AIGLFISFLSIFLFMCNHVSALASNYWLSLWT**[HA][HA]**DDPIVN-GTQEHTK^{1013}. The underlined portion represents the predicted TM 12. The calculated molecular mass of this polypeptide is 7.4 kDa. This is the first time a distinct photolabelling site has been identified in this region of MRP1. The results in figure 7C show IAALTC$_4$ photoaffinity labels a 7 kDa tryptic peptide in the digested MRP1-variant 1222. As with MRP1-variant 574, this peptide has been previously identified with several other photoreactive drugs [22,23]. Based on the molecular mass of the photoaffinity labelled peptide and the trypsin cleavage site in the vicinity of position 1222, photoaffinity labelling occurs within the following sequence: ^{203}LECVGNC-IVLFAALFAVIS-**[HA][HA]**RHSLSAGLVGLSVSYSLQVTTYLNWLVR^{1249}. The underlined regions represent the predicted location of TM 16 and TM 17. The calculated molecular mass of this peptide, including the HA epitopes is 7 kDa. The illustrations in figures 6 and 7 show topological drawings of MRP1 with the relative position of each HA epitope and the polypeptides that are produced by trypsin digestion. The asterisk (*) above HA epitopes: 574, 1001, and 1222 indicate the location of isolated IAALTC$_4$ photolabelling sites.

The photolabelling of the N2 polypeptide with IAALTC$_4$ in MRP1-variants 4 and 163 were particularly interesting. This is the first time that a photolabelling site has been demonstrated within MSD0. Using [^{3}H]LTC$_4$, a previous study examining LTC$_4$ binding sites in MRP1 concluded that MSD0 does not contain a photolabelling site [36]. To further confirm the photoaffinity labelling of the N2 fragment with IAALTC$_4$, we made use of the glycosylation status of the N2 fragment. A previous study indicated that N2 could be deglycosylated to produce a 25 kDa fragment [21]. To confirm the results of the latter study, MRP1 was incubated with and without PNGase F, digested with trypsin and the resultant peptides examined by Western blot using the MRPr1 mAb. The first lane of figure 8A shows that the MRPr1 mAb reacts with MRP1 and the trypsin-derived N1 fragment from MRP1-enriched plasma membranes. The second lane of figure 8A shows

the same sample treated with PNGase F; the sizes of both MRP1 and N1 were decreased due to deglycosylation. With trypsin digestion, the 45-55 kDa N2 fragment was detected (figure 8A, lane 3). After deglycosylation with PNGase F, N2 was reduced to 25-30 kDa (figure 8A, lane 4). Based on these results, we surmised that the $IAALTC_4$-labelled N2 fragment would appear as a 25-30 kDa band after deglycosylation. To test this, MRP1 was photolabelled with $IAALTC_4$ then digested with trypsin (1:10). The peptides were immunoprecipitated with the MRPr1 mAb followed by treatment with PNGase F. Lanes 1 and 2 of figure 8B show that the photolabelled MRP1 band decreased in size after treatment with PNGase F. Trypsin digestion of MRP1 shows that N1 and N2 were photolabelled by $IAALTC_4$ (lane 3). After the digested sample was deglycosylated, a 28 kDa fragment labelled with $IAALTC_4$ was generated. This band corresponds to the deglycosylated N2 fragment (lane 4). This demonstrates that MRPr1 can immunoprecipitate the photolabelled MSD0. To confirm this result, we used the same approach on MRP1-variants 4 and 163 (figures 8C and 8D). Both of these mutants have an HA epitope in MSD0 that would allow us to immunoprecipitate N2. The deglycosylated 28 kDa or N2 fragment was clearly photolabelled in MRP1-variants 4 and 163. In contrast, the native and deglycosylated N2 fragments were not detected in MRP1-variant 271 (figure 8E).

Discussion

MRP1 has been shown to interact with and mediate the transport of un-conjugated anti-cancer drugs in addition to normal cell metabolites. Previously, we have mapped the binding domains of several un-conjugated substrates that are transported by MRP1 [22,23]. In this study, it was of interest to determine the binding sites of LTC_4 in MRP1. For this, a photoreactive analog of LTC_4 was synthesized ($IAALTC_4$) and shown to specifically photoaffinity label MRP1. $IAALTC_4$ binding to MRP1 was saturable and was inhibited by molar excess of endogenous (LTC_4 and GSH) and exogenous (MK571, vincristine and verapamil) substrates. Together, these results show $IAALTC_4$ binds to physiologically relevant sites in MRP1.

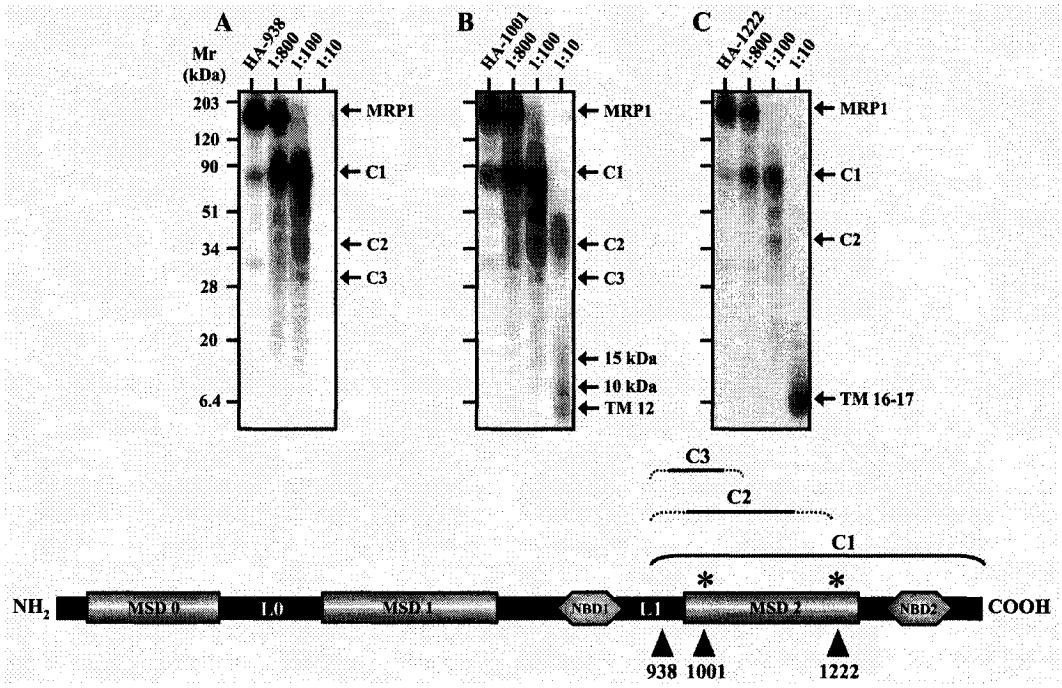

Figure 7

Photoaffinity labelling and digestion of C-terminal MRP1-HA variants. Three different MRP1 HA-variants (938, 1001, and 1222) were photolabelled with IAALTC$_4$, digested with trypsin (trypsin:protein), and immunoprecipitated with an anti-HA antibody. The location of each HA epitope is indicated on a topological illustration of MRP1. The size and location of peptides are also shown; the asterisks (*) show localised photolabelling sites.

The increase in photolabelling observed in the presence of 100 μM GSSG was unexpected. We were unable to find any previous report that examined the effect of GSSG on LTC$_4$ binding. Although the cause of this is elusive, we will present one possible explanation. Perhaps the cellular GSH/GSSG ratio influences the interaction between MRP1 and LTC$_4$. In such a system, GSH reduces the affinity of LTC$_4$ for MRP1 while GSSG increases affinity. Thereby, the redox state of a cell would affect the physiological release of LTC$_4$.

Interestingly, none of the MRP1 substrates completely inhibit IAALTC$_4$ labelling. To help understand this, we determined several kinetic parameters pertaining to MRP1-IAALTC$_4$ interactions. The K_m value of 0.26 μM obtained for IAALTC$_4$ shows that the interaction occurs with a high affinity relative to many MRP1 substrates. This K_m value

is within the high affinity range that we (0.17 μM) and others (approximately 0.10 μM) have measured for [^{3}H]LTC$_4$, [13]. Taken together, it would appear as if MRP1 substrates are not able to completely inhibit photolabelling due to the high affinity IAALTC$_4$ shares with its parent compound LTC$_4$. This is further illustrated by the observation that the most effective inhibitors of photolabelling, LTC$_4$ and MK571, are higher affinity substrates than the other compounds (GSH, GSSG, verapamil, and vincristine) [46-49].

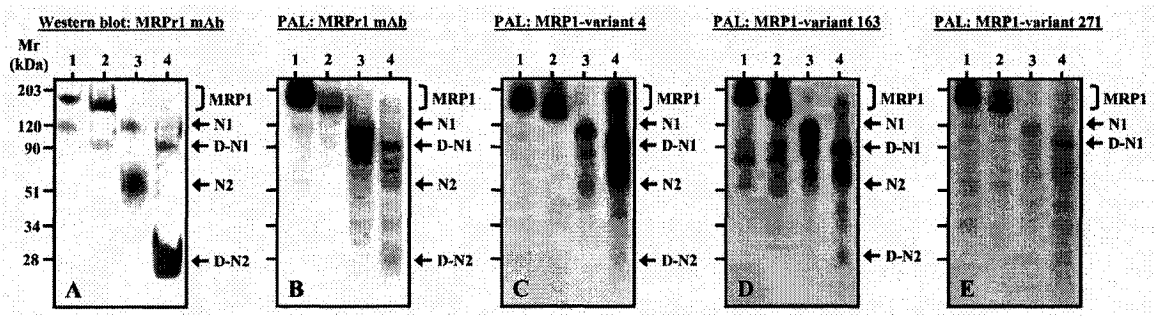

Figure 8

Deglycosylation of the photolabelled N2 peptide. In each panel, lane 1 contains MRP1-enriched plasma membrane, lane 2 has MRP1 deglycosylated with PNGase F, lane 3 shows MRP1 digested with trypsin (1:10, trypsin:protein), lane 4 shows MRP1 digested and deglycosylated. MRPr1 antibody was used for the Western blot (panel A). Panels B to E show MRP1 HA-variants (4, 163 and 271) that were photoaffinity labelled (PAL) with IAALTC$_4$ followed by immunoprecipitation with MRPr1 (panel B) or anti-HA antibodies (panels C to E).

The present study demonstrates for the first time that a photoreactive analog of LTC$_4$ photolabels MSD0 and TM 12 of MRP1, in addition to sequences in TM 10-11 and TM 16-17. Previously, we have reported the significance of TM 10-11 and TM 16-17 with several photoreactive compounds: IACI, IAARh123, and IAAGSH [22,23]. Using two different photoreactive drugs ([^{125}I]LY475776 and an analog of agosterol A (AG-A)), it was also shown that sequences within TM 16-17 are photoaffinity labelled [53]. Furthermore, specific amino acid substitutions within TM 10-11 and TM 16-17 have been

shown to alter drug binding and transport [24-27]. Collectively, these findings point to the importance of these two regions in forming a substrate binding site.

In addition to the above mentioned TM helices, we demonstrate that $IAALTC_4$ photolabelled a polypeptide encompassing TM 12 and a portion of the extra-cellular loop between TM 12 and TM 13. Interestingly, a previous photolabelling study using murine *mdr*1b P-glycoprotein identified a similar binding site [54]. In that study, a 7-*p*-benzoyldihydrocinnamol (7-BzDC) analog of Taxol was used. 7-BzDC-Taxol photolabels a region encompassed by TM 7 and half of TM 8 plus the intervening extra-cellular loop of *mdr*1b. This region of *mdr1b* is topologically equivalent to TM 12 of MRP1. In addition, mutations in TM 7 of P-gp1 have been found to decrease drug resistance [55,56]. Given this, the present report is the first to implicate this region in an MRP1 binding site.

The results presented in this study indicate that a region within the boundary of the N2 peptide directly interacts with $IAALTC_4$. Both MSD0 and an N-terminal portion of L0 are found within the N2 peptide. A previous study showed that efficient photolabelling of MRP1 by $[^3H]LTC_4$ is dependent on part of the L0 region [57], but not MSD0 [58]. Interestingly, L0 itself is not photolabelled by $[^3H]LTC_4$ [58]. Furthermore, a portion of L0 between amino acids Asp^{204} and Lys^{280} is important for $[^3H]LTC_4$ transport. Despite these findings, the precise function of L0 is still not well defined. Similarily, the role of MSD0 within MRP1 in substrate binding or transport remains unclear. Earlier studies have shown LTC_4 transport to drastically decrease when MSD0 or TM1 is removed [10]. Other studies show that MRP1-mediated transport of LTC_4 was reduced when portions of MSD0 are exchanged with equivalent regions of MRP2 or (ABCC2) [10,58]. Furthermore, two studies found that mutating specific Cys residues within MSD0 dramatically reduces LTC_4 transport [29,32]. Therefore, much of the work to date indicates that at least some portion of MSD0 is critical for MRP1-mediated transport. Conversely, one report showed that LTC_4 transport is unaffected in a truncated MRP1 mutant lacking MSD0 [59]. In the current study we showed that the N2 fragment is photolabelled with $IAALTC_4$ (figures 5A and 5B). The N2 fragment corresponds to a region of MRP1 that contains MSD0 and an NH_2-terminal portion of L0. These findings are supported by the deglycosylation of N2, whereby the native and deglycosylated N2 fragments were

photolabelled by IAALTC$_4$. The MRPr1 mAb was used to confirm the identity this deglycosylated and photolabelled N2 fragment (figure 8B). Furthermore, the same IAALTC$_4$-labelled fragment was purified from MRP1-variants 4 and 163 using the anti-HA mAb (figures 8C and 8D). Taken together, our results show that MSD0 directly interacts with LTC$_4$.

A previous study found that [^{3}H]LTC$_4$ does not photolabel MSD0; Photolabelling of the C-proximal half of MRP1 with [^{3}H]LTC$_4$ is limited to TM 14-17, thereby excluding TM 12 [36]. This discrepancy may stem from our different experimental systems. While our report used HA-variants of MRP1 for IAALTC$_4$ photolabelling, the previous study photolabelled co-expressed truncated fragments of MRP1; neither study used unmodified full-length MRP1. Alternatively, the photoreactive moiety added to LTC$_4$ (ie, IAALTC$_4$) could extend beyond the immediate region of LTC$_4$ binding domain(s) and photolabel a nearby domain such as TM 12. [^{3}H]LTC$_4$ is a useful compound because it is functionally and structurally identical to native LTC$_4$. Conversely, its UV cross-linking efficiency is different from our rapid photoreactive analog. Furthermore, it is conceivable that photolabelling with [^{3}H]LTC$_4$ would not allow for the detection of weakly photolabelled sequences, whereas the high specific activity of [^{125}I] allowed us to see photolabelling of the N2 fragment.

To understand the relevance of the regions photolabelled by IAALTC$_4$, we examined the structures of ABC transporters that are currently available. Two high resolution structures of ABC proteins that are similar to MRP1 have been solved. These are the lipid A transporters, MsbA, from *Escherichia coli* (EC-MsbA) and from *Vibrio cholera* (VC-MsbA) [60,61]. Each transporter is a dimmer composed of two subunits, each containing six transmembrane passes. The shape of the EC-MsbA dimmer resembles an upside-down V. The arms of this structure are separated by 40 Å on the cytoplasmic side of the plasma membrane. The VC-MsbA structure is similar although the arms are closer together. A recent study used these structures to model the MRP1 substrate binding site(s) [25]. This work proposes that specific amino acids in TM 10-11 and TM 16-17 make up an "aromatic basket" for substrate binding and are located at the edges of the V-like gap. We have also identified these same transmembrane domains as essential for substrate binding. As indicated in table 1 of Figure 9, all of the photoreactive drugs that

we have previously examined interact directly with TM 10-11 and TM 16-17, including $IAALTC_4$.

Interestingly, the MsbA structures predict that TM 1 in each subunit is located adjacent to TM 5 and TM 6 [60,61]. This information sheds light on our finding that TM 12 was photolabelled by $IAALTC_4$. The MsbA TM 1 and TM 5-6 are topologically equivalent to TM 12 and TM 16-17. Therefore, TM 12 may be photolabelled because of its proximity to the TM 16-17 binding region. TM 12 may also contribute amino acids that directly interact with LTC_4. In either case, this study demonstrates how photolabelling studies in conjunction with the newly resolved ABC protein structures will surely improve the understanding of other drug binding studies.

In summary our findings revealed several interesting attributes of LTC_4 binding with MRP1. (i) Its binding sites were found within TM 10-11 and TM 16-17, which are regions that interact with other MRP1 substrates. (ii) The photolabelling of TM 12 confirms structural data from other ABC transporters, and places this TM helix within close proximity to TM 16-17. TM 12 may also make up part of the multidrug binding site. Finally, (iii) $IAALTC_4$ interacted with, and photolabelled the MSD0 domain of MRP1. This observation was confirmed using several mAbs to specifically isolate the N2 fragment in both its native and deglycosylated form. These results demonstrate two important characteristics of MRP1. First, the interaction of LTC_4 with TM 10-11 and TM 16-17 furthers the possibility that ABC transporters share structural motifs to make up a multidrug binding site. Second, the interactions between LTC_4 and TMD0 indicate that MRP1 may contain separate regions necessary for binding its endogenous substrate.

Acknowledgments

We thank Nicholas Patocka for assistance with preparation of figure 5.

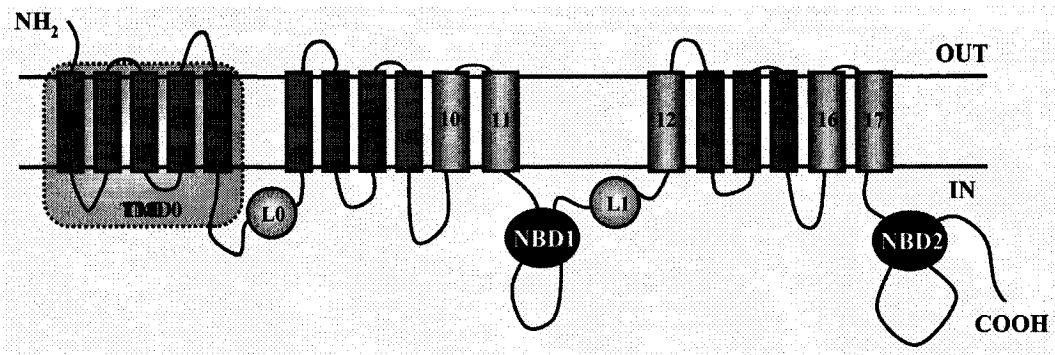

TABLE 1

Summary of the photolabelling intensity in various regions of MRP1 by different photoreactive compounds

Compound	*TMD0*	*L0*	*TM 10-11*	*L1*	*TM 12*	*TM 16-17*
IACI	-	-	+	-	-	++
IAARh123	-	-	+	-	-	+++
IAAGSH	-	+	++	+	-	+++
$IAALTC_4$	+	-	+	-	+	++++

Figure 9

Topological illustration of photolabelling sites in MRP1 for several compounds. The above diagram illustrates the predicted topological organization of the transmembrane segments in MRP1. The regions that have been found to interact with photoreactive compounds are shaded in gray: TMD0, L0, TM 10, TM 11, L1, TM 12, TM 16, and TM 17.

References

1. Riordan, J. R., and Ling, V. (1979) *J Biol Chem* 254(24), 12701-12705
2. Scala, S., Akhmed, N., Rao, U. S., Paull, K., Lan, L. B., Dickstein, B., Lee, J. S., Elgemeie, G. H., Stein, W. D., and Bates, S. E. (1997) *Mol Pharmacol* 51(6), 1024-1033
3. Gottesman, M. M., and Pastan, I. (1993) *Annu Rev Biochem* 62, 385-427
4. Mirski, S. E., Gerlach, J. H., and Cole, S. P. (1987) *Cancer Res* 47(10), 2594-2598
5. Cole, S. P. (1990) *Cancer Chemother Pharmacol* 26(4), 250-256
6. Cole, S. P., Bhardwaj, G., Gerlach, J. H., Mackie, J. E., Grant, C. E., Almquist, K. C., Stewart, A. J., Kurz, E. U., Duncan, A. M., and Deeley, R. G. (1992) *Science* 258(5088), 1650-1654

7. Borst, P., and Schinkel, A. H. (1997) *Trends Genet* 13(6), 217-222
8. Germann, U. A. (1996) *Eur J Cancer* 32A(6), 927-944
9. Cole, S. P., Sparks, K. E., Fraser, K., Loe, D. W., Grant, C. E., Wilson, G. M., and Deeley, R. G. (1994) *Cancer Res* 54(22), 5902-5910
10. Gao, M., Yamazaki, M., Loe, D. W., Westlake, C. J., Grant, C. E., Cole, S. P., and Deeley, R. G. (1998) *J Biol Chem* 273(17), 10733-10740
11. Hooijberg, J. H., Broxterman, H. J., Kool, M., Assaraf, Y. G., Peters, G. J., Noordhuis, P., Scheper, R. J., Borst, P., Pinedo, H. M., and Jansen, G. (1999) *Cancer Res* 59(11), 2532-2535
12. Holland, I. B. (2003) *ABC proteins: from bacteria to man*, Academic Press, London; San Diego, Calif.
13. Loe, D. W., Almquist, K. C., Deeley, R. G., and Cole, S. P. (1996) *J Biol Chem* 271(16), 9675-9682
14. Loe, D. W., Stewart, R. K., Massey, T. E., Deeley, R. G., and Cole, S. P. (1997) *Mol Pharmacol* 51(6), 1034-1041
15. Drazen, J. M., Israel, E., and O'Byrne, P. M. (1999) *N Engl J Med* 340(3), 197-206
16. Samuelsson, B., Dahlen, S. E., Lindgren, J. A., Rouzer, C. A., and Serhan, C. N. (1987) *Science* 237(4819), 1171-1176
17. Wijnholds, J., Evers, R., van Leusden, M. R., Mol, C. A., Zaman, G. J., Mayer, U., Beijnen, J. H., van der Valk, M., Krimpenfort, P., and Borst, P. (1997) *Nat Med* 3(11), 1275-1279
18. Robbiani, D. F., Finch, R. A., Jager, D., Muller, W. A., Sartorelli, A. C., and Randolph, G. J. (2000) *Cell* 103(5), 757-768
19. Cole, S. P., and Deeley, R. G. (1998) *Bioessays* 20(11), 931-940
20. Bakos, E., Hegedus, T., Hollo, Z., Welker, E., Tusnady, G. E., Zaman, G. J., Flens, M. J., Varadi, A., and Sarkadi, B. (1996) *J Biol Chem* 271(21), 12322-12326
21. Hipfner, D. R., Almquist, K. C., Leslie, E. M., Gerlach, J. H., Grant, C. E., Deeley, R. G., and Cole, S. P. (1997) *J Biol Chem* 272(38), 23623-23630

22. Daoud, R., Julien, M., Gros, P., and Georges, E. (2001) *J Biol Chem* 276(15), 12324-12330
23. Karwatsky, J., Daoud, R., Cai, J., Gros, P., and Georges, E. (2003) *Biochemistry* 42(11), 3286-3294
24. Ito, K., Oleschuk, C. J., Westlake, C., Vasa, M. Z., Deeley, R. G., and Cole, S. P. (2001) *J Biol Chem* 276(41), 38108-38114
25. Campbell, J. D., Koike, K., Moreau, C., Sansom, M. S., Deeley, R. G., and Cole, S. P. (2004) *J Biol Chem* 279(1), 463-468
26. Koike, K., Oleschuk, C. J., Haimeur, A., Olsen, S. L., Deeley, R. G., and Cole, S. P. (2002) *J Biol Chem* 277(51), 49495-49503
27. Zhang, D. W., Cole, S. P., and Deeley, R. G. (2002) *J Biol Chem* 277(23), 20934-20941
28. Zhang, D. W., Cole, S. P., and Deeley, R. G. (2001) *J Biol Chem* 276(37), 34966-34974
29. Leslie, E. M., Letourneau, I. J., Deeley, R. G., and Cole, S. P. (2003) *Biochemistry* 42(18), 5214-5224
30. Ito, K., Olsen, S. L., Qiu, W., Deeley, R. G., and Cole, S. P. (2001) *J Biol Chem* 276(19), 15616-15624
31. Haimeur, A., Deeley, R. G., and Cole, S. P. (2002) *J Biol Chem* 277(44), 41326-41333
32. Yang, Y., Chen, Q., and Zhang, J. T. (2002) *J Biol Chem* 277(46), 44268-44277
33. Leier, I., Jedlitschky, G., Buchholz, U., Cole, S. P., Deeley, R. G., and Keppler, D. (1994) *J Biol Chem* 269(45), 27807-27810
34. Leier, I., Jedlitschky, G., Buchholz, U., and Keppler, D. (1994) *Eur J Biochem* 220(2), 599-606
35. Loe, D. W., Almquist, K. C., Cole, S. P., and Deeley, R. G. (1996) *J Biol Chem* 271(16), 9683-9689
36. Qian, Y. M., Qiu, W., Gao, M., Westlake, C. J., Cole, S. P., and Deeley, R. G. (2001) *J Biol Chem* 276(42), 38636-38644
37. Kast, C., and Gros, P. (1997) *J Biol Chem* 272(42), 26479-26487
38. Kast, C., and Gros, P. (1998) *Biochemistry* 37(8), 2305-2313

39. Lowry, O. H., Rosebrough, N. J., Farr, A. L., and Randall, R. J. (1951) *J Biol Chem* 193(1), 265-275

40. Nare, B., Prichard, R. K., and Georges, E. (1994) *Mol Pharmacol* 45(6), 1145-1152

41. Georges, E., Zhang, J. T., and Ling, V. (1991) *J Cell Physiol* 148(3), 479-484

42. Fairbanks, G., Steck, T. L., and Wallach, D. F. (1971) *Biochemistry* 10(13), 2606-2617

43. Coligan, J. E. (2001) Current protocols in protein science. In., Wiley, New York

44. Towbin, H., Staehelin, T., and Gordon, J. (1979) *Proc Natl Acad Sci U S A* 76(9), 4350-4354

45. Leier, I., Jedlitschky, G., Buchholz, U., Center, M., Cole, S. P., Deeley, R. G., and Keppler, D. (1996) *Biochem J* 314 (Pt 2), 433-437

46. Jedlitschky, G., Leier, I., Buchholz, U., Center, M., and Keppler, D. (1994) *Cancer Res* 54(18), 4833-4836

47. Loe, D. W., Deeley, R. G., and Cole, S. P. (1998) *Cancer Res* 58(22), 5130-5136

48. Rappa, G., Lorico, A., Flavell, R. A., and Sartorelli, A. C. (1997) *Cancer Res* 57(23), 5232-5237

49. Gekeler, V., Ise, W., Sanders, K. H., Ulrich, W. R., and Beck, J. (1995) *Biochem Biophys Res Commun* 208(1), 345-352

50. Jedlitschky, G., Leier, I., Buchholz, U., Barnouin, K., Kurz, G., and Keppler, D. (1996) *Cancer Res* 56(5), 988-994

51. Hipfner, D. R., Gao, M., Scheffer, G., Scheper, R. J., Deeley, R. G., and Cole, S. P. (1998) *Br J Cancer* 78(9), 1134-1140

52. Hipfner, D. R., Almquist, K. C., Stride, B. D., Deeley, R. G., and Cole, S. P. (1996) *Cancer Res* 56(14), 3307-3314

53. Mao, Q., Qiu, W., Weigl, K. E., Lander, P. A., Tabas, L. B., Shepard, R. L., Dantzig, A. H., Deeley, R. G., and Cole, S. P. (2002) *J Biol Chem* 277(32), 28690-28699

54. Wu, Q., Bounaud, P. Y., Kuduk, S. D., Yang, C. P., Ojima, I., Horwitz, S. B., and Orr, G. A. (1998) *Biochemistry* 37(32), 11272-11279

55. Loo, T. W., and Clarke, D. M. (1996) *J Biol Chem* 271(26), 15414-15419

56. Loo, T. W., and Clarke, D. M. (1993) *J Biol Chem* 268(5), 3143-3149
57. Westlake, C. J., Qian, Y. M., Gao, M., Vasa, M., Cole, S. P., and Deeley, R. G. (2003) *Biochemistry* 42(48), 14099-14113
58. Konno, T., Ebihara, T., Hisaeda, K., Uchiumi, T., Nakamura, T., Shirakusa, T., Kuwano, M., and Wada, M. (2003) *J Biol Chem* 278(25), 22908-22917
59. Bakos, E., Evers, R., Szakacs, G., Tusnady, G. E., Welker, E., Szabo, K., de Haas, M., van Deemter, L., Borst, P., Varadi, A., and Sarkadi, B. (1998) *J Biol Chem* 273(48), 32167-32175
60. Chang, G., and Roth, C. B. (2001) *Science* 293(5536), 1793-1800
61. Chang, G. (2003) *J Mol Biol* 330(2), 419-430

General Conclusion

Since the discovery of ABC transporters, they have been linked to many medical conditions such as drug resistance in cancer, cystic fibrosis, and retinal dystrophies. For the most part, these conditions have been treated with conventional clinical treatments. More recently, treatment paradigms have been shifting towards more informed procedures for prevention and treatment of diseases. For this new strategy to continue, emphasis needs to be placed on research into fundamental science. Ideally, treatment in the near future will be armed with a greater fundamental knowledge of how cell, tissues, and organs within the body function at the molecular level in combination with more traditional therapies. For health conditions related to ABC transporters, there is a need for a better understanding of how they function. This requires insight into their biochemistry and their drug interactions at the molecular-level. With this knowledge it may be possible to target specific ABC transporters and side effects do to unforeseen pharmacokinetic interactions. For example, initial clinical trials with the P-gp1 inhibitor PSC 833 was not effective due to unforeseen toxic pharmacokinetic interactions. With a better understanding of the structure and mechanisms of specific ABC transporters it may be possible to target them with a greater specificity. Indeed, current studies indicate that the next generation of inhibitors do appear to target MDR transporters such as P-gp1 and MRP1 with greater specificity, thereby reducing detrimental pharmacokinetic interactions. To this end, the studies within this thesis add to the fundamental knowledge of these clinically relevant ABC proteins.

The scientific study presented in chapter 2 addresses a long standing phenomenon in P-gp1 research, the development of collateral sensitivity. Only one year after the discovery of P-gp1 in multidrug resistant cells, the first report appeared showing that these cells displayed collateral sensitivity to local anaesthetics, steroid hormones and some Triton X compounds 1. Furthermore, the degree of collateral sensitivity correlated with the degree of drug resistance. Many studies have reported that multidrug resistant

cells show collateral sensitivity to verapamil, an excellent substrate of P-gp1 [2-8]. Although several attempts to uncover the mechanism behind this effect have been made, finding clear answers remained elusive.

The findings presented in chapter 2 detail the first clear mechanism of verapamil-induced sensitivity in P-gp1-expressing cells. Verapamil activates ATPase activity in P-gp1 thereby creating an elevated ATP demand. This induces increased ATP production by oxidative phosphorylation resulting in an overactive electron transport chain. ROS produced from the electron transport chain deplete cellular GSH and damages biomolecules, the final result being apoptosis. Although these findings shed light on verapamil collateral sensitivity for the first time in many years, they also inspire many new questions and possibilities for further exploration. For example, the direct role of P-gp1 in this process could be further elucidated using newly developed RNAi technology. Moreover, detailed studies in apoptosis such as monitoring cytochrome *c* release and caspase activation would improve our understanding of the mechanism. These examples would help uncover the detail surrounding this mechanism of collateral sensitivity. I also believe that it would be important to investigate the role of verapamil sensitivity in human cancer cell lines with high P-gp1 expression, as well as exploring this process in animal models. These studies would help establish the clinical significance of verapamil collateral. Furthermore, the results presented in Appendix 1 indicate that other compounds mediate a similar affect. A systematic exploration of P-gp1 substrates might uncover compounds that can be used clinically to target drug resistant cancers. Any further studies together with the findings in chapter 2 should provide a greater understanding of collateral sensitivity which may eventually help develop new strategies for targeting drug resistant tumours.

In an effort to develop a better understanding of the way in which MRP1 interacts with its physiological substrates, photoreactive analogs of GSH and LTC_4 were generated that can be covalently linked to MRP1 binding sites. Once bound to MRP1, the substrate interactions can be examined and the location of binding domains can be elucidated. This technique has been especially useful with ABC transporters since it remains one of the most effective ways of examining the molecular interactions with drug substrates. In addition to the information gained from classic photolabelling studies, several other

techniques have been invaluable in exploring the nature of multidrug binding sites in ABC proteins. For example, mutagenesis of single amino acids in MRP1 has very successfully provided insight into the location of binding sites. This work has provided a great deal of information on which amino acids are involved in binding. The amino acids that have been directly investigated include (1) residues that are conserved between murine and human Mrp1/MRP1 and other MRP family members; (2) non-conserved residues; (3) specific amino acids with structural significance such as cysteines; and (4) groups of amino acids with specific chemical characteristics such as aromatic rings, hydrophobicity, or charged R-groups. The large number of these amino acid modifications and their effects of substrate binding and transport have recently been reviewed [9]. More recently, mass spectrometry has been used to locate photolabelled regions in P-gp1 and MRP1 [10-12]. In conjunction, the photoaffinity labelling studies and amino acid mutagenesis of MRP1 have provided impressive insight into the complex binding characteristics and structure of this multidrug transporter, especially since X-ray structures have been difficult to obtain.

The study in chapter 3 examines the interactions between GSH and MRP1 using a radiolabelled photoaffinity compound, IAAGSH. One of the most fascinating findings in this section was that both verapamil and vincristine increase GSH binding; this observation correlates with previous studies showing that GSH transport can be increased with verapamil and vincristine. Together, these observations firmly link the processes of drug binding and transport and shed light on the basic function of this MDR transporter. In addition, the specific photolabelled regions in MRP1 were identified. These regions include an intracellular GSH-specific binding sites which helps explain how the hydrophilic GSH molecule gains access to MRP1.

The binding of LTC_4 to MRP1 is characterised in Chapter 4 using a photoaffinity analog, $IAALTC_4$. Our results show that $IAALTC_4$ has very similar binding affinity to MRP1 and transport characteristics as native LTC_4. Furthermore, the study shows that $IAALTC_4$ photolabels drug labelling regions, as well as two novel regions. The photolabelling of a previously identified drug binding site made up of TM 10-11 and TM 16-17 with IAAGSH and $IAALTC_4$ demonstrates that this site interacts with both exogenous *and* endogenous substrates. $IAALTC_4$ was also observed to photolabel TM

12, a region that has not previously been implicated in MRP1 binding. TM 12 may be located close to TM 16-17, and thus proximal to the multidrug binding site. Lastly, IAALTC$_4$ is the first compound to interact directly with the five α-helices that make up MSD0 in MRP1. This novel finding indicates that MSD0 may form an LTC$_4$-specific binding site. The photolabelling studies in chapters 3 and 4 provide the most precise information on GSH and LTC$_4$ binding sites in MRP1 to date.

Although locating the physiological binding sites in MRP1 is a critical step towards understanding how the protein interacts with its substrates, these studies also point to new directions of research. One of the most interesting possibilities would be to determine the binding affinity of AAGSH and AALTC4 within different binding regions. This could be done under a variety of conditions such as during or after ATP hydrolysis, or in the presence of other MRP1 substrates. Specifically, it would be interesting to understand how verapamil and apigenin enhance the binding of AAGSH, and which binding sites would be favoured. The MRP1 HA-variants are particularly well suited for studying the binding affinity within different regions of the MRP1 protein. Additionally, a higher resolution map of binding sites using mass spectrometry would be a natural step in the discovery of drug binding sites. It is my hope that these and other studies will soon provide a very detailed picture of how multidrug transporters interact with their substrates.

Although chemotherapy is an effective means of treating cancer, the selective pressure of a toxic therapy often leads to rapid outgrowth of drug-resistant cells in human tumours. Certain ABC transporters such as P-gp1 and MRP1 cause multidrug resistance both *in vitro* and *in vivo*. Attempts have been made to counteract the MDR phenotype that accompanies the expression of P-gp1 and MRP1, but it remains difficult to specifically inhibit these transporters. I believe this drug resistance can be overcome by using current treatments in conjunction with strategies stemming from fundamental knowledge in domains such as signaling pathways, cellular metabolism, and protein biochemistry. The studies within this thesis directly contribute to the fundamental knowledge needed to develop new strategies against multidrug transporters. The inherent vulnerability of cells that express high levels of P-gp1 to ROS provides an interesting means of targeting resistant cells. Perhaps new drugs can be developed to more

effectively take advantage of this system. Indeed, several other compounds do elicit this same effect (see appendix I). Furthermore, the insight gained on the location of the multidrug binding site in MRP1 is valuable knowledge, especially since X-ray structural data remains elusive. This information will help determine how drugs interact with this perplexing binding site, and may eventually lead to a way of specifically inhibiting multidrug transporters. Through a culmination of fundamental knowledge of ABC transporters we can hope that their full nature will be revealed, and that this knowledge will improve the life of people affected by diseases related to them.

References

1. Bech-Hansen, N. T., Till, J. E., and Ling, V. (1976) J Cell Physiol 88(1), 23-31
2. Cano-Gauci, D. F., Seibert, F. S., Safa, A. R., and Riordan, J. R. (1995) Biochem Biophys Res Commun 209(2), 497-505
3. Croop, J. M., Guild, B. C., Gros, P., and Housman, D. E. (1987) Cancer Res 47(22), 5982-5988
4. Stow, M. W., and Warr, J. R. (1991) Biochim Biophys Acta 1092(1), 7-14
5. Stow, M. W., and Warr, J. R. (1993) FEBS Lett 320(2), 87-91
6. Vickers, S. E., Stow, M. W., and Warr, J. R. (1993) Cell Biol Int 17(5), 477-485
7. Warr, J. R., Anderson, M., and Fergusson, J. (1988) Cancer Res 48(16), 4477-4483
8. Warr, J. R., Quinn, D., Elend, M., and Fenton, J. A. (1995) Cancer Lett 98(1), 115-120
9. Haimeur, A., Conseil, G., Deeley, R. G., and Cole, S. P. (2004) Curr Drug Metab 5(1), 21-53
10. Ecker, G. F., Csaszar, E., Kopp, S., Plagens, B., Holzer, W., Ernst, W., and Chiba, P. (2002) Mol Pharmacol 61(3), 637-648
11. Pleban, K., Kopp, S., Csaszar, E., Peer, M., Hrebicek, T., Rizzi, A., Ecker, G. F., and Chiba, P. (2005) Mol Pharmacol 67(2), 365-374
12. Wu, P., Oleschuk, C. J., Mao, Q., Keller, B. O., Deeley, R. G., and Cole, S. P. (2005) Mol Pharmacol

Appendix 1

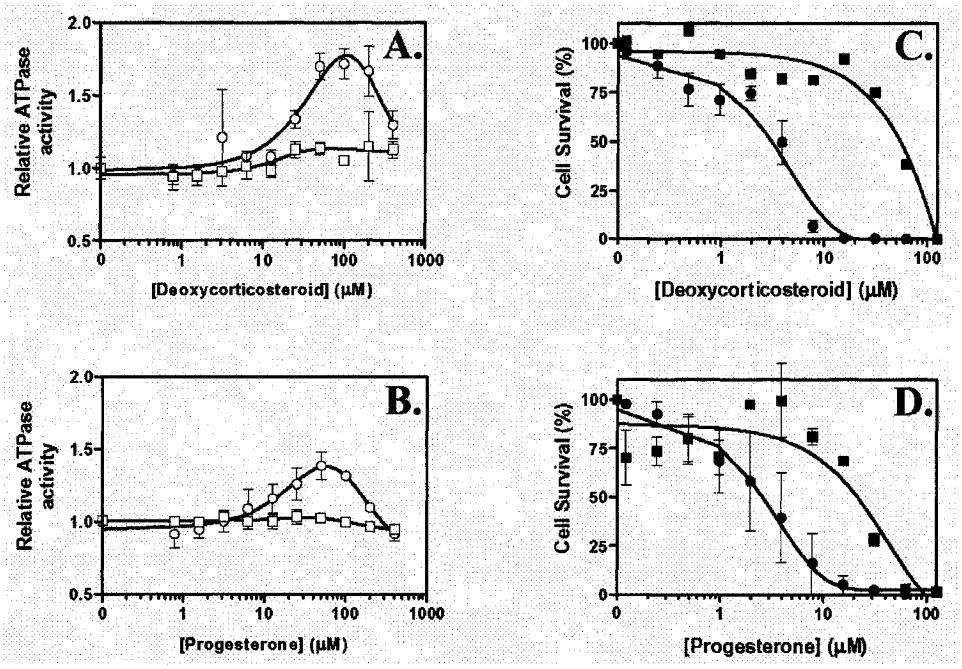

Chapter 2 Supplemental figure. *Effects of deoxycorticosteroid and progesterone on cell survival and P-gp1 ATPase in AUXB1 and CH^{R}C5.* Panels A and B, ATPase activity of AUXB1 (white squares) and CH^{R}C5 (white circles) was measured using purified plasma membranes exposed to increasing concentrations of deoxycorticosteroid and progesterone. Panel C and D, survival of AUXB1 (black squares) and CH^{R}C5 (black circles) exposed to increasing concentrations of deoxycorticosteroid and progesterone was determined by staining colonies with methylene blue and quantified by spectrophotometry.

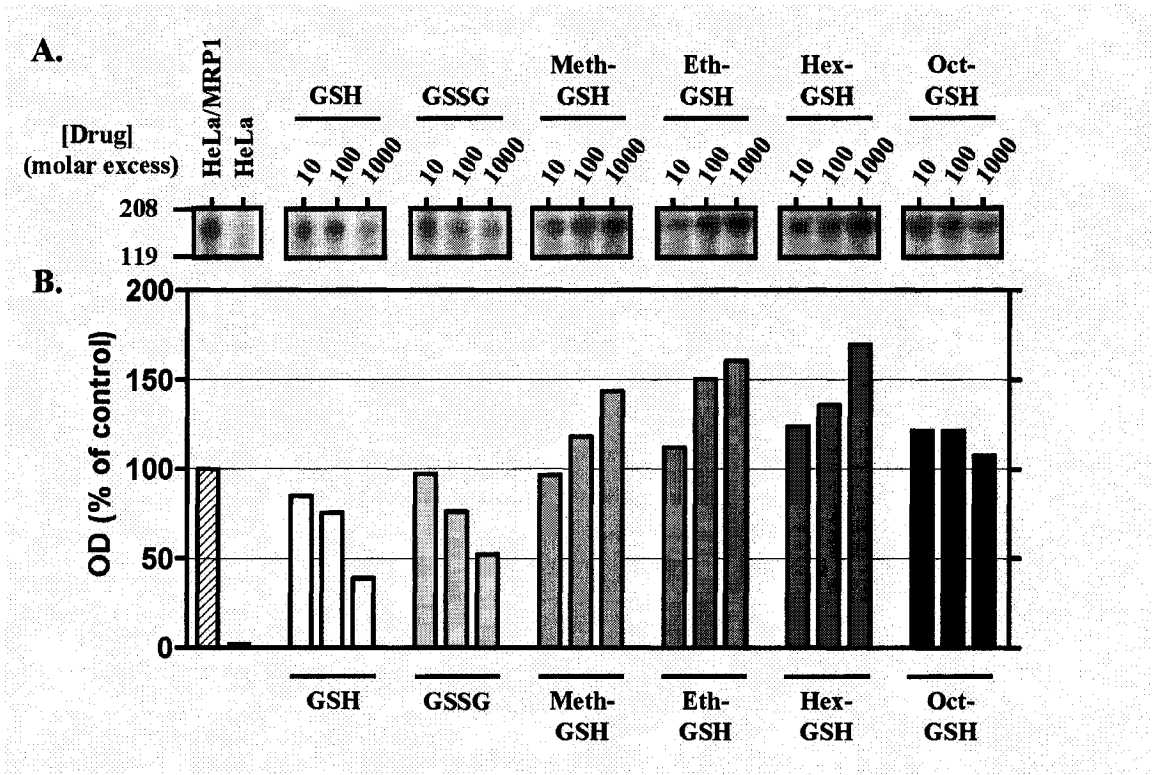

Chapter 3 supplemental figure. *Effect of GSH and its derivatives on the photoaffinity labelling of MRP1 by IAAGSH.* Panel A shows HeLa or HeLa/MRP1 plasma membranes photoaffinity labelled with 1 μM IAARh123 in the absence or presence of increasing molar excess (10, 100, and 1000) of: reduced glutathione (GSH), oxidized glutathione (GSSG), S-Methylglutathione (Meth-GSH), S-Ethylglutathione (Eth-GSH), S-Hexylglutathione (Hex-GSH), and S-Octylglutathione (Oct-GSH). Panel B demonstrates the relative decrease in photolabelling of MRP1 with IAARh123 in the presence of the same compounds. These results are representative of at least three individual experiments.

Appendix 2